

**Genetics and physiology of the  
thermophilic acetogenic bacteria  
*Thermoanaerobacter kivui* lacking  
key genes coding for electron  
re-cycling enzymes**

Dissertation for attaining the PhD degree of  
Natural Sciences

submitted to the Faculty of Biosciences of the Johann Wolfgang  
Goethe-University in Frankfurt am Main, Germany

by

**Surbhi Jain**

from Alwar, India

Frankfurt am Main, 2021

(D30)

accepted by the Faculty of Biosciences of the  
Johann Wolfgang Goethe University as a dissertation

Dean: Prof. Dr. Sven Klimpel

1<sup>st</sup> expert assessor: Prof. Dr. Volker Müller

2<sup>nd</sup> expert assessor: Prof. Dr. Claudia Büchel

Date of the disputation: 18.01.2022

(Printed with the support of German Academic exchange service (DAAD))

# Table of contents

<b>Abbreviations</b> .....	<b>V</b>
<b>1. Introduction</b> .....	<b>1</b>
<b>1.1 Acetogenic bacteria and acetogenesis</b> .....	<b>1</b>
1.1.1 Autotrophic metabolism.....	2
1.1.2 Heterotrophic metabolism .....	5
<b>1.2 Energy conservation in acetogenic bacteria</b> .....	<b>7</b>
<b>1.3 Electron bifurcation as a new mode of energy coupling</b> .....	<b>9</b>
<b>1.4 Role of HDCR</b> .....	<b>10</b>
<b>1.5 Physiology and bioenergetics of <i>Thermoanaerobacter kivui</i></b> .....	<b>11</b>
1.5.1 H <sub>2</sub> + CO <sub>2</sub> metabolism in <i>T. kivui</i> .....	13
1.5.2 CO metabolism in <i>T. kivui</i> .....	13
<b>1.6 Aim of the Thesis</b> .....	<b>14</b>
<b>2. Materials and methods</b> .....	<b>15</b>
<b>2.1 Organisms</b> .....	<b>15</b>
<b>2.2 List of plasmids</b> .....	<b>16</b>
<b>2.3 List of primers</b> .....	<b>18</b>
<b>2.4 Media and supplements for cultivation of <i>T. kivui</i></b> .....	<b>20</b>
2.4.1 Preparation of anaerobic media .....	20
2.4.2 Carbonate-buffered complex medium .....	21
2.4.3 Carbonate-buffered minimal medium .....	22
2.4.4 Carbonate-free medium .....	23
2.4.5 Trace element solution.....	24
2.4.6 Vitamin solution.....	25
<b>2.5 Cell growth</b> .....	<b>26</b>
2.5.1 Anaerobic cultivation of <i>T. kivui</i> .....	26
2.5.2 Carbon source used for the growth of <i>T. kivui</i> .....	26
2.5.3 Stock cultures .....	27
2.5.4 Cultivation of <i>Escherichia coli</i> .....	27
2.5.5 Determination of optical density .....	27
2.5.6 Purity control.....	28
<b>2.6 Plasmid construction</b> .....	<b>28</b>

2.6.1 Isolation of genomic DNA from <i>T. kivui</i> .....	28
2.6.2 Plasmid isolation from <i>E. coli</i> .....	29
2.6.3 Determination of DNA concentration .....	29
2.6.4 DNA amplification by polymerase chain reaction (PCR).....	29
2.6.5 Plasmid construction by Gibson Assembly .....	30
2.6.6 Production of chemically competent cells of <i>E. coli</i> .....	30
2.6.7 DNA transfer into <i>E. coli</i> .....	31
2.6.8 DNA digestion with restriction endonucleases .....	31
2.6.9 DNA separation by agarose gel electrophoresis.....	31
<b>2.7 DNA transfer into <i>T. kivui</i>.....</b>	<b>32</b>
2.7.1 DNA transfer into naturally competent <i>T. kivui</i> .....	32
2.7.2 Plating of <i>T. kivui</i> .....	32
2.7.3 Genotype analysis.....	34
<b>2.8 Cell suspension experiments .....</b>	<b>35</b>
2.8.1 Preparation of resting cells.....	35
2.8.2 Protein determination according to Schmidt (1963).....	35
2.8.3 Cell suspension experiments .....	36
<b>2.9 Measurement of metabolites .....</b>	<b>37</b>
2.9.1 Determination of acetate <i>via</i> gas chromatography.....	37
2.9.2 Determination of hydrogen gas <i>via</i> gas chromatography.....	37
2.9.3 Determination of formate, glucose and mannitol <i>via</i> HPLC analysis.....	38
<b>2.10 Measurement of enzyme activities .....</b>	<b>38</b>
2.10.1 Preparation of cell free extract.....	38
2.10.2 Protein determination according to Bradford (1976) .....	39
2.10.3 Measurement of CO-dehydrogenase activity.....	39
2.10.4 Measurement of methylene-THF dehydrogenase activity.....	40
<b>2.11 Chemicals and Gases.....</b>	<b>40</b>
<b>3. Results.....</b>	<b>42</b>
<b>3.1 Physiology of <i>T. kivui</i>.....</b>	<b>42</b>
3.1.1 Growth studies .....	42
3.1.2 Adaptation to growth on maltose and trehalose.....	44
3.1.3 Growth of <i>T. kivui</i> on mannitol with and without formate in carbonate free medium ...	45
3.1.4 Autotrophic growth of <i>T. kivui</i> .....	46
<b>3.2 Generation and characterization of a <math>\Delta hdcR</math> mutant of <i>T. kivui</i>.....</b>	<b>47</b>

3.2.1 Deletion of the <i>hdcr</i> gene cluster .....	47
3.2.2 Complementation of <i>T. kivui</i> $\Delta$ <i>hdcr</i> strain <i>in cis</i> .....	51
3.2.3 Growth studies with <i>T. kivui</i> $\Delta$ <i>hdcr</i> .....	54
3.2.4 Cell suspension experiments with <i>T. kivui</i> $\Delta$ <i>hdcr</i> .....	56
<b>3.3 Generation and characterization of a monofunctional CODH (<i>cooS</i>) deletion mutant of <i>T. kivui</i> .....</b>	<b>58</b>
3.3.1 Identification and organization of genes involved in CO metabolism .....	58
3.3.2 Deletion of <i>cooS</i> gene in <i>T. kivui</i> .....	60
3.3.3 Complementation of the <i>cooS</i> deletion mutant .....	65
3.3.4 The <i>cooS</i> mutant does not grow on CO .....	67
3.3.5 Measurement of CO-dehydrogenase activity in cell-free extracts of <i>T. kivui</i> $\Delta$ <i>cooS</i> ...70	
3.3.6 Cell suspension experiments with <i>T. kivui</i> $\Delta$ <i>cooS</i> .....	70
<b>3.4 Generation and characterization of a <math>\Delta</math><i>hydAB</i> mutant of <i>T. kivui</i> .....</b>	<b>72</b>
3.4.1 Identification and organization of electron bifurcating hydrogenase genes .....	72
3.4.2 Deletion of the <i>hydA<sub>1</sub>B</i> genes in <i>T. kivui</i> .....	73
3.4.3 Growth experiments with <i>T. kivui</i> $\Delta$ <i>hydA<sub>1</sub>B</i> .....	77
3.4.4 Cell suspension experiments with <i>T. kivui</i> $\Delta$ <i>hydA<sub>1</sub>B</i> .....	78
<b>3.5 Electron carrier specificity of the methylene-THF dehydrogenase in crude extracts of <i>T. kivui</i> .....</b>	<b>80</b>
<b>4. Discussion.....</b>	<b>81</b>
<b>4.1 Effect of deletion of hydrogen-dependent CO<sub>2</sub> reductase (<i>hdcr</i>) in <i>T. kivui</i>.....</b>	<b>83</b>
4.1.1 The physiological role of HDCR in the metabolism of <i>T. kivui</i> .....	84
<b>4.2 Effect of deletion of <i>cooS</i> in <i>T. kivui</i> .....</b>	<b>88</b>
<b>4.3 Effect of deletion of electron bifurcating hydrogenase (<i>hydAB</i>) in <i>T. kivui</i> .....</b>	<b>94</b>
4.3.1 The physiological role of hydrogenase in the metabolism of <i>T. kivui</i> .....	95
<b>5. Conclusion .....</b>	<b>98</b>
<b>6. Zusammenfassung .....</b>	<b>100</b>
<b>7. Appendix.....</b>	<b>105</b>
<b>7.1 Deletion of the <i>hdcr</i> gene cluster in <i>T. kivui</i>.....</b>	<b>105</b>
7.1.1 UFR of <i>hdcr</i> gene cluster .....	105
7.1.2 DFR of <i>hdcr</i> gene cluster .....	105
<b>7.2 Deletion of <i>cooS</i> gene in <i>T. kivui</i>.....</b>	<b>106</b>
7.2.1 UFR of <i>cooS</i> gene.....	106
7.2.2 DFR of <i>cooS</i> gene.....	106

<b>7.3 Deletion of <i>hydAB</i> gene in <i>T. kivui</i></b> .....	<b>107</b>
7.3.1 UFR of <i>hydAB</i> gene .....	107
7.3.2 DFR of <i>hydAB</i> gene .....	107
<b>8. References</b> .....	<b>109</b>
<b>9. Acknowledgements</b> .....	<b>127</b>
<b>10. Curriculum vitae</b> .....	<b>128</b>

## Abbreviations

5-FOA	5-fluoroorotic acid
ABC	ATP-binding cassette
Ack	acetate kinase
Acs/CODH	acetyl-CoA synthase / carbon monoxide dehydrogenase
BSA	Bovine serum albumin
CM	cytoplasmic membrane
CoFeSP	corrinoid iron-sulphur protein
DFR	downstream flanking region
DSMZ	Deutsche Sammlung von Mikroorganismen und Zellkulturen
DTE	Dithioerythritol
$\epsilon$	molar extinction coefficient [ $\text{mM}^{-1} \times \text{cm}^{-1}$ ]
$E_0'$	standard redox potential [mV]
Ech	Energy-converting hydrogenase
Etf	Electron transfer flavoprotein
Fd	Ferredoxin
Fno	Ferredoxin:NAD <sup>+</sup> oxidoreductase
HDCR	Hydrogen dependent carbon dioxide reductase
Hyd	Hydrogenase
Kbp	kilo basepair
MOPS	2-(N-morpholino)propanesulfonic acid
MV	methyl viologen
NaDt	sodium dithionite
Nfn	NADH-dependent reduced ferredoxin:NADP <sup>+</sup> oxidoreductase
NCBI	National Center for Biotechnology Information ( <a href="https://www.ncbi.nlm.nih.gov/">https://www.ncbi.nlm.nih.gov/</a> )
OD <sub>600</sub>	optical density at 600 nm
PMSF	phenylmethylsulfonyl fluoride
Pta	phosphotransacetylase

PTS	phosphotransferase system
Rnf	Rhodobacter nitrogen fixation
rpm	rounds per minute
SLP	substrate-level-phosphorylation
THF	tetrahydrofolate
Tris	2-amino-2-hydroxymethyl-propane-1,3-diol
UFR	upstream flanking region
v/v (%)	volume/volume percent
WLP	Wood-Ljungdahl pathway
WT	wild type



# 1. Introduction

## 1.1 Acetogenic bacteria and acetogenesis

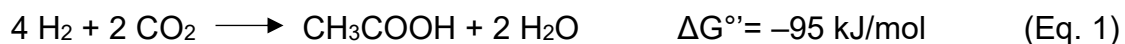
Acetogenic bacteria, acetogens in short, are strictly anaerobes which are able to use CO<sub>2</sub> as a terminal electron acceptor. Acetogens can grow chemolithoautotrophically on CO<sub>2</sub> with the use of molecular H<sub>2</sub> as electron donor and generate acetate *via* reductive acetyl-CoA or Wood-Ljungdahl pathway (Ljungdahl, 1986; Müller, 2003; Ragsdale, 2008; Ragsdale and Pierce, 2008). The dominant end product of this pathway is acetate, but acetogenic bacteria are not limited to this. Various metabolic end products such as ethanol, butanol or acetone are known. Besides fixing CO<sub>2</sub> into cell carbon, this metabolic pathway is coupled to the conservation of energy (Ljungdahl, 1994; Müller, 2003). The Wood-Ljungdahl pathway is distributed in various microbial groups such as methanogenic archaea as well as in sulfate reducing bacteria and considered as one of the oldest pathways to conserve energy (Lane and Martin, 2012; Martin, 2012).

Acetogenesis was first discovered in 1932 (Fischer et al., 1932). Shortly after 4 years, the first acetogen *Clostridium aceticum* isolation from soil sample was reported (Wieringa, 1939). This bacterium reduces CO<sub>2</sub> with H<sub>2</sub> as electron donor. However, this isolate was lost after few years. In 1942, the second thermophilic acetogenic bacterium *Clostridium thermoacetica* (later named as *Moorella thermoacetica*) was isolated (Fontaine et al., 1942). *M. thermoacetica* was used to further investigate and understand the metabolic pathway of acetogenesis. This strain could produce three moles of acetate from one mole of glucose. After some years, *M. thermoacetica* was described to grow on hydrogen and carbon dioxide as substrates (Daniel et al., 1990). To date, over 100 species classified in 23 different genera have been described (Müller and Frerichs, 2013). A large number of the isolates belong to the species *Clostridium* or *Acetobacterium* (Drake et al., 2008). The ecological niche of acetogenic bacteria is found in diverse habitats. They grow at ambient temperatures (Balch et al., 1977) under high-salt conditions (Pikuta et al., 2003) and even at elevated temperatures ( $\geq 50$  °C) (Leigh et al., 1981). Acetogens have been isolated

from the gastrointestinal tracts of cows (Kelly et al., 2016), from humans or termites (Graber and Breznak, 2004; Kamlage et al., 1997; Tanner et al., 1993), sediments (Balch et al., 1977), tundra (Simankova et al., 2000) and forest soils (Kuhner et al., 1997), salt marshes (Küsel et al., 2001) and acidic ponds formed from pumped water from coal mines (Küsel et al., 2000).

### 1.1.1 Autotrophic metabolism

Acetogenic bacteria are capable of growing chemolithoautotrophically with  $H_2 + CO_2$ .  $CO_2$  is used as a carbon source as well as an electron acceptor (Wood and Ljungdahl, 1991). *Moorella thermoacetica* served as a model organism for Harland G. Wood and Lars G. Ljungdahl to elucidate the biochemical and enzymological characteristics of the Wood-Ljungdahl pathway (Wood and Ljungdahl, 1991). During lithotrophic growth, the organism uses 4 molecules of  $H_2$  and 2 molecules of  $CO_2$  for acetate formation (Eq. 1) (Fischer et al., 1932).



The WLP is separated into a carbonyl- and a methyl branch, catalyzing the reduction of two molecules of  $CO_2$  to one molecule of acetyl-CoA (Fig. 1). In the first reaction of the methyl branch one molecule of  $CO_2$  is reduced to formate by a formate dehydrogenase (Fdh). The electron donor for this reaction varies between different acetogens for example *M. thermoacetica* uses NADPH as an electron donor (Li et al., 1966) whereas in *Acetobacterium woodii* and *Thermoanaerobacter kivui* electrons are derived from molecular  $H_2$  or reduced ferredoxin can serve as an electron donor for the reduction of  $CO_2$  to formate. The enzyme that catalyzes this reaction is hydrogen-dependent  $CO_2$  reductase (HDCR) (Schuchmann and Müller, 2013). In the next endergonic step, formate produced is activated by formyl-THF synthetase, whereupon the formyl group is bound to the cofactor THF driven by ATP hydrolysis (Himes and Harmony, 1973; Lovell et al., 1988). By splitting off water, the formyl-THF is converted to methenyl-THF catalyzed by formyl-THF cyclohydrolase. Subsequently, two reduction reactions occur, where the THF-bound methenyl group is reduced to methylene-THF via a methylene-THF dehydrogenase. The

electron donor for the first reduction step is either NADPH (*M. thermoacetica*, *T. kivui*) (O'Brien et al., 1973; Katsyv et al., 2021, submitted) or NADH (*A. woodii*, *Clostridium formicoaceticum*) (Ragsdale and Ljungdahl, 1984; Moore et al., 1974). In the second reduction step, methylene-THF is reduced to methyl-THF by methylene-THF reductase (MTHFR). Four classes of MTHFR with different subunit compositions are found in acetogens (Öppinger et al. 2021). MTHFR varies in the use of electron donors for example in *Blautia producta*, it forms a FAD-containing octamer that reduces methylene-THF using NADH as electron donor (Wohlfarth et al., 1990), whereas, MTHFR from *C. formicoaceticum* consists of a heterooctamer of four MetF subunits and four MetV-Subunits and reduces methylene-THF using ferredoxin (Clark and Ljungdahl, 1984). In *A. woodii* MTHFR forms a heterotrimer of MetF, MetV and RnfC<sub>2</sub> that uses NADH to reduce methylene-THF (Bertsch et al., 2015). In the terminal step of the methyl branch, the methyl group is transferred onto a corrinoid/iron-sulfur protein (CoFeSP) by methyltransferase.

In the carbonyl branch, another molecule of CO<sub>2</sub> is reduced to enzyme bound CO, required for the generation of acetyl-CoA. The reaction is ferredoxin dependent and carried out by the key enzyme of the WLP, the bifunctional acetyl-CoA synthase/ CO dehydrogenase (ACS/CODH). First, CO<sub>2</sub> is reduced with electrons from Fd<sup>2-</sup> to CO on the β subunit of the ACS/CODH (Pezacka and Wood, 1984; Raybuck et al., 1988; Seravalli et al., 1997). Later the α-subunit of the ACS/CODH assembles CO, the methyl group and coenzyme A (CoA) which catalyzes the acetyl-CoA synthesis (Ragsdale et al., 1982; Ragsdale et al., 1983; Ragsdale and Wood, 1985).

This acetyl-CoA formed serves as a precursor to anabolic metabolism and is converted to acetyl-phosphate by phosphotransacetylase (Pta) (Drake et al., 1981). Acetyl-phosphate is further converted to final product acetate by acetate kinase (Ack) with the gain of one molecule of ATP (Schaupp and Ljungdahl, 1974). In this pathway, one ATP is consumed in the input reaction during the conversion of formate to formyl-THF and one ATP is generated in the final reaction, the acetate kinase reaction. Thus, there is no net ATP synthesis by substrate level phosphorylation in the Wood-Ljungdahl pathway.

Therefore, a chemiosmotic mechanism has been established for the ATP synthesis under autotrophic growth (Heise et al., 1989).

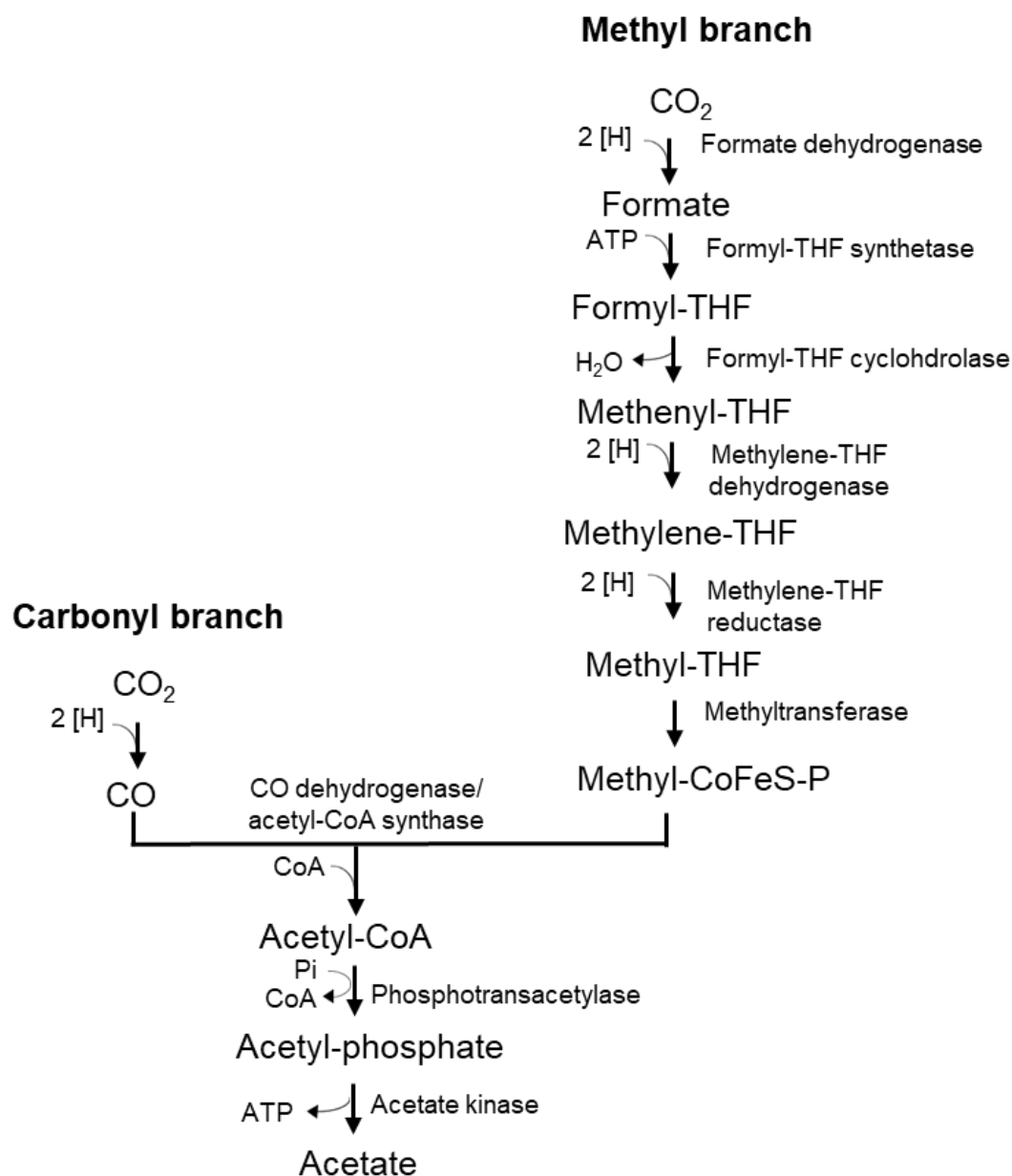
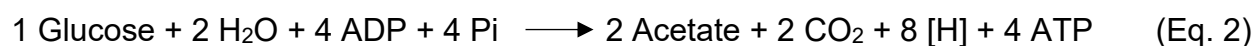


**Fig. 1. Scheme of the Wood-Ljungdahl pathway in acetogens (modified after Ljungdahl, 1986).** Two molecules of  $\text{CO}_2$  are reduced to 1 molecule of acetate. THF, tetrahydrofolate; CoFeSP, corronoid / iron-sulfur protein, CoA, coenzyme-A, Pi, inorganic phosphate; [H], reducing equivalent, corresponding two protons and two electrons.

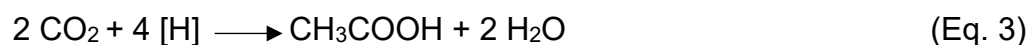
### 1.1.2 Heterotrophic metabolism

The unique feature of acetogens is the coupling of the WLP with various electron donors, which makes them versatile and enables them to compete in the ecosystem. They can grow heterotrophically on wide spectrum of potential substrates such as hexose like glucose or fructose, pentoses like xylose, organic acids such as pyruvate or lactate, alcohols (methanol, ethanol, propanol, butanol as well as diols (1,2-propandiol, 2,3-butandiol, ethylene glycol etc.). Some acetogens can use C1 compounds such as methanol and formate, which are metabolized through the Wood-Ljungdahl pathway (Drake et al., 1997).

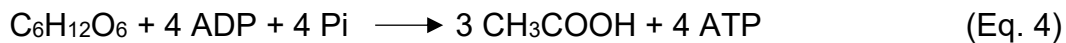
Oxidation of C<sub>6</sub> sugars is carried out by *via* the Embden-Meyerhof-Parnas pathway (also known as glycolysis) and 2 moles of produces pyruvate. From this module, 2 moles of ATP are generated *via* substrate level phosphorylation and 2 moles of NADH are formed (Fig. 2). 2 moles of pyruvate are further converted to 2 moles of acetyl-CoA by pyruvate:ferredoxin oxidoreductase, generating 2 moles of CO<sub>2</sub> and 2 moles of reduced ferredoxin. Acetyl-CoA are further converted to acetate by phosphotransacetylase and acetate kinase, producing 2 moles of ATP. In total, 1 mole of glucose is converted to 3 moles of acetate and 4 moles of ATP:



CO<sub>2</sub> formed in this reaction is not an end product but serves as terminal electron acceptor. The reducing equivalents released during oxidation of glucose are used to reduce these two moles CO<sub>2</sub> *via* Wood-Ljungdahl pathway and convert 2 moles of CO<sub>2</sub> to one mole of acetate (Gorst and Ragsdale, 1991; Ragsdale, 1991; Ljungdahl, 1994; Müller et al., 2004; Drake et al., 2006):



Overall, in glucose oxidation 3 moles of acetate are produced and 4 mol ATP:



Since acetate is the sole end product, this pathway is named as homoacetogenesis.

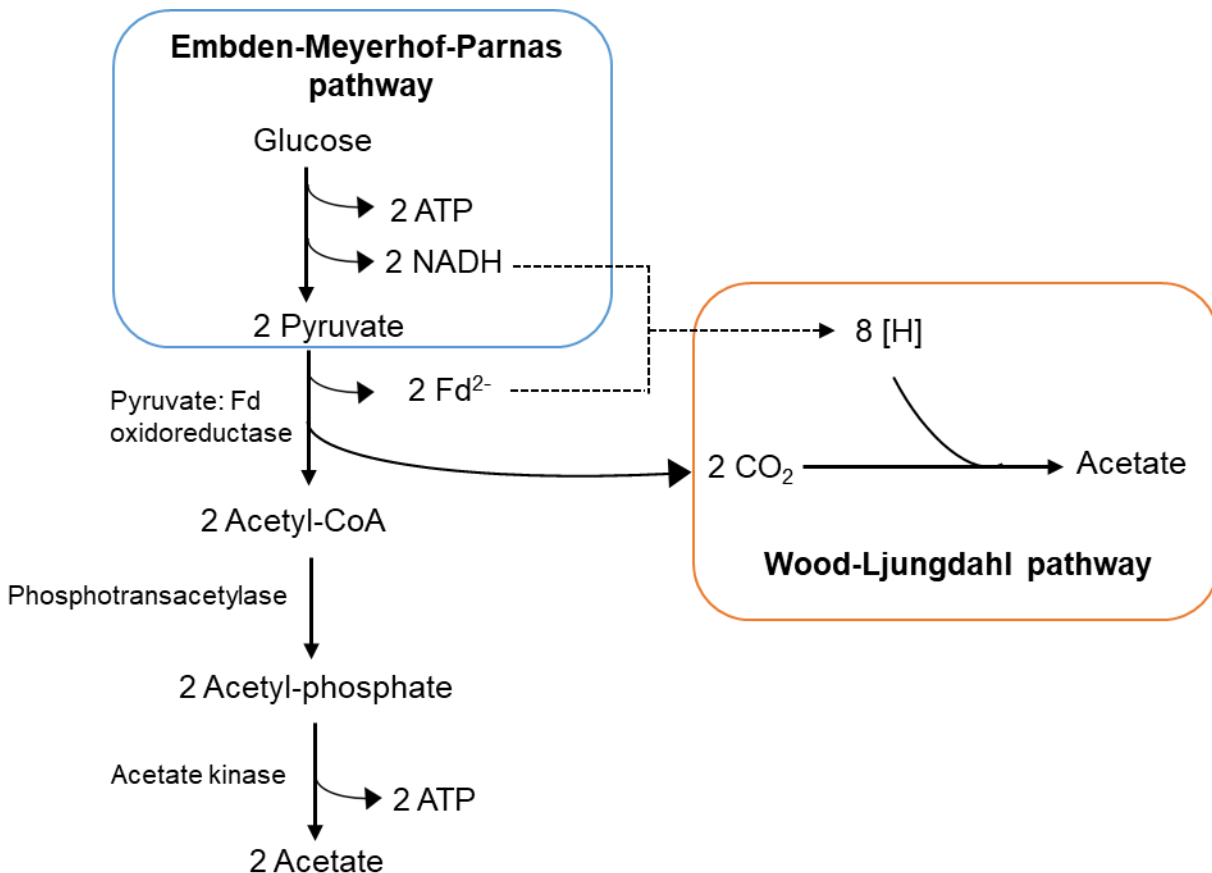


**Fig. 2. Scheme of homoacetogenesis in acetogens as carried out by combining the Embden-Meyerhof-Parnas- and the Wood-Ljungdahl pathway.** One molecule glucose is oxidized to three molecules of acetate. ATP yield *via* substrate level phosphorylation is 4 molecules of ATP per mol glucose. Fd<sub>red</sub>, reduced ferredoxin; [H], reducing equivalent.

The above examples of heterotrophy and autotrophy describes the fundamental principles of acetogenic metabolism. The other characterized metabolic pathways for the use of alternative electron acceptors are merely variants of the basic metabolic pathways described. Coupling of WLP with different metabolic modules argues for the competitiveness of acetogens in many ecological habitats.

## 1.2 Energy conservation in acetogenic bacteria

Energy can be conserved in the form of ATP through substrate level phosphorylation (SLP) where ATP is generated through direct phosphorylation or through phosphorylation driven by a chemiosmotic ion gradient. During oxidation of glucose, 4 moles of ATP are generated by substrate level phosphorylation where the WLP functions as an electron sink for the regeneration of redox equivalents. Whereas, in case of the autotrophic reduction of CO<sub>2</sub> in the Wood-Ljungdahl pathway, acetate kinase generates one mole of ATP per two moles of CO<sub>2</sub> by substrate chain phosphorylation, but one ATP is consumed to generate formyl-THF in the methyl branch, the net ATP balance of this pathway by SLP is zero (Hugenholtz and Ljungdahl, 1990; Müller, 2003). Therefore, this process is coupled to an additional energy conservation mechanism that utilizes a chemiosmotic gradient to gain net ATP (Heise et al., 1989; Hugenholtz et al., 1987). The mechanism allows storing metabolic energy by translocation of ions across the membrane which leads to the generation of an electrical and/or ion gradient. This ion gradient is used by a membrane-bound ATP synthase for ATP generation (Heise et al., 1989; Müller et al., 2001). There are two membrane bound enzyme complexes in acetogenic bacteria, the Rnf- and the Ech complex (Schuchmann and Müller, 2014). These both complexes are membrane-bound respiratory enzymes that uses reduced ferredoxin as reductant (Biegel and Müller, 2010; Biegel et al., 2011; Schoelmerich and Müller, 2019).

The Rnf complex (Fig. 3 A) consists of 6 subunits encoding one soluble, two membrane-associated, and three putative membrane-integral proteins (Biegel et al., 2011). *Acetobacterium woodii* is the model organism of Rnf-containing acetogens (Balch et al., 1977). It was shown in 1989 that growth and acetate formation of *A. woodii* is Na<sup>+</sup>-dependent (Heise et al., 1989). Resting cells of *A. woodii* generate a sodium ion gradient across the cytoplasmic membrane during acetogenesis from H<sub>2</sub> + CO<sub>2</sub>. If this gradient is destroyed, acetogenesis stops ((Aufurth et al., 1998; Heise et al., 1989; Müller and Bowien, 1995). The Rnf complex has ferredoxin:NAD<sup>+</sup> oxidoreductase (Fno) activity and causes reduction of NAD<sup>+</sup> ( $\Delta E_0' = -320$  mV) which is coupled with oxidation of reduced ferredoxin ( $\Delta E_0' = -450$  mV) (Biegel and Müller, 2010). *rnf* genes were first reported in

*Rhodobacter capsulatus*, where the complex uses an ion gradient as a driving force to couple the endergonic oxidation of NADH with a simultaneous reduction of ferredoxin, which is required for nitrogen fixation (Schmehl et al., 1993); (Jouanneau et al., 1998). Based on the origin and postulated function of the complex, the enzyme has been named "Rnf complex" - from "Rhodobacter nitrogen fixation" (Schmehl et al., 1993). The generation of a  $\Delta rnf$  mutant in *A. woodii* proved the Rnf complex in *A. woodii* is energy-conserving and membrane-bound coupling site for generating the sodium ion gradient (Westphal et al., 2018). In addition to energy conservation, the Rnf complex regenerates the reducing equivalent NADH which is required for reductive processes in WLP.

Genome sequencing of some acetogenic bacteria revealed that some possess *ech* genes encoding a membrane associated energy-converting hydrogenase (Ech) complex as found in *M. thermoacetica* (Pierce et al., 2008) and *Thermoanaerobacter kivui* (Hess et al., 2014) (Fig. 3B). *T. kivui* has 2 *ech* gene clusters encoded in its genome (Hess et al., 2014). The Ech complex couples the exergonic oxidation of reduced ferredoxin (Fd) to H<sup>+</sup> reduction, thereby translocating protons across the cytoplasmic membrane. Ech belongs to the group 4 [NiFe] hydrogenases responsible for H<sub>2</sub> evolution by translocating protons (Hedderich and Forzi, 2005); (Vignais and Billoud, 2007; Schut et al., 2016b; Schoelmerich and Müller, 2020). However, in *T. kivui* it is evident that Ech complex is involved in H<sup>+</sup> as well as in Na<sup>+</sup> transport to produce H<sub>2</sub> from reduced ferredoxin (Schoelmerich and Müller, 2019). Experiments on resting cells of *T. kivui* grown with carbon monoxide as substrate showed the coupled oxidation of CO with the generation of hydrogen and the simultaneous establishment of a transmembrane electrochemical ion gradient. Translocation of protons over the cytoplasmic membrane generates ATP with the establishment of proton motive force (Tersteegen and Hedderich, 1999; Hedderich and Forzi, 2005; Welte et al., 2010). These data demonstrate the coupling of an energy-conserving hydrogenase with an ATP synthase for the generation of ATP (Schoelmerich and Müller, 2019).



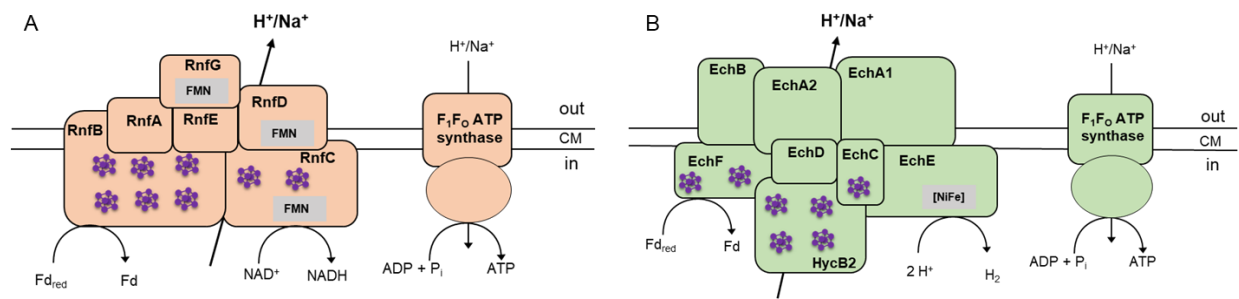


**Fig. 3. Model of respiratory enzyme complexes for energy conservation in acetogens (modified after (Katsyv and Müller, 2020)).** (A) Rnf complex in *A. woodii*. (B) Ech complex in *T. kivui*. CM, cytoplasmic membrane; Fd<sub>red</sub>, reduced ferredoxin; FMN, flavin mononucleotide.

### 1.3 Electron bifurcation as a new mode of energy coupling

Reduced ferredoxin is required for energy conservation as well as for the carbonyl branch of WLP. But the question arose how reduced ferredoxin is generated from H<sub>2</sub>, since it is an endergonic process where the redox potential of molecular hydrogen ( $E_0'$  [H<sub>2</sub>/H<sup>+</sup>] = -414 mV) does not allow for direct reduction of ferredoxin ( $E_0'$  [Fd<sup>2-</sup>/Fd] = -500 mV) (Thauer et al., 1977). This energetic barrier is overcome by electron bifurcation, a new mechanism of coupling endergonic and exergonic redox reactions (Buckel and Thauer, 2013). This mechanism was first reported for butyryl-CoA dehydrogenase/Etf complex (Bcd/Etf) in *Clostridium kluyveri* (Li et al., 2008). *A. woodii* also possesses a soluble electron bifurcating hydrogenase, HydABCD (Fig. 4), which couples reduction of ferredoxin and NAD<sup>+</sup> with oxidation of H<sub>2</sub> through flavin-based electron bifurcation (Schuchmann and Müller, 2012). The genome of *T. kivui* contains a 3 subunit electron bifurcating hydrogenase (HydABC) (Hess et al., 2014) which has recently been purified and has shown NADPH specificity (Katsyv et al., 2021, submitted). To date, many bacterial electron-bifurcating enzyme complexes have been identified in acetogens (Müller et al., 2018).

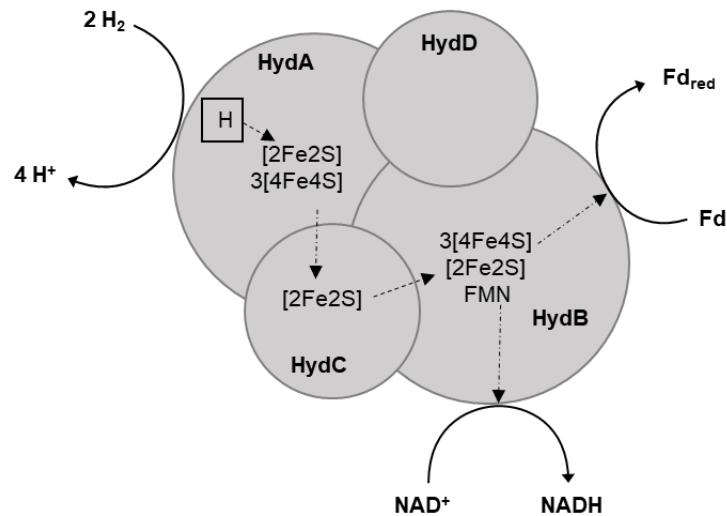


**Fig. 4. Schematic model of electron bifurcating hydrogenase, HydABCD, of *A. woodii* (modified after Schuchmann and Müller, 2012).** Fd<sub>red</sub>, reduced ferredoxin; [Fe-S], iron-sulfur cluster; FMN, Flavin mononucleotide.

## 1.4 Role of HDCR

The hydrogen-dependent CO<sub>2</sub> reductase (HDCR) is involved in the first step of the methyl branch in the WLP, where it catalyzes the reduction of CO<sub>2</sub> to formic acid or formate. Some acetogenic microorganisms use only ferredoxin-dependent formate dehydrogenase while others use in combination with two small subunits to form a hydrogen-dependent carbon dioxide reductase (HDCR). The enzyme complex has been purified from *A. woodii* (Schuchmann and Müller, 2013). The specialty of this soluble enzyme complex, which is not anchored in the membrane, is the direct use of molecular hydrogen as electron donor for CO<sub>2</sub> reduction to formate. As an alternative to molecular hydrogen, HDCR may also use reduced ferredoxin as an alternative electron donor. This enzyme also works in the reverse direction which makes it applicable for hydrogen storage. Recently, the discovery of the first thermostable HDCR in *T. kivui* (Fig. 5) has been reported with a higher catalytic rate than its mesophilic homologue (Schwarz et al., 2018). In addition to the two catalytic subunits of hydrogenase (HydA2) and molybdenum/tungsten containing formate dehydrogenase (FdhF1), HDCR consists of two electron transfer subunits (HycB2 & HycB3) (Nicolet et al., 1999; Ceccaldi et al., 2017).

The reduction of CO<sub>2</sub> to formate with H<sub>2</sub> is energetically feasible ( $E_0'$  [CO<sub>2</sub>/formate] = -420 mV;  $E_0'$  [2 H<sup>+</sup>/H<sub>2</sub>] = -414 mV) and has high turnover frequencies (TOF) of 101,600 h<sup>-1</sup> in *A. woodii* (Schuchmann and Müller, 2013) and 10,000,000 h<sup>-1</sup> in *T. kivui* (Schwarz et al., 2018). This makes HDCR interesting for biotechnological applications (Pereira, 2013; Müller, 2019).

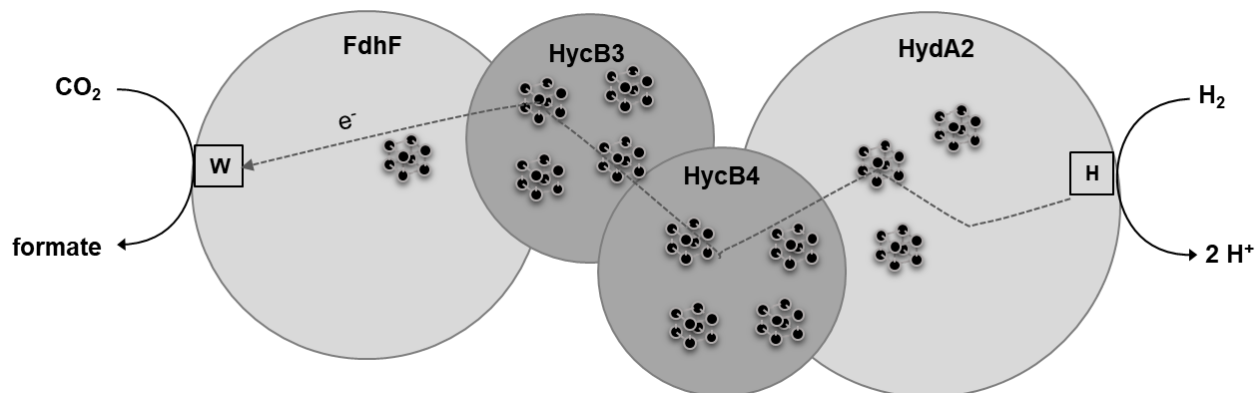


**Fig. 5. Model of hydrogen-dependent CO<sub>2</sub> reductase, HDCR, in *T. kivui* (modified after Schwarz et al., 2018).** Shown are the two catalytic subunits of hydrogenase (HydA2) and formate dehydrogenase (FdhF2), as well as the two electron transfer subunits of HycB3 and HycB4. W, tungsten.

## 1.5 Physiology and bioenergetics of *Thermoanaerobacter kivui*

*T. kivui* is a thermophilic acetogenic bacterium, isolated from Lake Kivu in central Africa and characterized as *Acetogenium kivui* in 1981 (Leigh et al., 1981). Later, the acetogenic bacterium was assigned to the genus *Thermoanaerobacter*. *T. kivui* was initially assigned to the Gram-negative bacteria on the basis of Gram staining. Based on its cell wall structure, *T. kivui* was reclassified as the Gram-positive bacterium (Leigh and Wolfe, 1983). *T. kivui* is a chemolithotrophic, thermophilic and non-spore forming acetogen that grows optimally at 66°C and pH 6.4 (Leigh et al., 1981). It is rod-shaped and often appears in pairs or chains (Fig. 6). The genome of *T. kivui* comprises 2.9 Mbp with a GC content of 35 % and 2,378 protein encoding open reading frames (Hess et al., 2014).

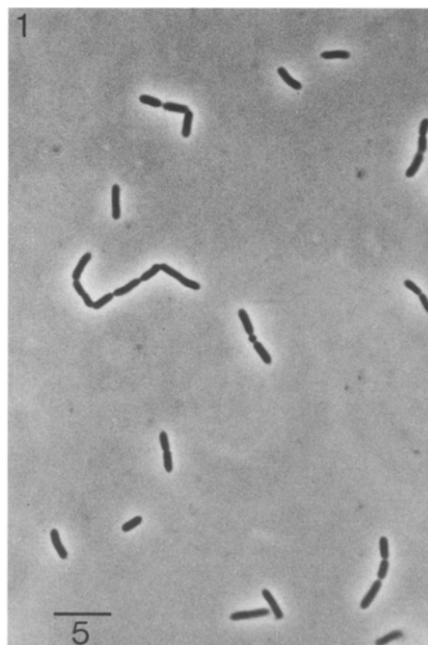


**Fig. 6. Phase contrast photomicrograph of *T. kivui*.** Cells were grown on hydrogen and carbon dioxide (Leigh et al., 1981). Bar scale in  $\mu\text{m}$ .

*T. kivui* grows heterotrophically on glucose, fructose, mannose, pyruvate and formate as well as autotrophically on  $\text{H}_2+\text{CO}_2$ , producing acetate as the main product (Leigh et al., 1981). It has been adapted to grow on CO (Weghoff and Müller, 2016), the third major component of synthesis gas. The ability of *T. kivui* to utilize CO or synthesis gas increases the biotechnological interest in this bacterium (Müller, 2019). Recently, the growth of *T. kivui* on mannitol has been reported (Moon et al., 2019). In this study *T. kivui* was adapted to grow maltose and trehalose. Interestingly, *T. kivui* does not require the addition of vitamins as well as it can grow on minimal medium (Leigh et al., 1981; Yang and Drake, 1990) and produces high titers of acetate ( $>600 \text{ mM}$ ) with high yields ( $>2.5 \text{ mol mol}^{-1}$  glucose) (Klemps et al., 1987), which makes it interesting for industrial applications.

### 1.5.1 H<sub>2</sub> + CO<sub>2</sub> metabolism in *T. kivui*

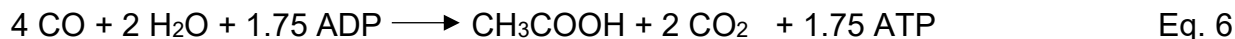
The reactions of the WLP and energy conservation from H<sub>2</sub> + CO<sub>2</sub> in *T. kivui* slightly differ from those described above for acetogens, in general. Reduction of 2 mol of CO<sub>2</sub> to 1 mol of acetate is catalyzed by the Wood-Ljungdahl pathway with H<sub>2</sub> as an electron donor where 4 moles of hydrogen are oxidized by an electron-bifurcating hydrogenase. The electron bifurcating hydrogenase of *T. kivui* has 3 subunits, HydABC, which reduces ferredoxin and NADP<sup>+</sup> and has two Ech complexes for energy conservation (Hess et al., 2014); (Schoelmerich and Müller, 2019). The genome also encodes for NfnAB-transhydrogenase which converts NADPH to NADH and Fd<sup>2-</sup> (Hess et al., 2014; Katsyv et al., 2021, submitted). CO<sub>2</sub> reduction in first step of the methyl branch is catalyzed by HDCR (Schwarz et al., 2018). The electron donor of methylene-THF dehydrogenase was unknown and addressed in this study.

### 1.5.2 CO metabolism in *T. kivui*

Despite of its toxicity, some bacteria and archaea use carbon monoxide as electron and carbon source for growth (Henstra et al., 2007; Sokolova et al., 2009; Robb and Techtmann, 2018). The redox potential of the CO/CO<sub>2</sub> couple of -520 mV (Thauer et al., 1977), makes CO a potent electron donor for biological processes. *T. kivui* is one of the few acetogens which grows on CO and produces acetate (Weghoff and Müller, 2016). Oxidation of CO can remove this waste gas from the environment and convert it to CO<sub>2</sub> and H<sub>2</sub>, which serves as the intermediates for acetogenesis (Diekert and Thauer, 1978; Savage et al., 1987; Daniel et al., 1990; Diender et al., 2015), methanogenesis (Daniels et al., 1977; Rother and Metcalf, 2004) and sulphate reduction (Parshina et al., 2005). CO dependent acetogenesis involves the principle of CO oxidation in the presence of water to CO<sub>2</sub> and H<sub>2</sub> according to:



Overall, CO is oxidized to acetate in *T. kivui* according to:



Oxidation of CO in microorganisms is catalyzed by monofunctional CODHs or bifunctional CODHs. The monofunctional CODH is well characterized in the carboxydrotrophic bacterium *Carboxydotherrmus hydrogenoformans* and phototrophic bacterium *Rhodospirillum rubrum* which couples CO oxidation to H<sub>2</sub> evolution by a nickel-containing CODH (CooS) often present together with an electron transfer protein (CooF) (Ragsdale, 2000; Ensign and Ludden, 1991; Kerby et al., 1992; Singer et al., 2006). *T. kivui* also contains *cooS*, encoding for monofunctional CODH, the downstream of it is localized by the gene *cooF<sub>1</sub>* (Hess et al., 2014). It was one of the aims of this study to identify the CODH catalyzing oxidation of the growth substrate CO.

## 1.6 Aim of the Thesis

Physiological studies toward the importance of heterotrophic and autotrophic metabolism of the thermophilic acetogenic bacterium, *T. kivui* have not been carried out yet, due to the lack of genetic tools. Therefore, the objective of this work was to create markerless deletion of genes encoding key enzymes of Wood-Ljungdahl pathway (WLP) in *T. kivui*. The hydrogen-dependent carbon dioxide reductase (HDCR), monofunctional carbon monoxide dehydrogenase (CooS) and electron bifurcating hydrogenase (HydABC) should be deleted using the recently developed genetic system (Basen et al., 2018). Deletion mutants were used to gain insights into the physiological relevance of the autotrophic growth on H<sub>2</sub> + CO<sub>2</sub> or CO and heterotrophic growth on glucose or mannitol.

## 2. Materials and methods

### 2.1 Organisms

The microorganisms used in this study are listed in Tab. 1.

**Tab. 1. List of organisms used**

Strain	Genotype	Reference
<i>T. kivui</i> DSM 2030	Wild type	(Leigh et al., 1981)
<i>T. kivui</i> TKV_MB001	$\Delta pyrE$	(Basen et al., 2018)
<i>T. kivui</i> TKV_MB013	$\Delta pyrE, \Delta hdcR$	This study
<i>T. kivui</i> TKV_MB019	P <sub>slp</sub> <i>hdcR</i>	This study
<i>T. kivui</i>	CO adapted Wild type*	(Weghoff and Müller, 2016)
<i>T. kivui</i>	CO adapted $\Delta pyrE$	This study
<i>T. kivui</i>	$\Delta pyrE, \Delta cooS$	This study
<i>T. kivui</i>	CO adapted $\Delta pyrE, \Delta cooS$	This study
<i>T. kivui</i>	P <sub>slp</sub> <i>cooS</i>	This study
<i>T. kivui</i>	$\Delta pyrE, \Delta hydA_1B$	This study
<i>E. coli</i> DH5 $\alpha$	$\Delta(ara-leu)$ 7697 <i>araD139 fhuA</i> $\Delta lacX74 galK16 galE15 e14-$ $\phi 80dlacZ\Delta M15 recA1 relA1 endA1$ <i>nupG rpsL (StrR) rph spoT1</i> $\Delta(mrr-$ <i>hsdRMS-mcrBC)</i>	New England Biolabs®

## 2.2 List of plasmids

Plasmid used in this work are listed in Tab. 2.

**Tab. 2. Plasmids used in this study**

Plasmid name	Description	Source
pMBTkv005	Derivative of pMU131 Contains ampicillin resistance cassette and the gene <i>pyrE</i> (Tkv_c14380) under the control of the aminoglycoside 3'-phosphotransferase promoter from <i>S. aureus</i> .	Henke, 2017
pMBTkv0012	Contains UFR and DFR of <i>hdcr</i> gene cluster (TKV_c19960-TKV_c19990), <i>pyrE</i> (Tkv_c14380), ampicillin resistance cassette	Peiter, 2017
pJM006	UFR (Tkv_c24500) and DFR (Tkv_c24520), in between <i>adhE</i> (Teth514_0627) under control of the S-layer protein promoter from <i>T. kivui</i> , followed by <i>pyrE</i> (Tkv_c14380) under control of the gyrase promoter from <i>Thermoanaerobacter</i> sp. strain X514, ampicillin- and kanamycin cassette	Moon, 2018
pSJ002	<i>hdcr</i> gene cluster (TKV_c19960-TKV_c19990) inserted between UFR (Tkv_c24500) and DFR (Tkv_c24520), under the control of S-layer protein promoter from <i>T. kivui</i> , followed by <i>pyrE</i> under control of the gyrase promoter from <i>Thermoanaerobacter</i> sp. strain X514, ampicillin- and kanamycin resistance cassette	This study



---

pMBTkv002b	Contains UFR and DFR of <i>pyrE</i> (Tkv_c14380), and kanamycin resistance cassette	Geiger, 2016
pSJ006	Contains UFR and DFR of <i>cooS</i> (Tkv_c08080), <i>pyrE</i> (Tkv_c14380), ampicillin-resistance cassette	This study
pSJ008	<i>cooS</i> (TKV_c08080) inserted between UFR (Tkv_c24500) and DFR (Tkv_c24520), under the control of S-layer protein promoter from <i>T. kivui</i> , followed by <i>pyrE</i> under control of the gyrase promoter from <i>Thermoanaerobacter</i> sp. strain X514, ampicillin- and kanamycin resistance cassette	This study
pSJ0011	Contains UFR and DFR of <i>hydA<sub>1B</sub></i> (Tkv_c19580-Tkc_c19600), <i>pyrE</i> (Tkv_c14380), ampicillin-resistance cassette	This study

---

## 2.3 List of primers

All primers used in this study are listed in Tab. 3.

**Tab. 3. Primers used in this study**

Primer name	Sequence (5'-3')	Application
NP005	GATAGGTGATACAATTGAAGTGC	Verification for <i>hdcr</i> gene cluster deletion (fw)
NP006	CGCCTCTTGCAAACCCG	Verification for <i>hdcr</i> gene cluster deletion (rv)
NP001	GCTCGGTACCCGGGGATCCTAA AGTTTAGTGCATTACCCCTAAAAT AATGG	Binding inside the <i>hdcr</i> gene locus to verify clean deletion (fw)
SJ003	AGCCGCATGCCTGCAGGTCGAC TCTAGATTCATATTGAGGCAATA GTTCAATAGCC	Binding inside the <i>hdcr</i> gene locus to verify clean deletion (rv)
P9fw	AAAGATGGTAAACAGGAAAAGG	Binding inside the <i>hdcr</i> gene locus to verify clean deletion (fw)
NP007	CAGGTGTTAAATCTCCCAAAT	Binding inside the <i>hdcr</i> gene locus to verify clean deletion (rv)
PBseq10	GCTCCGGCTATTAGAGTTTC	Binding inside the <i>hdcr</i> gene locus to verify clean deletion (fw)
P18brev	GCGTTATGCCTACCTATATCTTC	Binding inside the <i>hdcr</i> gene locus to verify clean deletion (rv)
SJ0010	GAGGAGGATTGACTGTATGAAAG ATGGTAAACAGGAAAA	Amplification for <i>hdcr</i> gene insertion in pSJ002 (fw)
SJ0011	TTTTAAATTAATTTTATACTTTTT TTCTCGGTGTATATTTAG	Amplification for <i>hdcr</i> gene insertion in pSJ002 (rv)
SJ0012	GAGAAAAAAGTATAAAATTTAAT TTAAAAATTTACAGCAA	Amplification of backbone for pSJ002 (fw)
SJ0013	TTTACCATCTTTCATACAGTCAAT CCTCCTCCTTG	Amplification of backbone for pSJ002 (rv)

$\Delta$ cooS_UFR_ FP	<u>ACCCGGGGATCCGCAGGAAGAT</u> TGGAAGTCAT	Amplification of UFR for pSJ006 (fw)
$\Delta$ cooS_UFR_ RP	<u>CCCATATTTTTCAATTATTATCAC</u> AACTCCTTTT	Amplification of UFR for pSJ006 (rv)
$\Delta$ cooS_DFR_ FP	<u>GGAGTTGTGATAATAATTGAAAA</u> ATATGGGAGGAA	Amplification of DFR for pSJ006 (fw)
$\Delta$ cooS_DFR_ RP	<u>GCAGGTCGACTCTAGACTGGTC</u> GGGGCAACAGGAT	Amplification of DFR for pSJ006 (rv)
$\Delta$ cooS_BB_FP	<u>GCCCCGACCAGTCTAGAGTCGA</u> CCTGCAGGCATG	Amplification of backbone for pSJ006 (fw)
$\Delta$ cooS_BB_RP	<u>CAATCTTCCTGCGGATCCCCGG</u> GTACCGAGCTCG	Amplification of backbone for pSJ006 (rv)
$\Delta$ cooS_FP	GGGCTTTATAAAGCGAAATGGG	Verification for <i>cooS</i> gene deletion (fw)
$\Delta$ cooS_RP	GCCTGTTGATAAGTCATAAAACC TGC	Verification for <i>cooS</i> gene deletion (rv)
CooS binding _FP	GCGTGATCCAAAATGTGGTTTCG G	Binding inside the <i>cooS</i> gene to verify clean deletion (fw)
CooS binding _RP	CAAGCCATTGTGGTGCAGAAGC	Binding inside the <i>cooS</i> gene to verify clean deletion (rv)
MB_IG_0005	CTCGTTCTTCAAACACTTTCATTA GG	Verification for <i>pyrE</i> gene deletion (fw)
MB_IG_0006	GGAATGGTGACACAAGTAATTGA G	Verification for <i>pyrE</i> gene deletion (rv)
CooS BB compl. _FP	<u>CTACTCAATATATAAAATTTAATT</u> TAAAATTTACAGCAAGCAG	Amplification of backbone for pSJ008 (fw)
CooS BB compl. _RP	<u>TGTAATTATCACTCATACAGTCAA</u> TCCTCCTCCTTGATTTG	Amplification of backbone for pSJ008 (rv)
CooS compl._FP	<u>GGAGGATTGACTGTATGAGTGAT</u> AATTACATTTATTCTGCTG	Amplification for <i>cooS</i> gene insertion in pSJ008 (fw)
CooS compl._RP	<u>GTGAAATTTTTAAATTTAATTTAT</u> ATATTGAGTAGTTTGCGCC	Amplification for <i>cooS</i> gene insertion in pSJ008 (rv)
$\Delta$ hydA <sub>1</sub> B_UFR_ FP	<u>GTACCCGGGGATCCCCACCTTC</u> ATATGACACAGCCC	Amplification of UFR for pSJ0011 (fw)

$\Delta hydA_1B$ _UFR_	<u>GGGAGGTGTGGTTTAAAAAAAT</u>	Amplification of UFR for pSJ0011 (rv)
RP	TAAGGTCTTTGTTAGAGTTGGG	
$\Delta hydA_1B$ _DFR_	<u>GAACCTTAATTTTTTTTAAACCAC</u>	Amplification of DFR for pSJ0011 (fw)
FP	ACCTCCCACAA	
$\Delta hydA_1B$ _DFR_	<u>GGTCGACTCTAGAGCGATGACAA</u>	Amplification of DFR for pSJ0011 (rv)
RP	CAACAGGAG	
$\Delta hydA_1B$ _BB_	<u>GTTGTCATCGCTCTAGAGTCGAC</u>	Amplification of backbone for pSJ007
FP	CTGCAGGC	(fw)
$\Delta hydA_1B$ _BB_	<u>ATGAAGGTGGGGATCCCCGGGT</u>	Amplification of backbone for pSJ007
RP	ACCGAGCT	(rv)
$\Delta hydA_1B$ _FP	CGAGGTGAAAAAAGTGA CTCT	Verification for <i>hydA<sub>1</sub>B</i> gene deletion
		(fw)
$\Delta hydA_1B$ _RP	GGGGTAAAACATGGGAAATTGG	Verification for <i>hydA<sub>1</sub>B</i> gene deletion
		(rv)
<i>hydA<sub>1</sub>B</i> int _FP	GCTTTTGGACCACAAGGCTT	Binding inside the <i>hydA<sub>1</sub>B</i> gene to
		verify clean deletion (fw)
<i>hydA<sub>1</sub>B</i> int _RP	TCTCAAAGAGAAGGGTTTGC	Binding inside the <i>hydA<sub>1</sub>B</i> gene to
		verify clean deletion (rv)

The nucleotides underlined are regions homologous to the fragment that they are supposed to be fused with.

## 2.4 Media and supplements for cultivation of *T. kivui*

### 2.4.1 Preparation of anaerobic media

The preparation of anaerobic media was modified according to (Hungate, 1969) and (Bryant, 1972). Media were prepared and dispensed in either 20 ml Hungate tubes (Glasgerätebau Ochs, Bovenden/Lenglern, Germany), with 5 ml media or 120 ml serum bottles (Glasgerätebau Ochs, Bovenden/Lenglern, Germany) with 20 or 50 ml medium or in 1 l serum bottles (Glasgerätebau Ochs, Bovenden/Lenglern, Germany) with 200 or 500 ml medium. In order to make the medium strictly anoxic, media were flushed with N<sub>2</sub> + CO<sub>2</sub> (80/20 [v/v]) or N<sub>2</sub> (100%) for 20 minutes, and then the bottles were sealed with butyl

rubber stoppers. The medium was sterilized for 25 minutes at 121 °C in an autoclave (Sanoclav, Maschinenbau Wolf GmbH, Bad Überkingen, Germany). The sterilized media were stored at room temperature. The appropriate growth substrate was added before inoculation from an anoxic and sterile stock solution.

#### 2.4.2 Carbonate-buffered complex medium

*T. kivui* was routinely cultivated in carbonate-buffered complex medium (modified according to (Leigh et al., 1981)). The composition is listed in Tab. 4.

**Tab. 4. Carbonate-buffered complex medium for the cultivation of *T. kivui***

Components	Amount	Final concentration
Na <sub>2</sub> HPO <sub>4</sub> × 2 H <sub>2</sub> O	8.9 g/l	50 mM
NaH <sub>2</sub> PO <sub>4</sub> × 2 H <sub>2</sub> O	7.8 g/l	50 mM
K <sub>2</sub> HPO <sub>4</sub>	0.22 g/l	1.2 mM
KH <sub>2</sub> PO <sub>4</sub>	0.22 g/l	1.2 mM
NH <sub>4</sub> Cl	0.3 g/l	4.7 mM
(NH <sub>4</sub> ) <sub>2</sub> SO <sub>4</sub>	0.22 g/l	1.7 mM
NaCl	0.45 g/l	7.5 mM
MgSO <sub>4</sub> × 7 H <sub>2</sub> O	0.1 g/l	0.37 mM
CaCl <sub>2</sub> × 2 H <sub>2</sub> O	6.0 mg/l	42.0 µM
FeSO <sub>3</sub> × 7 H <sub>2</sub> O	2.0 mg/l	7.2 µM
KHCO <sub>3</sub>	5.4 g/l	54.0 mM
Cystein-HCl × H <sub>2</sub> O	0.5 g/l	3.0 mM
Yeast extract	2.0 g/l	0.2 % [w/v]
Trace element solution (DSM 141)	10 ml/l	1.0 % [v/v]

Vitamin solution (DSM 141)	10 ml/l	1.0 % [v/v]
Resazurin	1.0 mg/l	4.4 $\mu$ M

The pH was adjusted to 7.5 after flushing with N<sub>2</sub>/CO<sub>2</sub> (80/20 [v/v]).

### 2.4.3 Carbonate-buffered minimal medium

The minimal medium used for cultivation of *T. kivui* had the following composition (modified after (Leigh et al., 1981) (Tab. 5)

**Tab. 5. Carbonate buffered minimal medium for the cultivation of *T. kivui***

Components	Amount	Final concentration
Na <sub>2</sub> HPO <sub>4</sub> × 2 H <sub>2</sub> O	8.9 g/l	50 mM
NaH <sub>2</sub> PO <sub>4</sub> × 2 H <sub>2</sub> O	7.8 g/l	50 mM
K <sub>2</sub> HPO <sub>4</sub>	0.22 g/l	1.2 mM
KH <sub>2</sub> PO <sub>4</sub>	0.22 g/l	1.2 mM
NH <sub>4</sub> Cl	0.3 g/l	4.7 mM
(NH <sub>4</sub> ) <sub>2</sub> SO <sub>4</sub>	0.22 g/l	1.7 mM
NaCl	0.45 g/l	7.5 mM
MgSO <sub>4</sub> × 7 H <sub>2</sub> O	0.1 g/l	0.37 mM
CaCl <sub>2</sub> × 2 H <sub>2</sub> O	6.0 mg/l	42.0 $\mu$ M
FeSO <sub>3</sub> × 7 H <sub>2</sub> O	2.0 mg/l	7.2 $\mu$ M
KHCO <sub>3</sub>	5.4 g/l	54.0 mM
Cystein-HCl × H <sub>2</sub> O	0.5 g/l	3.0 mM
Trace element solution (DSM 141)	10 ml/l	1.0 % [v/v]
Vitamin solution (DSM 141)	10 ml/l	1.0 % [v/v]

---

Resazurin	1.0 mg/l	4.4 $\mu$ M
-----------	----------	-------------

---

The pH was adjusted to 7.5 after flushing with N<sub>2</sub>/CO<sub>2</sub> (80/20 [v/v]).

All components were dissolved in water under stirring, and then the trace element solution (Tab. 7), vitamin solution (Tab. 8), and resazurin (1 mg/l) were added to the solution. The medium was flushed with N<sub>2</sub> + CO<sub>2</sub> (80/20 [v/v]) for 20 minutes in order to remove the oxygen.

#### 2.4.4 Carbonate-free medium

Carbonate free medium was prepared for the cultivation of *T. kivui* without external CO<sub>2</sub> or KHCO<sub>3</sub>. The buffer capacity of the medium was increased by addition of KHPO<sub>4</sub>. The composition is listed in the Tab. 6.

**Tab. 6. Carbonate free medium for the cultivation of *T. kivui***

Components	Amount	Final concentration
Na <sub>2</sub> HPO <sub>4</sub> × 2 H <sub>2</sub> O	8.9 g/l	50 mM
NaH <sub>2</sub> PO <sub>4</sub> × 2 H <sub>2</sub> O	7.8 g/l	50 mM
NH <sub>4</sub> Cl	0.3 g/l	4.7 mM
(NH <sub>4</sub> ) <sub>2</sub> SO <sub>4</sub>	0.22 g/l	1.7 mM
NaCl	0.45 g/l	7.5 mM
MgSO <sub>4</sub> × 7 H <sub>2</sub> O	0.1 g/l	0.37 mM
CaCl <sub>2</sub> × 2 H <sub>2</sub> O	6.0 mg/l	42.0 $\mu$ M
FeSO <sub>3</sub> × 7 H <sub>2</sub> O	2.0 mg/l	7.2 $\mu$ M
KPO <sub>4</sub> (1 M, pH 7.0)	27 ml	54 mM
Cystein-HCl × H <sub>2</sub> O	0.5 g/l	3.0 mM
Yeast extract	2.0 g/l	0.2 % [w/v]

---

Trace element solution (DSM 141)	10 ml/l	1.0 % [v/v]
Vitamin solution (DSM 141)	10 ml/l	1.0 % [v/v]
Resazurin	1.0 mg/l	4.4 $\mu$ M

---

The pH was adjusted to 7.5 after flushing with N<sub>2</sub> (100%).

The distilled water was boiled in round bottom flask to remove the CO<sub>2</sub> and to make it completely carbonate free. The water was then cooled down by sparging with N<sub>2</sub> for 20 min in order to remove oxygen and then all the components were added.

#### 2.4.5 Trace element solution

The trace element solution DSM 141 had the following composition (Tab. 7).

**Tab. 7. Trace element solution DSM 141**

---

Components	Amount	Final concentration
Nitrilotriacetic acid	1.5 g/l	7.9 mM
MgSO <sub>4</sub> × 7 H <sub>2</sub> O	3.0 g/l	11.0 mM
MnSO <sub>4</sub> × H <sub>2</sub> O	0.5 g/l	3.0 mM
NaCl	1.0 g/l	16.7 mM
FeSO <sub>4</sub> × 7 H <sub>2</sub> O	0.1 g/l	0.36 mM
CoSO <sub>4</sub> × 7 H <sub>2</sub> O	0.18 g/l	0.64 mM
CaCl <sub>2</sub> × 2 H <sub>2</sub> O	0.1 g/l	0.7 mM
ZnSO <sub>4</sub> × 7 H <sub>2</sub> O	0.18 g/l	0.63 mM
CuSO <sub>4</sub> × 5 H <sub>2</sub> O	0.01 g/l	40.0 $\mu$ M
KAl(SO <sub>4</sub> ) × 12 H <sub>2</sub> O	0.02 g/l	42.0 $\mu$ M

---



H <sub>3</sub> BO <sub>3</sub>	0.01 g/l	0.17 mM
Na <sub>2</sub> MoO <sub>4</sub> × 2 H <sub>2</sub> O	0.01 g/l	56.0 μM
NiCl <sub>2</sub> × 6 H <sub>2</sub> O	0.03 g/l	0.13 mM
Na <sub>2</sub> SeO <sub>3</sub> × 5 H <sub>2</sub> O	0.3 mg/l	1.1 μM
Na <sub>2</sub> WO <sub>4</sub> × 2 H <sub>2</sub> O	0.4 mg/l	1.2 μM

Nitritotriacetic acid was diluted in distilled water and the pH was set with KOH to 6.5. After adding all the minerals, the pH was set with KOH to 7.0. The trace element solution was stored at 4°C.

#### 2.4.6 Vitamin solution

The components of the vitamin solution DSM 141 (Wolin et al., 1963) for the cultivation of *T. kivui* are listed in Tab. 8.

**Tab. 8. Vitamin solution DSM 141**

Components	Amount	Final concentration
Biotin	2.0 mg/ml	8.2 μM
DL-Ca-panthothenic acid	5.0 mg/ml	10.0 μM
Folic acid	2.0 mg/ml	4.5 μM
Liponic acid	5.0 mg/ml	24.0 μM
Nicotinic acid	5.0 mg/ml	41.0 μM
Pyridoxin-HCl	10.0 mg/ml	49.0 μM
p-Aminobenzoic acid	5.0 mg/ml	37.0 μM
Riboflavin	5.0 mg/ml	13.0 μM
Thiamin-HCl	5.0 mg/ml	15.0 μM
Vitamin B <sub>12</sub>	0.1 mg/ml	74.0 nM

The bottle containing the vitamin solution was covered with aluminium foil and stored at 4°C.

## 2.5 Cell growth

### 2.5.1 Anaerobic cultivation of *T. kivui*

*T. kivui* was cultivated either in 20 ml Hungate tubes filled with 5 ml media or 120 ml serum bottles filled with 50 ml media containing the growth substrates listed below in Tab. 9. For growth on gases, cells were cultivated in 120 ml serum bottles (Glasgerätebau Ochs, Bovenden/Lenglern) filled with 20 ml minimal or complex medium. The culture was inoculated to a starting OD<sub>600</sub> of ~0.02 - 0.05 using sterile disposable syringes (Braun Melsungen AG, Melsungen, Germany). Pre-cultures were grown on the same carbon source, unless stated otherwise. Cultivation took place at 65 °C.

### 2.5.2 Carbon source used for the growth of *T. kivui*

Stock solution of growth substrates were passed through sterile filter (Filtropur S, 0.45 µm) and poured in 120 ml serum bottles with a 50 ml plastic syringe (BD Plastipak, Spain). Subsequently, solutions were flushed with N<sub>2</sub> for 20 minutes to remove oxygen, sealed with a rubber stopper and stored at room temperature or at 4 °C. Carbon sources tested are listed in Tab. 9.

**Tab. 9. Carbon source and their final concentration for the growth of *T. kivui***

Substrates	Concentration of stock solution	Final concentration
Glucose	1.25 M	25 mM
Sodium formate	2M	50-300 mM

---

Pyruvate	2 M	100 mM
Mannitol	0.625 M	25 mM
Maltose	0.5 M	25 mM
Trehalose	0.5 M	25 mM

---

For autotrophic growth of *T. kivui*, H<sub>2</sub> + CO<sub>2</sub> (80:20 [v/v]) at 2 × 10<sup>5</sup> Pa or 100% CO (2 × 10<sup>5</sup> Pa) were used as a carbon source. The glass vessels were filled with medium to 1/4<sup>th</sup> of the volume and the headspace was exchanged with the respective gases.

### 2.5.3 Stock cultures

To ensure stable long-term storage of the *T. kivui* strains, stock cultures were created. 500 µl of exponentially grown cells was added to 500 µl of 50% glycerol and was then frozen into liquid nitrogen and stored at -80°C.

### 2.5.4 Cultivation of *Escherichia coli*

*E. coli* DH5α was cultivated aerobically in Luria-Broth (LB) medium (modified after Green and Sambrook, 2012) in test tubes at 37 °C under shaking condition with a speed of 150 rpm. LB medium contained 10 g/l tryptone, 5 g/l yeast extract and 5 g/l NaCl. Solid medium on plates was prepared with 1.8 % agar and antibiotics for selection were added, if necessary (100 µg/ml ampicillin or 30 µg/ml kanamycin).

### 2.5.5 Determination of optical density

The optical density of cultures was measured in disposable plastic cuvettes (Sarstedt AG & Co., Nümbrecht, Germany) at a wavelength of 600 nm using a spectrophotometer (Spectronic 200, Thermo Scientific, USA). 1 ml of the culture was withdrawn with a disposable syringe (anaerobic cultures) or with a pipette (aerobic cultures). Medium

containing the redox and oxygen sensitive indicator dye resazurin was supplemented with trace amount of sodium dithionite ( $\text{Na}_2\text{S}_2\text{O}_4$ ), to reduce the resazurin present in the growth medium, for preventing interference with the absorbance of oxidized resazurin. If the optical density exceeded 0.5, the sample was diluted.

### 2.5.6 Purity control

Cultures were checked regularly for purity *via* light microscopy in a phase-contrast microscope (Zeiss, Jena, Germany).

## 2.6 Plasmid construction

### 2.6.1 Isolation of genomic DNA from *T. kivui*

Genomic DNA from *T. kivui* was isolated using the DNeasy Blood & Tissue Kit (Qiagen, Hilden, Germany). *T. kivui* cells were cultivated in a 5 ml Hungate tubes on 25 mM glucose. After reaching the stationary growth phase cells were disrupted according to the 'pretreatment for Gram-positive bacteria' protocol. The cells were spun down at 13000 rpm at 4 °C for 10 minutes. The pellet was re-suspended in 180 µl of TE buffer (20 mM Tris-HCl, pH 8.0, 2 mM EDTA, 1.2% Triton X-100 and 20 mg/ml lysozyme), and then incubated at 37 °C for 30 minutes. After subsequent addition of 25 µl Proteinase K and 200 µl lysis buffer, samples were mixed and incubated at 56 °C for 30 minutes. After subsequent addition of 25 µl Proteinase K and 200 µl lysis buffer, samples were mixed and incubated at 56 °C for 30 minutes. Then 200 µl ethanol (96–100%) was added to the samples and mixed. Subsequently, the procedure was continued from point 4 of the instructions "Purification of Total DNA from Bacterial Cells (Spin-Column Protocol)". The mixture was then poured into DNeasy mini spin column placed in 2 ml Eppendorf tube. The cells were spun down at 8000 rpm for 1 minute and the flow-through was discarded. The column was transferred in a new 2 ml collection tube. 500 µl of wash buffer 1 was added, centrifuged at 8000 rpm for 1 minute and the flow-through was discarded. Same

step was repeated with 500  $\mu$ l of wash buffer 2 and centrifuged for 3 minutes at 14000 rpm to dry the DNeasy membrane of the column. The flow-through was discarded, the column was transferred to a clean Eppendorf tube and 100  $\mu$ l of elution buffer or distilled water was directly added to the column membrane. After incubating at room temperature for 1 min, the DNA was eluted by centrifugation for 1 minute at 8000 rpm.

### **2.6.2 Plasmid isolation from *E. coli***

For plasmid isolation, 2 ml of *E. coli* cells were harvested by centrifugation at 13000 rpm for 1 minute. The supernatant was discarded and the pellet was used for isolating plasmid DNA. The isolation was carried out using 'GenElute™ HP Plasmid Miniprep kit (Sigma-Aldrich, St. Louis, Missouri, USA). The plasmid DNA was eluted in 30  $\mu$ l distilled water and stored at  $-20$  °C.

### **2.6.3 Determination of DNA concentration**

The concentration of DNA was determined photometrically at a wavelength of 260 nm using NanoDrop spectrophotometer (NanoDrop™ 2000C; Thermo Fisher Scientific, Waltham, Massachusetts, USA). The purity of DNA was controlled by determining the  $A_{260}/A_{280}$  and  $A_{260}/A_{230}$  ratios.

### **2.6.4 DNA amplification by polymerase chain reaction (PCR)**

The amplification of DNA fragments was performed *via* polymerase chain reaction according to (Mullis et al., 1986). Phusion® High-Fidelity Polymerase (New England Biolabs Inc., Ipswich, Massachusetts, USA) was routinely used for amplification or PrimeSTAR® GXL DNA Polymerase (Takara Bio Inc., Kusatsu, Shiga, Japan). All procedures were performed according to the supplier's instructions. A thermocycler (LabCycler48; SensoQuest GmbH, Göttingen, Germany) was used for the PCR.

### 2.6.5 Plasmid construction by Gibson Assembly

All the plasmids used in this study were prepared by Gibson Assembly (Gibson et al., 2009). Gibson assembly (NEB, Frankfurt am Main, Germany) was used for fusing two or more DNA fragments for the plasmid construction. DNA fragments were amplified by PCR with the primers containing homologous regions with the fragments that they were supposed to be fused with. Then, the PCR products were purified using the 'GenElute™ PCR Clean-up kit' (Sigma-Aldrich, St. Louis, Missouri, USA) according to the manufacturer's instruction and eluted in 15 µl distilled water. For the DNA fragments derived from plasmids isolated from *E. coli*, digestion with *DpnI* (NEB, Frankfurt/Main, Germany) was performed, to eradicate the residual template plasmids. 50–100 ng of the plasmid fragments were taken and mixed with DNA fragments in 1:2 molar ratio of plasmid to insert. The mixture was incubated at 50 °C for 30 minutes with 50% 2X NEBuilder HiFi DNA Assembly Master Mix (NEB, Frankfurt/Main, Germany). After incubation, *E. coli* was transformed directly with the DNA.

### 2.6.6 Production of chemically competent cells of *E. coli*

For the production of chemically competent cells of *E. coli*, a single colony of DH5α was transferred into 5 ml LB-medium and the culture was incubated at 37 °C for 16 hours. An aliquot of the grown culture was inoculated in 50 ml LB medium to an OD<sub>600</sub> of 0.05. The 50 ml culture was then cultivated with shaking at 37 °C up to an OD<sub>600</sub> of 0.4–0.6. Cells were harvested by centrifugation at 4 °C and 4,000 rpm for 10 minutes and resuspended in 10 ml of ice cold calcium chloride solution (100 mM CaCl<sub>2</sub>, 20% [v/v] glycerol). After incubation on ice for 15 minutes, the cells were pelleted by centrifugation at 4 °C and 4000 rpm for 10 minutes and resuspended in 2 ml of ice cold calcium chloride solution. The cells were then incubated for 1-2 hours on ice. Finally, the cells were distributed into 100 µl aliquots and immediately frozen in liquid nitrogen. The competent cells were stored at –80 °C for later use.

### **2.6.7 DNA transfer into *E. coli***

100 µl aliquots of stored competent cells were first thawed on ice and then 50 ng of plasmid was added. The mixture was incubated on ice for 30 minutes. The heat shock treatment at 42 °C was given for 45 seconds and the cells were then immediately incubated on ice for 2 minutes. 400 µl of super optimal broth, SOC medium (2 % [w/v] trypton, 0.5 % [w/v] yeast extract, 10 mM NaCl, 2.5 mM KCl, 10 mM MgCl<sub>2</sub>, 10 mM MgSO<sub>4</sub>, and 20 mM glucose) was added for the cells to recover and incubated at 37 °C for 45 minutes with shaking. Cells were then centrifuged at 8000 rpm for 2 minutes and the pellet was re-suspended in 100 µl of media and streaked on LB agar plates with antibiotics for selection. The plates were incubated overnight at 37 °C to get clear visible colonies. The colonies were inoculated to liquid LB medium and plasmids were isolated as described in section 2.4.2.

### **2.6.8 DNA digestion with restriction endonucleases**

For the verification of constructs, isolated plasmid DNA was digested with restriction endonucleases (New England Biolabs Inc., Ipswich, Massachusetts, USA). For 10 µl of sample, 1 µl CutSmart buffer and 0.5 µl of restriction endonuclease was added to 100–200 ng plasmid DNA, and the mixture was incubated at 37 °C for 1.5–2 hours. The DNA fragments were analyzed by agarose gel electrophoresis.

### **2.6.9 DNA separation by agarose gel electrophoresis**

Using agarose gel electrophoresis, DNA fragments were separated according to their lengths. DNA samples were mixed with 6x loading dye (Thermo Fisher Scientific, Dreieich, Germany) as well as 4 µl of DNA Standard GeneRuler 1kb (Thermo Fisher Scientific, Dreieich, Germany) and loaded onto an agarose gel (1 % agarose [w/v] in 1x

TAE buffer, which contains 1 mM EDTA, 40 mM Tris, 20 mM acetic acid, pH 8, 0.05% ethidium bromide). The separation was carried out at 120 V in an electrophoresis chamber. DNA fragments were visualized under UV-transilluminator (Intas Science Imaging Instruments GmbH, Göttingen, Germany) at a wavelength of 254 nm.

## **2.7 DNA transfer into *T. kivui***

### **2.7.1 DNA transfer into naturally competent *T. kivui***

*T. kivui* can naturally take up DNA (Basen et al., 2018). For the transformation, Hungate tubes containing 5 ml of carbonate-buffered minimal media, 50  $\mu$ M uracil and 25 mM glucose was inoculated with a pre-culture to an initial OD<sub>600</sub> of 0.05. After addition of 1  $\mu$ g of plasmid DNA, the culture was incubated at 65 °C for 16-18 hours.

### **2.7.2 Plating of *T. kivui***

After the incubation period at 65 °C, the cultures were cooled down at room temperature. Carbonate-buffered minimal medium with 1.5 % Bacto™ agar (Becton, Dickison and Company, Le Pont de Claix, France) was melted at 121 °C for 2 min and kept in an incubator at 60 °C until plating. The cells were serially diluted with sterile 1x saline solution (50 mM Na<sub>2</sub>HPO<sub>4</sub> × 2 H<sub>2</sub>O, 50 mM NaH<sub>2</sub>PO<sub>4</sub> × 2 H<sub>2</sub>O, 1.2 mM K<sub>2</sub>HPO<sub>4</sub>, 4.7 mM NH<sub>4</sub>Cl, 1.7 mM (NH<sub>4</sub>)<sub>2</sub>SO<sub>4</sub>, 7.5 mM NaCl, 0.37 mM MgSO<sub>4</sub> × 7 H<sub>2</sub>O, 42  $\mu$ M CaCl<sub>2</sub> × 2 H<sub>2</sub>O, 7.2  $\mu$ M FeSO<sub>3</sub> × 7 H<sub>2</sub>O, 53.6 mM NaHCO<sub>3</sub>). Immediately before plating, cysteine (to a final concentration of 200  $\mu$ g/ml), uracil (50  $\mu$ M), and 5 mM 5-FOA (in second round of selection) was supplemented. Depending on the mutant preparation, then substrates glucose (25 mM) or glucose (25 mM) + formate (50 mM) were added in 25 ml serum bottles containing melted agar medium.

100–200  $\mu$ l of undiluted or diluted culture was added into petri dishes (Sarsted AG & Co., Nürnberg, Germany) and the agar medium containing substrates was poured on top, so



that the cells were embedded in the medium. The plating was done under an air atmosphere. Subsequently, these plates were transferred to an anoxic tent (Coy Laboratory Products, Grass Lake, USA) with an atmosphere of N<sub>2</sub>/CO<sub>2</sub> (80/20 [v/v]) containing 2% [v/v] hydrogen gas (H<sub>2</sub>). When the medium was solidified and completely anaerobic, the plates were placed in an anoxic jar (Fig. 7) containing 2 small palladium catalysts (Oxid, Hampshire, England) and 50 g CaCl<sub>2</sub>. The atmosphere in the anoxic jar was changed to N<sub>2</sub>/CO<sub>2</sub> (80/20 [v/v]). The plates were incubated in the jar at 65 °C for 4-6 days.



**Fig. 7.**  
incubation of *T. kivui*

Sealed metal jar for anaerobic

### 2.7.3 Genotype analysis

In order to search for colonies having the desired gene deletions, PCR was performed. For this purpose, single colonies were picked from agar plates and transferred to 5 ml medium in Hungate tubes containing the corresponding substrates and supplements. Cultures were then incubated at 65 °C for 24-72 hours. 1 ml of the grown cell culture was transferred to a 1.5 ml eppendorf (Sarsted AG & Co., Nürnberg, Germany) and cells were pelleted by centrifugation at 13,000 rpm for 2 minutes. The cell pellet was re-suspended in 50-80 µl of distilled water. 1-2 µl of resuspended cells was used as template for the PCR to analyze the respective genotype of the isolates in a PCR reaction. Primers were chosen to amplify the gene of interest or its deletion derivative.

## 2.8 Cell suspension experiments

### 2.8.1 Preparation of resting cells

For the preparation of cell suspensions, *T. kivui* was cultivated on a larger scale in 1 l serum bottles (Glasgerätebau Ochs, Bovenden / Lenglern) filled with 500 ml complex medium. The media were inoculated to an initial OD<sub>600</sub> of ~0.03 - 0.05 with pre-cultures grown on the same carbon source and under the same growing conditions. Depending on the experiment, cultivation occurred either in the presence of 25 mM glucose or 25 mM glucose + 50 mM formate with N<sub>2</sub> + CO<sub>2</sub> (80/20 [v/v]) or 25 mM glucose + 100% CO in the headspace. Cultivation was done at 65 °C. Cells were grown until mid-exponential growth phase to an OD<sub>600</sub> of ~1.5. All the further steps were performed under strictly oxygen-free conditions in an anoxic chamber (Coy Laboratory Products, Grass Lake, USA) filled with N<sub>2</sub>/CO<sub>2</sub> (80/20 [v/v]) or 95-98% N<sub>2</sub> plus 2-5% H<sub>2</sub> atmosphere. Cells were harvested by centrifugation (Avanti™ J-25, JA-10 Fixed-Angle Rotor; Beckman Coulter, Brea, CA, United States) at 8,500 rpm and 4 °C for 10 minutes. Supernatant was discarded, cells were transferred into JA-25.50 tubes and washed twice in imidazole buffer (50 mM imidazole, 20 mM MgSO<sub>4</sub>, 20 mM KCl, 20 mM NaCl, 4 mM DTE, 4 μM resazurin, pH 7.0).

Cells from 500 ml cultures were finally suspended in in 5-10 ml buffer and kept in 20 ml gas tight Hungate tubes. The protein concentration was typically within the range of 30 mg/ml. The tight sealed Hungate tubes were taken out of the chamber and then H<sub>2</sub> was removed by exchanging the headspace with N<sub>2</sub>/CO<sub>2</sub> (80/20 [v/v]) or to N<sub>2</sub> (100%).

### 2.8.2 Protein determination according to Schmidt (1963)

Protein determination in resting cells was performed according to (Schmidt et al., 1963). 5, 10 or 50 μl of the resting cells were taken and the final volume of 1 ml was made by addition of distilled H<sub>2</sub>O. A calibration curve was prepared with 0, 0.2, 0.4, 0.6, 0.8 and 1

mg BSA (Carl Roth GmbH, Karlsruhe) in 1 ml of distilled H<sub>2</sub>O. In order to reduce measurement inaccuracies, samples were measured in triplicates. 125 µl of solution A (4 M NaOH) were added to the mixtures and were then boiled for 10 min at 100 °C and cooled on ice. Then 400 µl of solution B (60 mM K-Na-tartrate, 0.25 M NaOH, 10 mM CuSO<sub>4</sub> × 5 H<sub>2</sub>O, 38 mM KI, stored at 4 °C, protected from light) were added. The samples were incubated for 30 min at 37 °C and then cell debris was removed by centrifugation (13,000 rpm, 5 min). The absorbance of the supernatant was measured at 546 nm using a spectrophotometer (Spectronic 200, Thermo Scientific, USA) in plastic cuvettes.

### 2.8.3 Cell suspension experiments

As substrate, glucose or glucose + formate was added to 60 ml serum bottles filled with the final suspension volume of 10 ml imidazole buffer (50 mM imidazole, 20 mM MgSO<sub>4</sub>, 20 mM KCl, 20 mM NaCl, 4 mM DTE, 4 µM resazurin, pH 7.0) in the presence of 50 mM KHCO<sub>3</sub>. Cells were added to a protein concentration of 1-2 mg/ml. Subsequently, the gas phase was changed to N<sub>2</sub>/CO<sub>2</sub> (80/20 [v/v]) and then incubated at 65 °C in a water bath under shaking conditions (150 rpm). After the pre-incubation for 10 minutes, the experiment was started. At different time period, 50 µl gas samples were injected into the gas chromatograph using 0.1 ml Gastight<sup>®</sup> syringe to determine H<sub>2</sub> and 0.5-0.8 ml of samples were taken regularly to measure concentrations of substrate and products.

In the case of H<sub>2</sub> + CO<sub>2</sub> (80/20 [v/v], 2 × 10<sup>5</sup> Pa) as a substrate, 120 ml serum bottles were used and the preparation was done using the same procedure as described above. After the serum bottles were pre-warmed, the experiment started by flushing with 100% H<sub>2</sub> + CO<sub>2</sub>.

## 2.9 Measurement of metabolites

### 2.9.1 Determination of acetate *via* gas chromatography

The concentration of acetate was determined by gas chromatography (Clarus 580 GC; PerkinElmer, Waltham, Massachusetts, USA). For sample preparation, cells were spun down by centrifugation at 13,000 rpm for 1 minute and 200  $\mu$ l of supernatant was mixed with 200  $\mu$ l water, 50  $\mu$ l of 2 M phosphoric acid, 50  $\mu$ l of 200 mM 1-propanol (as an internal standard) and 500  $\mu$ l of acetone in a 2 ml glass vials (PerkinElmer, Waltham, Massachusetts, USA). Vials were closed with an aluminium cap with a septum (Supleco, Bellefonte, Pennsylvania, USA). 0.5  $\mu$ l of the prepared sample was injected at 250 °C by an auto-sampler and separated on a Stabilwax<sup>®</sup>-DA-column (30 m  $\times$  0.25 mm; Restek Co., Bellefonte, Pennsylvania, USA). Helium was used as carrier gas with a flow rate of 20 cm/sec and a split of 20:1. The oven was kept at 60 °C for 3 minutes and then heated to 180 °C with a rate of 10 °C/min. Metabolites were detected in a flame ionization detector at 250 °C.

### 2.9.2 Determination of hydrogen gas *via* gas chromatography

The concentration of H<sub>2</sub> was measured by gas chromatography (Clarus 580 GC; PerkinElmer, Waltham, Massachusetts, USA) during the experiment. 50  $\mu$ l of gas phase was taken using 0.1 ml Gastight<sup>®</sup> syringe (Hamilton Co., Reno, Nevada, USA) and injected at 100 °C and separated on a ShinCarbon ST 80/100 column (2 m  $\times$  0.53 mm; Restek Co., Bellefonte, Pennsylvania, USA). N<sub>2</sub> was used as carrier gas with a head pressure of 400 kPa and a split flow of 30 ml/s. The oven was held at 40 °C and the samples were analyzed with a thermal conductivity detector at 100 °C. Concentrations are given as total amount in headspace per volume of liquid phase.

### 2.9.3 Determination of formate, glucose and mannitol *via* HPLC analysis

The concentrations of glucose and mannitol were measured by high performance liquid chromatography equipped with P680 HPLC Pump, ASI-100 Automated Sample Injector and Thermostatted Column Compartment TCC-100 (Dionex, Sunnyvale, California, USA). For the sample preparation, cells were spun down by centrifugation at 13,000 rpm for 5 minutes. 200  $\mu$ l of supernatant was passed through a filter (Millex<sup>®</sup>- LH) in 2 ml vials containing 400  $\mu$ l flat bottom glass insert (Agilent Technologies). A C<sub>18</sub>- based column (HyperREZ XP Carbohydrate H<sup>+</sup>; Thermo Fisher Scientific, Waltham, Massachusetts, USA) was used for separation. Degassed sulfuric acid (5 mM) was used as eluent at a flow rate of 0.6 ml/min. The oven was kept at 65 °C. 10  $\mu$ l of each sample was injected by auto-sampler and analyzed with a refractive index detector (RefractoMax 520; Dionex, Sunnyvale, California, USA) at 55 °C.

## 2.10 Measurement of enzyme activities

### 2.10.1 Preparation of cell free extract

For the preparation of cell-free extract, *T. kivui* were cultivated in 500 ml of complex medium with 25 mM glucose as carbon and energy source or in 200 ml of complex medium in the presence of 100% CO (2 × 10<sup>5</sup> Pa) with 1bar overpressure in 1 l serum bottles. Cells were harvested in the mid exponential growth phase by centrifugation (Avanti™ J-25 and JA-10 Fixed-Angle Rotor; Beckman Coulter, Brea, California, USA) at 8,500 rpm and 4 °C for 10 minutes. Subsequently, cells were washed three times with lysis buffer (50 mM Tris-HCl, 25 mM MgSO<sub>4</sub> × 7H<sub>2</sub>O, 2 mM DTE, 4  $\mu$ M resazurin, 20% glycerin, pH 7.5). Then, cells were spun down by centrifugation at 8,500 rpm and 4 °C for 10 minutes (JA-25.50 Fixed-Angle Rotor, Beckman Coulter, Brea, California, USA). After the last centrifugation step, the cells were resuspended in 3 ml lysis buffer with few crystals of DNaseI and 40  $\mu$ M phenylmethylsulfonyl fluoride (PMSF). The cells were disrupted in a French Pressure Cell Press (SLM AMINCO, SLM Instruments, Inc.,

Urbana, Illinois, USA) at a pressure of 110 MPa. Cell debris and whole cells were removed by centrifugation at  $14,300 \times g$  (Centrifuge 5417R; Eppendorf, Hamburg-Eppendorf, Germany) for 20 minutes at  $4^\circ\text{C}$ . The supernatant containing the cell-free extract was transferred into anoxic Hungate tubes and the gas phase was changed to  $\text{N}_2$  (100%).

### 2.10.2 Protein determination according to Bradford (1976)

Protein determination in cell-free extract was performed according to (Bradford, 1976). The samples to be examined were diluted appropriately so that they were within the standard calibration values (0, 2.5, 5, 7.5 and  $10 \mu\text{g}$  BSA). The final volume was made to  $200 \mu\text{l}$  by distilled water. Measurements were done in duplicates from the respective samples and for the calibration curve. Then  $1 \text{ ml}$  of Bradford solution ( $0.1 \text{ g/l}$  Serva Blue G250, 5% ethanol [v/v], 10% o-phosphoric acid [v/v], filtered twice, covered with aluminium foil, stored at  $4^\circ\text{C}$ ) was added to the mixture and incubated for 5 min at room temperature and then the absorbance was measured at  $595 \text{ nm}$  in plastic cuvettes using a spectrophotometer (Spectronic 200, Thermo Scientific, USA).

### 2.10.3 Measurement of CO-dehydrogenase activity

Measurement of CODH activity in the cell-free extracts of *T. kivui* was carried out in  $1.8 \text{ ml}$  anoxic cuvettes (Hellma HmbH & Co.KG, Mühlheim, Germany) sealed by rubber stoppers in 100%  $\text{CO}$  ( $2 \times 10^5 \text{ Pa}$ ) atmosphere containing overall liquid volume of  $1 \text{ ml}$ . The assay buffer contained  $50 \text{ mM}$  Tris-HCl,  $2 \text{ mM}$  DTE and  $4 \mu\text{M}$  resazurin at  $\text{pH } 7.5$ . Before the measurement, the cuvettes were incubated at  $60^\circ\text{C}$ .

The measurement was performed with a UV/Vis Spectrophotometer (SPECORD® S 600, Analytic Jena, Jena, Germany). Methylviologen (MV) was used as an electron acceptor. Reaction was started by addition of  $10 \mu\text{l}$  of a  $1 \text{ M}$  MV ( $10 \text{ mM}$ ) to the buffer using a precision syringe (Pressure-Lok®; VICI precision sampling, Baton Rouge, Louisiana, USA). Reduction of MV was monitored at  $604 \text{ nm}$  ( $\epsilon=13.8 \text{ mM}^{-1}\cdot\text{cm}^{-1}$ ).

#### 2.10.4 Measurement of methylene-THF dehydrogenase activity

The measurement of methylene THF-dehydrogenase activity was conducted in the cell free extract of *T. kivui* in 1.8 ml anoxic cuvettes (Hellma HmbH & Co.KG, Mühlheim, Germany), sealed by rubber stoppers at 60°C. The assay buffer used was 50 mM MOPS, 10 mM NaCl, 20 mM MgSO<sub>4</sub>, 4 µM resazurin, 2 mM DTE at pH 7.0. Methylene-THF was used as an electron donor, which was synthesized non-enzymatically with 0.5 mM THF in DMSO and 1.5 mM formaldehyde. The reaction will lead to the formation of a racemic mixture and resulting in of 0.25 mM active methylene-THF. The reaction was started by the addition of 1 mM NAD<sup>+</sup> or 1 mM NADP<sup>+</sup>. Activity of MTHF-DH was measured by following reduction of 1 mM NADP<sup>+</sup> at 340 nm ( $\epsilon=6.22 \text{ mM}^{-1}\cdot\text{cm}^{-1}$ ).

#### 2.11 Chemicals and Gases

The chemicals used were purchased from Merck KGaA (Darmstadt, Germany), Applichem GmbH (Darmstadt, Germany), Carl Roth GmbH & Co. KG (Karlsruhe, Germany), SERVA Electrophoresis GmbH (Heidelberg, Germany) and Sigma-Aldrich Chemie GmbH (Steinheim, Germany). The gases were supplied by Praxair Deutschland GmbH (Düsseldorf, Germany).



## 3. Results

### 3.1 Physiology of *T. kivui*

*T. kivui* was isolated from Lake Kivu in Africa. To elucidate the genetics and metabolism of this thermophilic acetogenic bacterium, the autotrophic and heterotrophic growth on various substrates were examined. In the original publication, studies have revealed that *T. kivui* grows on mannose, glucose, fructose, pyruvate, formate and H<sub>2</sub> + CO<sub>2</sub> (Leigh et al., 1981; Klemps et al., 1987; Daniel et al., 1990; Voneysmond et al., 1990; Yang and Drake, 1990; Lupas et al., 1994; Hess et al., 2014; Freude and Blaser, 2016). Recently, growth of *T. kivui* on mannitol and CO as a sole carbon source has been observed (Moon et al., 2019; Weghoff and Müller, 2016). Previous studies had concluded the inability of *T. kivui* to grow on maltose and trehalose (Leigh et al., 1981).

#### 3.1.1 Growth studies

First, experiments were conducted to study growth of *T. kivui* with different carbon and energy sources in carbonate-buffered complex media. The substrates used were glucose, pyruvate, maltose and trehalose. For the experiment, pre-cultures were grown on the same carbon source. When *T. kivui* was transferred to complex media in the presence of 25 mM glucose, the growth rate obtained was 0.53 h<sup>-1</sup>, corresponding to a doubling time of 1.3 hours (Fig. 8A). The maximum OD<sub>600</sub> obtained was 2.8. Growth on 100 mM pyruvate, proceeded with lower growth rate of 0.13 h<sup>-1</sup> with the doubling time of 5 hours (maximum OD<sub>600</sub>= 1) (Fig. 8B).

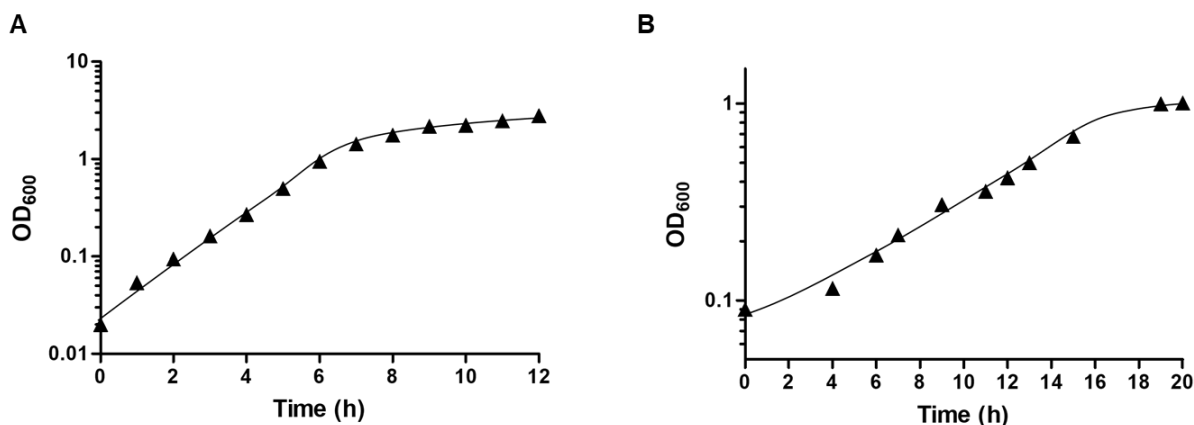


**Fig. 8. Growth of *T. kivui* in carbonate-buffered complex medium.** Cultures were grown in bicarbonate containing complex media at 65°C on (A) 25 mM glucose or (B) 100 mM pyruvate. Shown is one representative experiment out of three independent replicates.

Next, growth of *T. kivui* was investigated in carbonate-buffered minimal media. For genetic studies, minimal media without uracil was used for the selection of uracil prototrophs. When the organism was cultivated on 25 mM glucose in bicarbonate-buffered minimal media, the maximum optical density obtained was 2.0. The growth rate and doubling time was 0.4 h<sup>-1</sup> and 1.7 hours (Fig. 9).

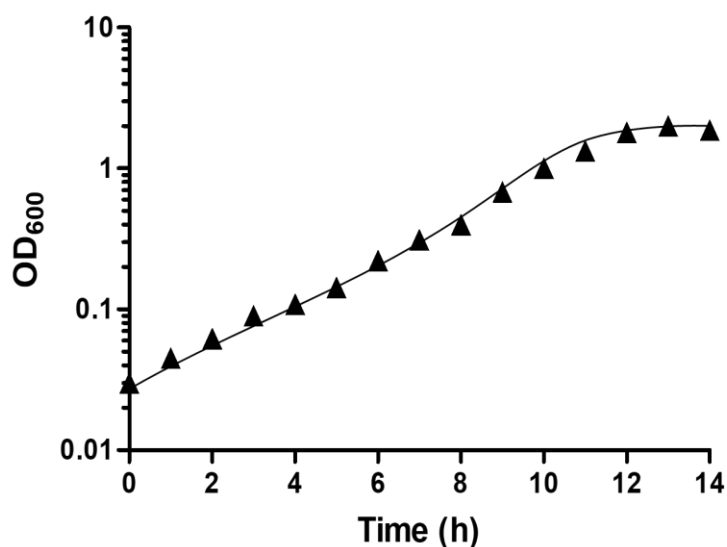


**Fig. 9. Growth of *T. kivui* in carbonate-buffered minimal medium.** Cultures were grown in bicarbonate containing minimal media at 65°C on 25 mM glucose. Shown is one representative experiment out of three independent replicates.

### 3.1.2 Adaptation to growth on maltose and trehalose

After transfer of a glucose-adapted preculture to fresh medium containing 25 mM maltose or 25 mM trehalose, no growth was obtained. Interestingly, when the same preculture were transferred to a media containing higher concentration of maltose or trehalose (50 mM), the cells grew after a long lag phase to final OD<sub>600</sub> of 1.8 and 0.75, respectively (Fig. 10).

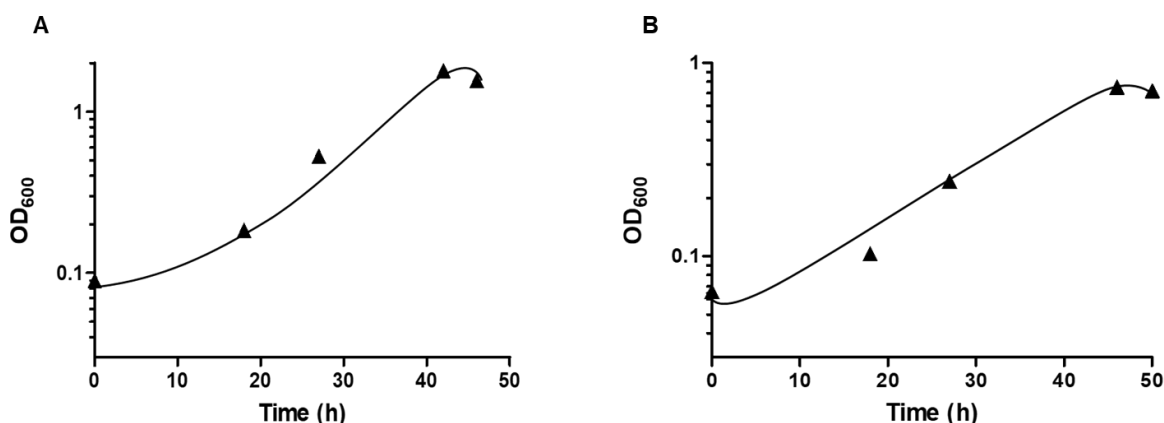


**Fig. 10. Adaptation of *T. kivui* to growth on maltose or trehalose in carbonate-buffered complex medium.** Cultures were transferred to bicarbonate-containing complex media at 65°C on (A) 50 mM maltose (B) 50 mM trehalose. Pre-cultures were grown on 25 mM glucose.

Next, the adapted cultures were used as precultures for subsequent inoculation of media containing 25 mM of maltose or trehalose. As depicted in Fig. 11A, growth on 25 mM maltose was observed without a lag phase with the rate of 0.3 h<sup>-1</sup> (doubling time = 2.3 h). The maximum OD<sub>600</sub> observed was 1.12. With 25 mM trehalose the growth rate decreased to 0.25 h<sup>-1</sup> (doubling time = 2.7 hours). The maximum OD<sub>600</sub> obtained was 0.73 after 11 hours (Fig. 11B).

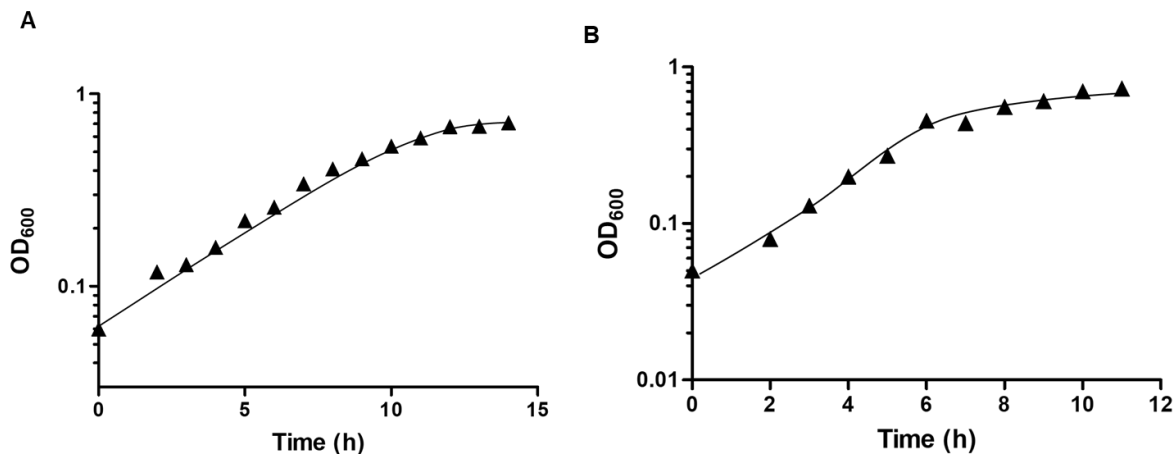


**Fig. 11. Growth of *T. kivui* on maltose and trehalose in carbonate-buffered complex medium.** Cultures were grown in bicarbonate-containing complex media at 65°C on (A) 25 mM maltose (B) 25 mM trehalose. Pre-cultures were grown on 50 mM maltose or 50 mM trehalose. Shown is one representative experiment out of three independent replicates.

### 3.1.3 Growth of *T. kivui* on mannitol with and without formate in carbonate free medium

Growth of acetogens even on sugars is CO<sub>2</sub>-dependent (Drake et al., 2006; Schuchmann and Müller, 2016), this was also true for acetogenesis from mannitol by *T. kivui* (Moon et al., 2020). Formate can offer a substitute for CO<sub>2</sub> (Jain et al., 2020) and therefore, I tested whether growth of *T. kivui* on mannitol in the absence of CO<sub>2</sub>/bicarbonate is stimulated by formate. As can be seen in Fig. 12, growth of *T. kivui* in the absence of CO<sub>2</sub> or bicarbonate was slow. In the presence of formate, the growth rate was 0.26 h<sup>-1</sup> and the final yield was increased (OD<sub>600</sub> = 2.5). Growth on formate alone was also possible, but to much smaller ODs. During growth on mannitol plus formate, at the end of the experiment 19.7 ± 0.8 mM of mannitol and 40.3 ± 2.0 mM formate were consumed and 66.0 ± 15.5 mM of acetate was produced, indicating that formate was converted to acetate. This experiment demonstrated that CO<sub>2</sub>/bicarbonate can be replaced by formate.

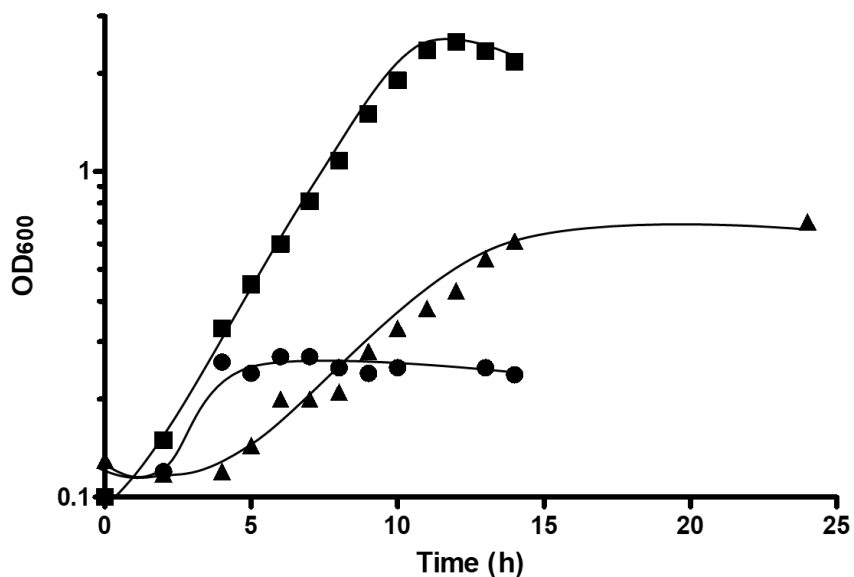


**Fig. 12. Growth of *T. kivui* on mannitol with and without formate in carbonate-free minimal medium.** Cultivation of *T. kivui* on 25 mM mannitol in carbonate-free minimal media with 50 mM formate (■) and without formate (▲) at 65°C. Growth on 50 mM formate (●) only is shown as a control. Growth was determined by measuring the optical density at 600 nm. Two biological duplicates were analyzed and one representative growth curve is depicted.

### 3.1.4 Autotrophic growth of *T. kivui*

Growth on H<sub>2</sub> + CO<sub>2</sub> (80/20 [v/v]) at  $2 \times 10^5$  Pa was re-investigated according to Leigh et al., (1981). Growth on H<sub>2</sub> + CO<sub>2</sub> proceeded with the growth rate of 0.13 h<sup>-1</sup> corresponding to a doubling time of 5.3 hours. The final OD<sub>600</sub> reached up to 0.7 (Fig. 13).

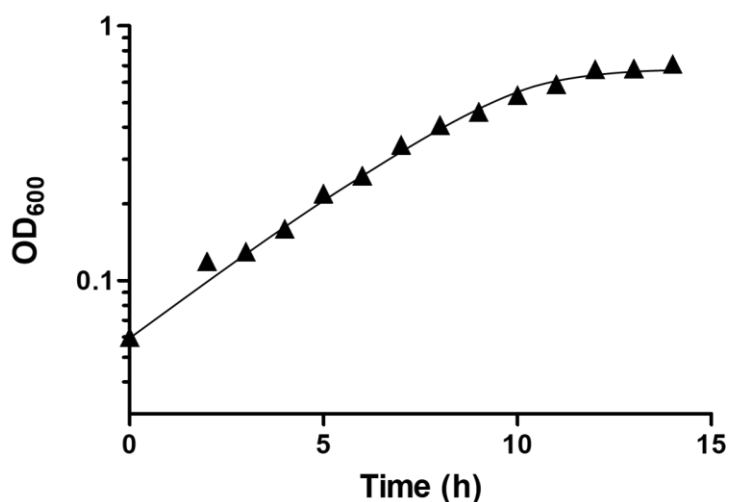


**Fig. 13. Growth of *T. kivui* on H<sub>2</sub> + CO<sub>2</sub> in complex medium.** *T. kivui* was grown in bicarbonate containing complex media at 65°C on H<sub>2</sub> + CO<sub>2</sub> (80/20 [v/v]) at  $2 \times 10^5$  Pa. Growth was examined by measuring the optical density at 600 nm. Three biological duplicates were analyzed and one representative growth curve is depicted.

Since the highest growth rates were observed with glucose in complex medium, *T. kivui* was routinely grown on glucose.

## 3.2 Generation and characterization of a $\Delta hdcr$ mutant of *T. kivui*

### 3.2.1 Deletion of the *hdcr* gene cluster

The hydrogen-dependent carbon dioxide reductase (HDCR) catalyzes the first step of the methyl branch in the Wood-Ljungdahl pathway and utilizes H<sub>2</sub> for the reduction of CO<sub>2</sub> to formate (Schuchmann and Müller, 2013). The *hdcr* gene cluster comprises of the genes *fdhF* (TKV\_c19990), *hycB3* (TKV\_c19980), *hycB4* (TKV\_c19970), *hydA2* (TKV\_c19960) and *fdhD* (TKV\_c19950). FdhF codes for formate dehydrogenase, HydA2 for the hydrogenase subunits and HycB3-HycB4 are two small electron-transferring subunits (Schwarz et al., 2018). The function of FdhD is unknown.

FdhF1, HycB2, FdhD, HycB3, and HydA2 of *A. woodii* has 45%, 41%, 33%, 50% and 66% identity to the corresponding subunits of *T. kivui*. The genes encoding a selenocysteine containing formate dehydrogenase and its corresponding small electron transferred subunits are missing in *T. kivui* (Fig. 14).

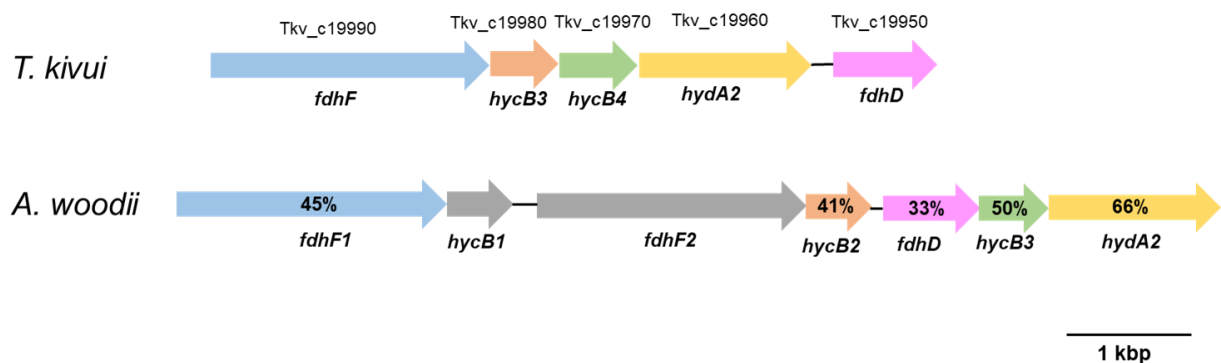


**Fig. 14. Genetic organization of HDCR subunits in *T. kivui* and *A. woodii*.** Shown is the percentage identity of amino acid sequence to the respective gene in *T. kivui*. The identity determination was carried out by BlastP based on NCBI database.

To delete the genes from *fdhF* to *hydA2* (further referred as *hdcr*), plasmid pMBTkv012 was kindly provided by Nils Peiter. pMBTkv012 contains 999 bp upstream flanking region (UFR) (position: 1927301 - 1928300, see appendix 7.1.1) and 899 bp downstream flanking region (DFR) (position: 1921520 - 1922419, see appendix 7.1.2) of the *hdcr* gene cluster. For the generation of pMBTKV012, the backbone plasmid pMBTkv005 was used, which has an *E. coli* origin of replication, an ampicillin resistance cassette and the *pyrE* gene encoding the orotate phosphoribosyltransferase as selectable marker for introducing into the  $\Delta pyrE$  uracil-auxotrophic strain TKV\_002 (Basen et al., 2018). The deletion strategy carried out is described below (Fig. 15).

The transformants can only grow in minimal media if the plasmid was integrated in chromosome. Uracil prototrophs were selected in the first round. In the second round of selection, loss of the plasmid was forced by plating with the anti-metabolite 5-FOA (5 mM) on minimal media with uracil (50  $\mu$ M). Initially, by using glucose as sole substrate, the isolation of mutants after screening >50 colonies failed, and the genotype was reverted to the wild type. Next approach was used to add formate (50 mM) in the presence of

glucose (25 mM) during the selection procedure, since formate is produced by HDCR in the first step of methyl branch of WLP.

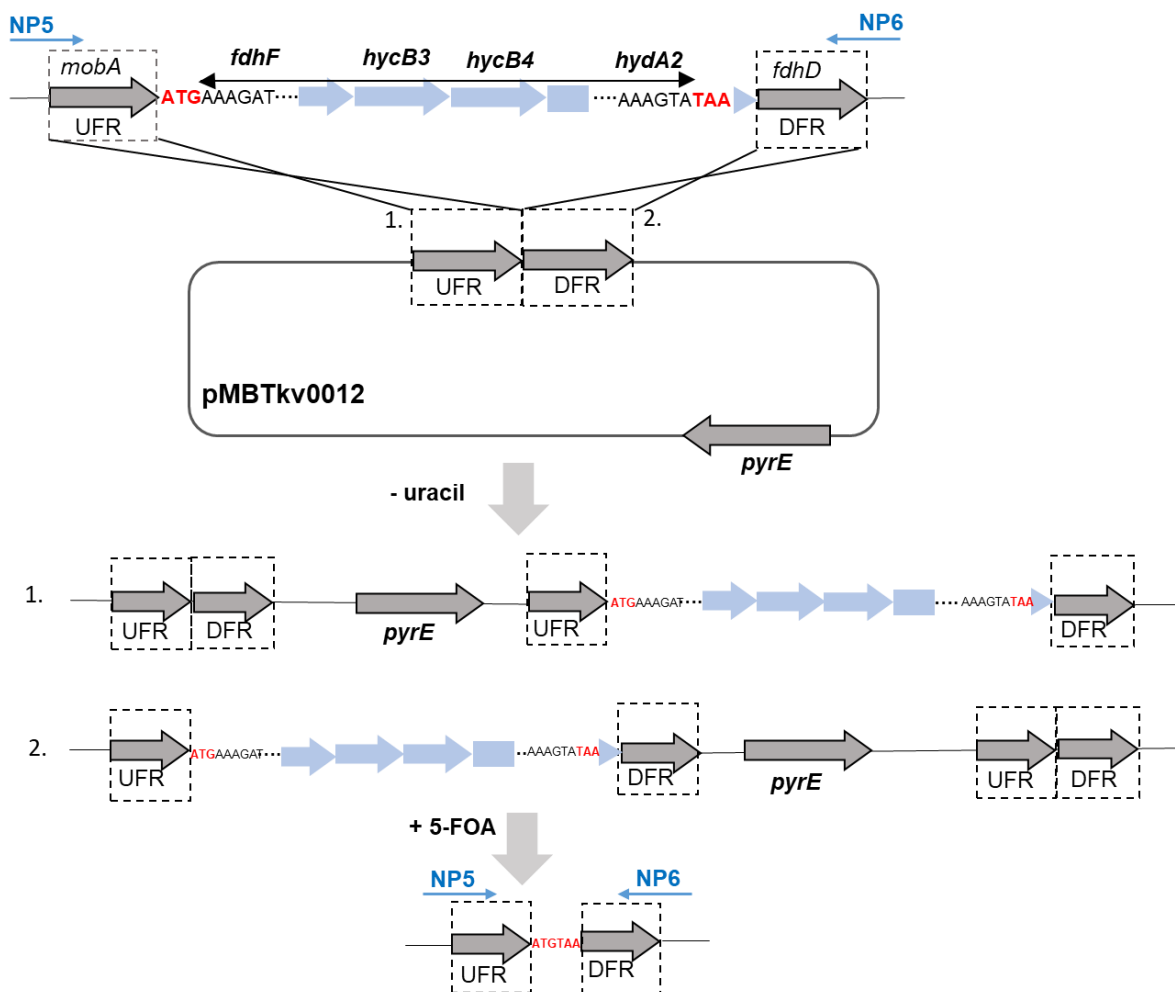


**Fig. 15. Scheme for the deletion of *hdcr* using plasmid pMBTk0012.** *T. kivui* was transformed with the plasmid (pMBTk0012) that contains a selection marker (*pyrE*), and the upstream flanking region (UFR) and downstream flanking region (DFR) of the *hdcr* gene cluster. *hdcr* gene deletion starts after 3 base pairs of UFR and ends before 3 base pairs of DFR. In the absence of uracil, isolates were selected which had integrated the plasmid in first round of selection by simple homologous recombination at the UFR or DFR region. After subsequent counter-selection with 5-FOA, the plasmid was disintegrated from the genome and two genotypes were obtained either  $\Delta pyrE$  mutant or  $\Delta pyrE$  mutant with the deletion of *hdcr* genes where, 4800 base pairs were deleted. *mobA*; gene of a putative molybdenum cofactor guanylyltransferase, *fdhD*; function unknown. Blue arrows marked are the primer binding sites of the oligonucleotides used for the detection of genotype with *hdcr* deletion.

After incubation of plates at 65 °C for 4-5 days, 6 colonies were obtained which out of 5 showed the genotype of the “clean” *hdcr* deletion. Genotype analysis was carried out by PCR with the primers NP5 and NP6, binding outside the *hdcr* gene in the *T. kivui* genome (Fig. 16A). The *hdcr* gene cluster of 4800 base pairs were deleted, therefore, PCR of



$\Delta hdcr$  isolates revealed the expected fragment size of 1.9 kb as seen in isolates 1 to 5 whereas the wild type had the fragment size of ~6.8 kb (Fig. 16B).

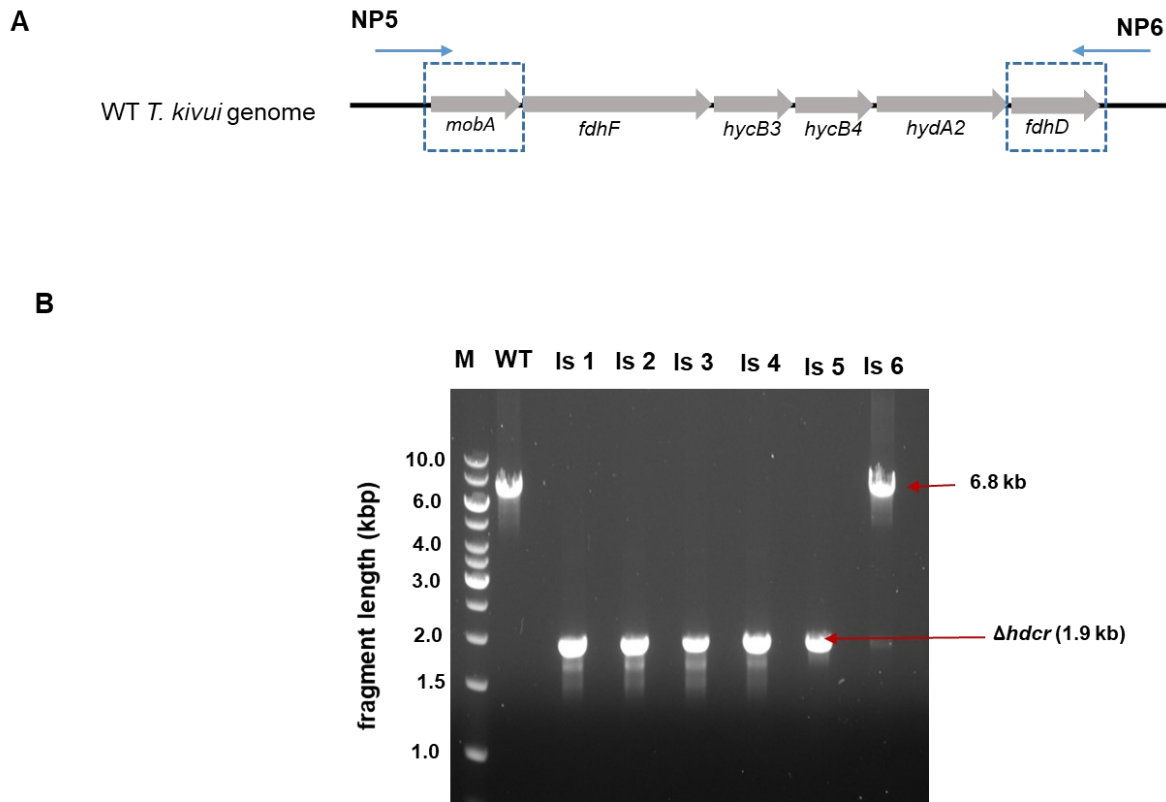


**Fig. 16. Genotypic analysis of *hdcr* deletion in *T. kivui*.** The loss of *hdcr* (4806 bp) was verified *via* PCR. A) Binding sites of the oligonucleotides NP5 & NP6, used for the detection of genotype with *hdcr* deletion. They bind outside the HDCR gene cluster in the genome. Expected sizes of PCR products, WT; 6856 bp,  $\Delta hdcr$ ; 1949 bp B) DNA fragments amplified from the isolates were analyzed on a 1.0 % agarose gel showing PCR products of *T. kivui*  $\Delta hdcr$  isolates (Is 1-5) and the wild type, WT (Is 6). Is, isolates; M, Gene Ruler 1 kb DNA ladder (Thermo Fisher Scientific).

Further, to confirm clean *hdcr* gene deletion, isolates 3, 4 and 5 were additionally verified by PCR with the primers NP1 & SJ3, P9fw & NP7 and PBseq10 & P18b rev, binding inside the *hdcr* gene at different locations (Fig. 17A). No DNA fragment in the isolates 3-5 was observed but the wild type showed the band of respective size (Fig. 17B-D). This verified the genes deleted from *fdhF* to *hydA2*. A single isolate was further verified by Sanger sequencing and named as *T. kivui* strain TKV\_MB013 and used for further studies.

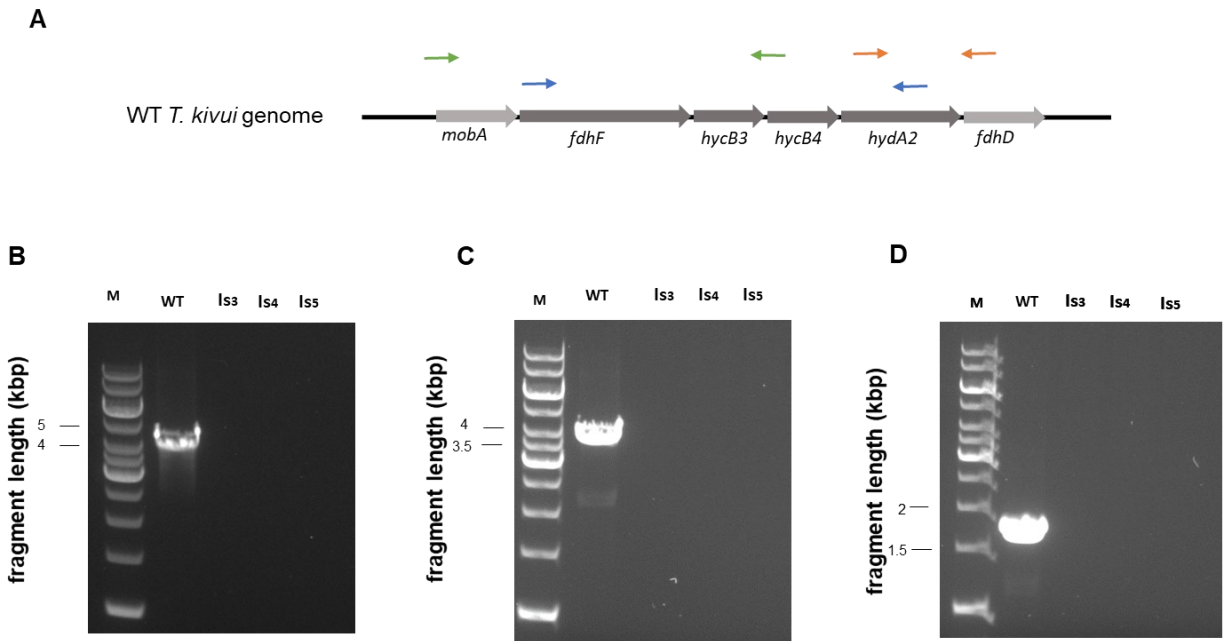


**Fig. 17. Verification of the deletion mutant *via* PCR with primers binding inside the *hdcr* genes.** A) Binding sites of the oligonucleotides in the *hdcr* gene cluster of *T. kivui*, NP1 & SJ3 (green); P9fw & NP7 (blue); PBseq10 & P18b rev (orange). Agarose gel verification with the primers NP1 and SJ3 (B), P9fw & NP7 (C) and PBseq10 & P18b rev (D). Is, Isolates (3-5); WT, wild type; M, GeneRuler 1 kb DNA Ladder (Thermo Fisher Scientific).

### 3.2.2 Complementation of *T. kivui* $\Delta$ *hdcr* strain *in cis*

For complementation of  $\Delta$ *hdcr* mutant, plasmid pSJ002 was prepared (Fig. 18). The genes (TKV\_c19960-TKV\_c19990) coding for *hdcr* gene cluster (*fdhF*, *hycB3*, *hycB4* and *hydA2*) were inserted between the convergent genes TKV\_c24500, encoding for general secretion pathway protein A (*exeA*) and TKV\_c24520, encoding for hydroxylamine reductase (*Hcp*). The *hdcr* genes were not inserted at its original locus to avoid any polar effects. Since the area in the genome between the genes TKV\_c24500 and TKV\_c24520 contains no ORFs and insertion of genes into that region is presumably did not have any effect on neighboring genes. The plasmid contains *hdcr* genes under the control of the S-layer protein promoter from *T. kivui*, followed by *pyrE* under the regulation of the gyrase promoter from *Thermoanaerobacter* sp. strain X514. Besides, the plasmid possesses an ampicillin and a kanamycin resistance cassette for the selection in *E. coli*. To construct

pSJ002, the backbone was amplified from pJM006 with the primers SJ0012 and SJ0013, and *hdcR* was amplified from *T. kivui* wild type genomic DNA with the primers SJ0010 and SJ0011. The amplified fragments were assembled by Gibson Assembly.

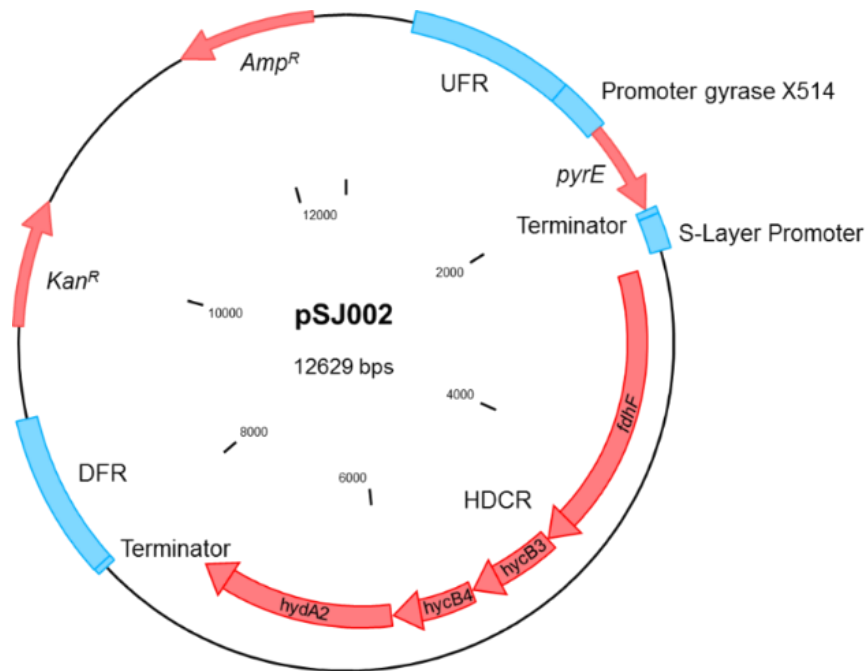


**Fig. 18. Physical map of plasmid pSJ002.** The plasmid was used for complementation of *hdcR* gene cluster back into the  $\Delta hdcR$  mutant strain. The plasmid contains the upstream flanking region (DFR) and downstream flanking region (DFR) of the genome region between *Tkv\_c24500* and *Tkv\_24520*; between UFR and DFR is *pyrE* (*Tkv\_c14380*), under regulation of gyrase promoter from *Thermoanaerobacter* sp. strain X514; *hdcR* gene under regulation of S-layer protein promoter from *T. kivui*; *amp<sup>R</sup>* & *kan<sup>R</sup>*, ampicillin and kanamycin resistance cassettes for selection in *E. coli*.

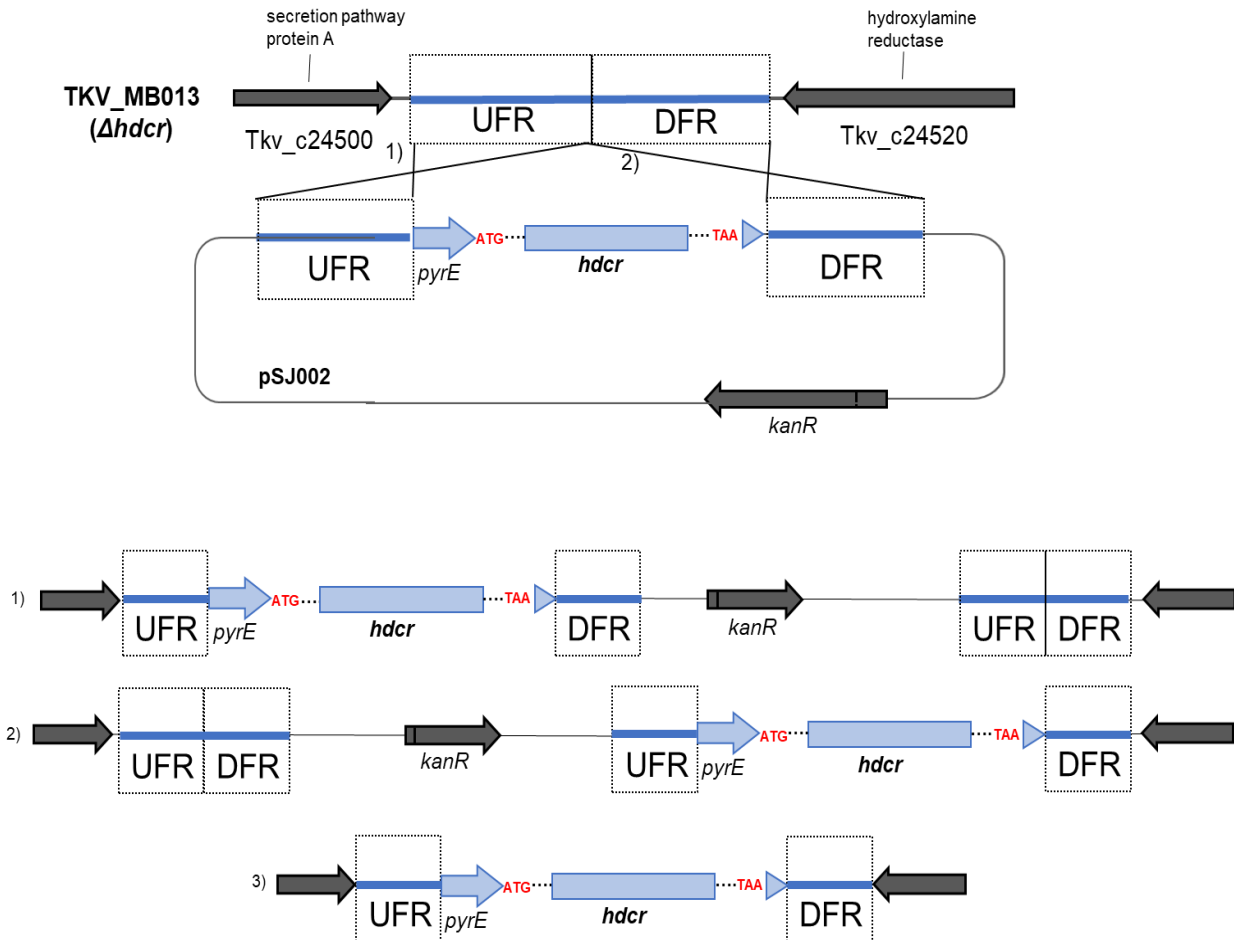


**Fig. 19. Scheme for the integration of HDCR gene cluster in *T. kivui*  $\Delta hdcr$  genome.** *T. kivui* was transformed with the plasmid pSJ002 that contains a selection marker (*kanR*), and the upstream flanking region (UFR) and downstream flanking region (DFR). The selection for isolates, which integrated parts of pSJ008 through single- (1 and 2) or double (3) homologous recombination in chromosome, was carried out in minimal medium without uracil.

The gene integration was carried out through homologous recombination as shown in the scheme (Fig. 19). Plasmid pSJ002 was transformed with *T. kivui*  $\Delta hdcr$  in minimal without uracil. The resulted strain is named as TKV\_MB019. The complementation of *hdcr* gene cluster was verified with the growth restoration ability on  $H_2 + CO_2$  or glucose, described in the next section.

### 3.2.3 Growth studies with *T. kivui* $\Delta hdcR$

To analyze the phenotype of the *hdcR* mutant, growth experiments with different substrates were performed. Therefore, pre-cultures were grown on glucose (25 mM) + formate (50 mM) in complex medium in Hungate tubes. The different substrates used and their final OD<sub>600</sub> are summarized in Tab. 10. In addition to wild type *T. kivui* strain, the complemented *hdcR* strain (TKV\_MB019) were used as control. As expected, the *hdcR* mutant did not grow on formate (300 mM), whereas the wild type grew well and reached an OD<sub>600</sub> of  $0.22 \pm 0.017$ . Next, the inability of  $\Delta hdcR$  strain to grow autotrophically with H<sub>2</sub> + CO<sub>2</sub> was also confirmed, since HDCR is an essential enzyme to catalyze the CO<sub>2</sub> reduction to formate. In contrast, the wild type grew to an OD<sub>600</sub> of  $0.57 \pm 0.02$ .

**Tab. 10. Optical density of *hdcR* deletion mutant on different carbon sources in Hungate tubes.** Using following substrates maximum OD<sub>600</sub> were measured from stationary phase cultures of *T. kivui*  $\Delta hdcR$  strain. Controls used were wild type *T. kivui* and *T. kivui*  $\Delta hdcR$  complemented strain.

Substrates	<i>T. kivui</i> wild type	<i>T. kivui</i> $\Delta hdcR$	<i>T. kivui</i> $\Delta hdcR$ complemented
	OD <sub>600</sub> *	OD <sub>600</sub> *	OD <sub>600</sub> *
25 mM glucose	$2.64 \pm 0.11$	$0.2 \pm 0.017$	$2.4 \pm 0.09$
25 mM glucose + 50 mM formate	$2.86 \pm 0.14$	$3.3 \pm 0.1$	$2.34 \pm 0.20$
H <sub>2</sub> + CO <sub>2</sub> (1 bar)	$0.57 \pm 0.02$	$0.02 \pm 0.002$	$0.48 \pm 0.004$
H <sub>2</sub> + CO <sub>2</sub> (1 bar) + 50 mM formate	$0.8 \pm 0.02$	$0.49 \pm 0.01$	$0.39 \pm 0.02$
25 mM mannitol	$2.46 \pm 0$	$0.02 \pm 0.01$	$1.08 \pm 0.02$
25 mM mannitol + 50 mM formate	$2.45 \pm 0$	$1.99 \pm 0.3$	$2.4 \pm 0.01$
300 mM formate	$0.22 \pm 0.017$	$0.01 \pm 0$	$0.16 \pm 0.02$
50 mM pyruvate	$0.15 \pm 0.01$	$0.03 \pm 0$	$0.15 \pm 0.0007$

OD<sub>600</sub>\* denotes optical density at 600 nm.

Interestingly, heterotrophic growth on sugars was also dependent on HDCR. When cells were cultivated in 120 ml serum bottles in the presence of 25 mM glucose as a substrate, the *T. kivui*  $\Delta h d c r$  mutant grew only to a  $OD_{600}$  of 0.22, while the wild type and the *h d c r* complemented strain grew till 2.8 and 2.9, respectively (Fig. 20A), however, growth was restored in the  $\Delta h d c r$  mutant by the addition of 50 mM formate. A maximum  $OD_{600}$  of 3.2 was reached (Fig. 20B).

Growth of the *T. kivui*  $\Delta h d c r$  mutant on  $H_2 + CO_2$  (80/20 [v/v],  $2 \times 10^5$  Pa) was not observed, as expected. In contrast, the wild type and *h d c r* complemented strain grew to a final  $OD_{600}$  of 0.8 and 0.67, respectively (Fig. 20C). Again, addition of formate restored the growth in  $\Delta h d c r$  mutant and the final  $OD_{600}$  observed was 0.65 (Fig. 20D). This is in line with the hypothesis that formate served as a terminal electron acceptor and restored the growth deficiency.

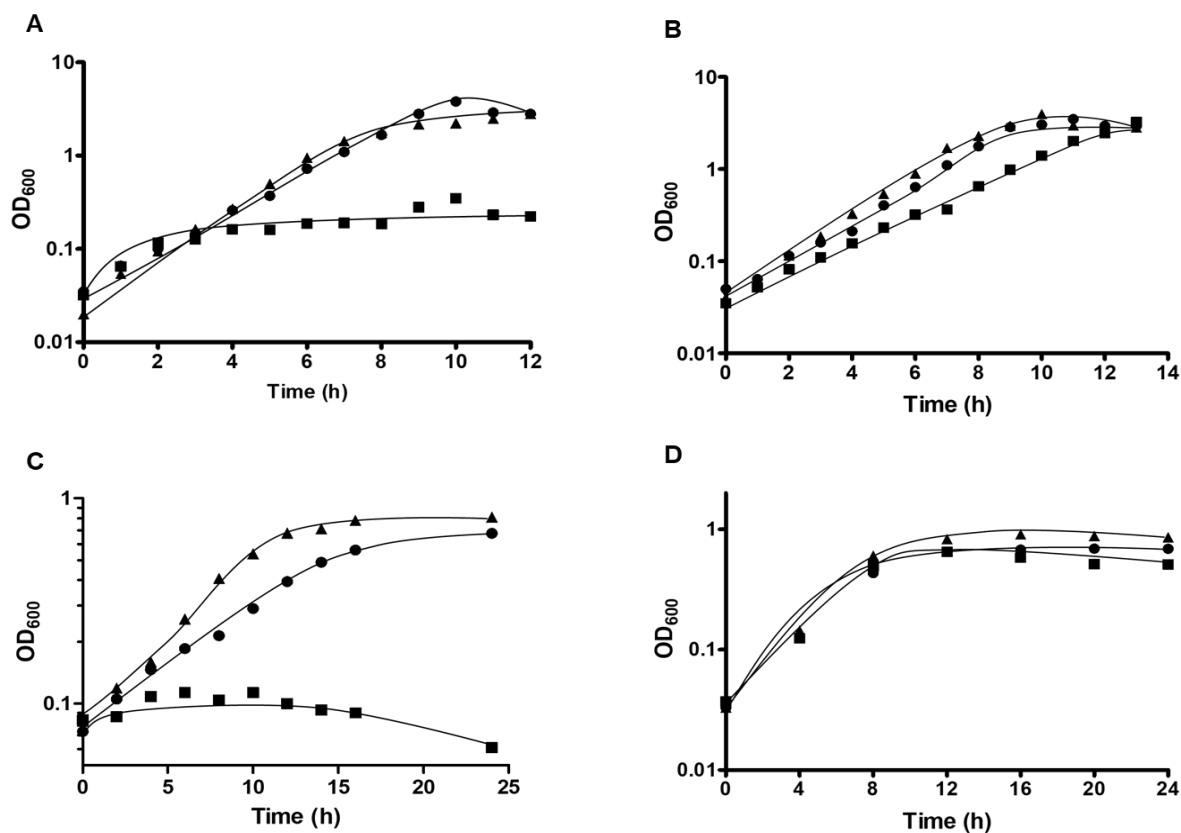


**Fig. 20. Growth of *T. kivui* wild type,  $\Delta hdcR$  mutant (TKV\_MB013) and *hdcR* complemented strain (TKV\_MB019).** Cells were grown in complex media at 65°C in 120 ml serum bottles on (A) 25 mM glucose, (B) 25 mM glucose + 50 mM formate, (C) H<sub>2</sub> + CO<sub>2</sub> (80/20 [v/v], 2 × 10<sup>5</sup> Pa) or (D) H<sub>2</sub> + CO<sub>2</sub> (80/20 [v/v], 2 × 10<sup>5</sup> Pa) + 50 mM formate. TKV\_MB013 (■), TKV\_MB019 (●) and wild type (▲). Growth was measured by following the optical density at 600 nm. Shown growth curve is one representative experiment out of three independent replicates.

### 3.2.4 Cell suspension experiments with *T. kivui* $\Delta hdcR$

Cell suspension experiments were performed in order to investigate the substrate consumption and product formation in non-growing cells of *T. kivui*  $\Delta hdcR$  strain. For these experiments, 500 ml of cultures in late exponential growth phase grown on 25 mM glucose + 50 mM formate were harvested and resting cells were prepared as described in materials and methods. Cells were added to a protein concentration of 1 mg/ml. After the cells were incubated at 65 °C for 10 mins in a pre-warmed water bath, the experiment was started by addition of 25 mM glucose + 50 mM formate or 25 mM glucose only.

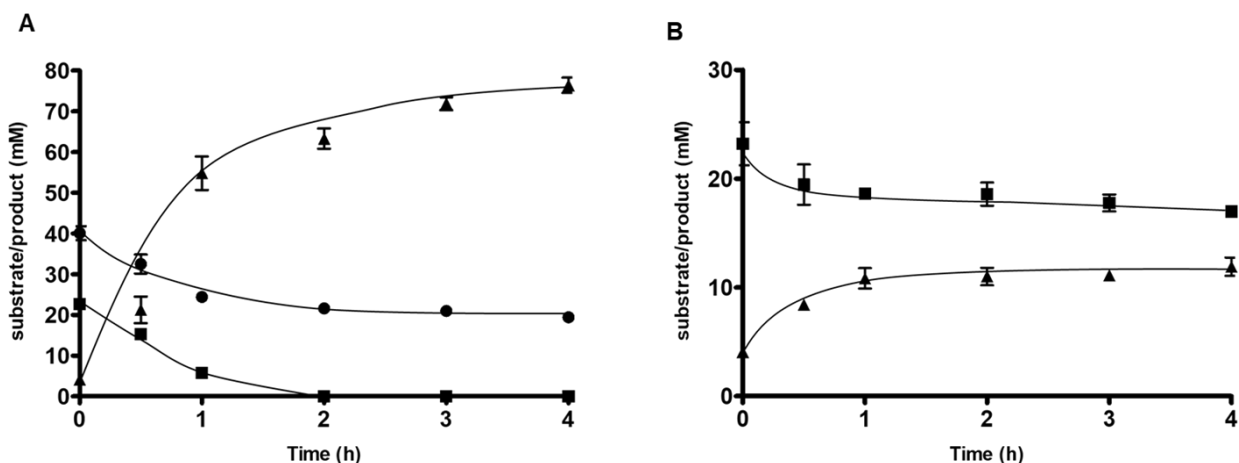


**Fig. 21. Acetate production and substrate consumption from resting cells of  $\Delta hdcr$  mutant.** Cells were grown on 25 mM glucose + 50 mM formate to the mid exponential phase and then harvested. The cells were washed and resuspended in minimal media according to a protein concentration of 1 mg/ml. The resting cells were incubated with (A) 25 mM glucose + 50 mM formate or (B) 25 mM glucose only, as substrates in pre-warmed water bath at 65 °C. 0.8 ml of samples were collected for the determination of glucose (■), acetate (▲) and formate (●) over the time. The concentrations of glucose and formate were determined by high performance liquid chromatography. Acetate concentrations was determined using gas chromatography. The experiments were carried out in biological triplicates.

After addition of glucose + formate,  $22.7 \pm 1.9$  mM glucose was completely consumed, while the formate concentration decreased from  $40.1 \pm 2.9$  to  $19 \pm 0.8$  mM, at the same time  $76.4 \pm 3.2$  mM acetate was produced (Fig. 21A). The amount of  $H_2$  detected was very low (0.3 mM). The ratio of acetate/glucose reached was  $3.0 \pm 0.3$ . In contrast with glucose only, substrate was consumed very little.  $23.2 \pm 3.4$  mM was converted to only  $11.9 \pm 1.45$  mM acetate (Fig. 21B).

The carbon and electron recoveries from cell suspension experiment were calculated. Carbon recovery from glucose + formate to acetate was stoichiometrically  $1.03 \pm 0.017$  (n=3), assuming that one  $CO_2$  was consumed for each formate consumed. The electron recovery was  $0.96 \pm 0.03$  (n=3), based on the oxidation of glucose and the reduction of formate and  $CO_2$  to acetate.



### 3.3 Generation and characterization of a monofunctional CODH (*cooS*) deletion mutant of *T. kivui*

#### 3.3.1 Identification and organization of genes involved in CO metabolism

For the identification of genes involved in CO metabolism, the genome sequence of *T. kivui* was searched for potential CO dehydrogenase genes. Two putative genes were identified, one encoding a potential monofunctional CODH annotated as *cooS* (Tkv\_c08080) (Hess et al., 2014). The downstream region of *cooS* is flanked by the gene *cooF<sub>1</sub>* (Tkv\_c08090), potentially encoding for protein known to be involved in CO metabolism for transferring electrons to a membrane-bound hydrogenase (Fox et al., 1996a; Schoelmerich and Müller, 2020) (Fig. 22). Upstream of *cooS* is a gene encoding a hypothetical protein with unknown function.

Additionally, the genome of *T. kivui* contains another putative CODH gene annotated as *acsA* (TKV\_c20100) that together with the gene *acsB* (TKV\_c19820), encoding the acetyl-CoA synthase, forms the CODH/ACS complex. The gene *acsA* is flanked by a second copy of *cooF* (*cooF<sub>2</sub>*) (TKV\_c20110), responsible for transferring electrons to membrane bound hydrogenase and *cooC<sub>2</sub>* (TKV\_c20090), a gene encoding potentially for nickel insertion. All three genes are transcribed in the same direction (Fig. 22).

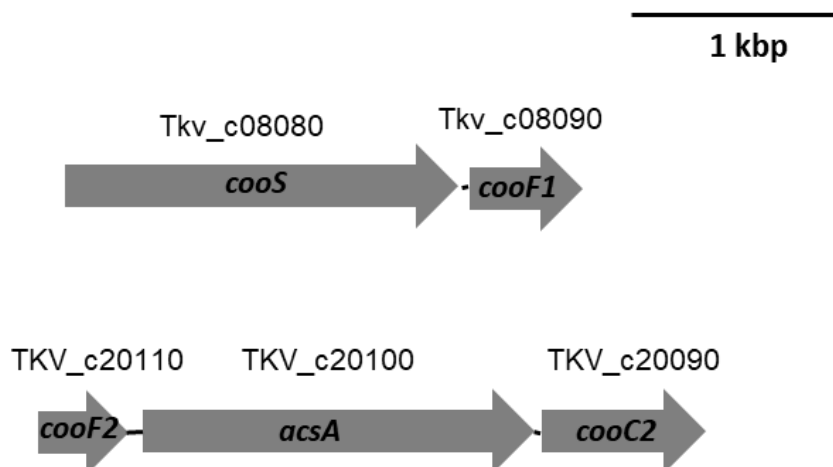


**Fig. 22. Genetic organization of CO dehydrogenase genes in *T. kivui*.** Two putative CODH genes found in the *T. kivui* genome: gene encoding for potential monofunctional CODH *cooS*, along with the adjacent gene *cooF<sub>1</sub>* and second CODH *acsA*, organized with *cooF<sub>2</sub>* and *cooC<sub>2</sub>*.

Previous studies on western blot analysis revealed the higher content of the monofunctional CODH, *CooS* in CO-grown cells (Weghoff and Müller, 2016). *CooS* is predicted to have a molecular mass of 68 kDa and contains a 4Fe-4S cluster and a Ni-4Fe-4S center where the oxidation of carbon monoxide occurs (Ragsdale and Kumar, 1996). The amino acid sequence of *CooS* and *CooF1* share 52 and 28% identity to respective genes of *A. woodii*. Despite this similarity, *A. woodii* does not grow on CO as a sole carbon and energy source (Bertsch and Müller, 2015). *Clostridium autoethanogenum*, a mesophilic acetogenic bacterium grows on CO as a sole carbon source and produces acetate, ethanol, 2,3-butanediol, and lactate (Liew et al., 2016a). *CooS* and *CooF* of *C. autoethanogenum* are 54 and 33% identical to that of *T. kivui*. The thermophilic anaerobic bacterium, *Carboxydotherrmus hydrogenoformans*, contains 5 CODH genes (Wu et al., 2005). *T. kivui* shares 35 and 38% identity to *CooS1* and adjacent *CooF*. In *Rhodospirillum rubrum* CODH complex is proposed as a site for transferring electrons to a membrane-bound hydrogenase (Fox et al., 1996b). *CooS* and *CooF* share 33 and 38% identity to that of *T. kivui*.

### 3.3.2 Deletion of *cooS* gene in *T. kivui*

To understand the molecular basis for the adaptation of *T. kivui* to grow on CO, we aimed to delete the *cooS* (Tk<sub>v</sub>\_c08080) gene from *T. kivui*. For deletion of *cooS*, plasmid pSJ006 was designed containing 1000 bp upstream (position: 773838 – 774838, see appendix 7.2.1) and 1000 bp downstream (position: 776721 - 777721, see appendix 7.2.2) of the *cooS* gene (Fig. 23). The backbone of pSJ006 was amplified from pMB\_TKV012 (Jain et al., 2020) containing an ampicillin resistance cassette and the *pyrE* gene which served as a selectable marker for introducing into the *T. kivui*  $\Delta pyrE$  (Basen et al., 2018). The backbone was amplified with the primers  $\Delta cooS\_BB\_FP$  &  $\Delta cooS\_BB\_RP$ . UFR and DFR was amplified from genomic DNA of *T. kivui* with the primers  $\Delta cooS\_UFR\_FP$  &  $\Delta cooS\_UFR\_RP$  and  $\Delta cooS\_DFR\_FP$  &  $\Delta cooS\_DFR\_RP$ . The amplified fragments were assembled by Gibson Assembly.

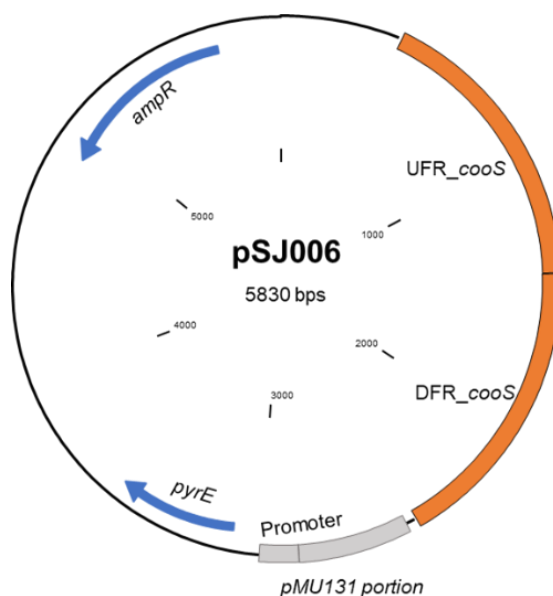


**Fig. 23. Physical map of plasmid pSJ006.** The plasmid was used for the deletion of the *cooS* (Tk<sub>v</sub>\_c08080) gene from *T. kivui* genome. The plasmid contains the upstream flanking region (DFR) and downstream flanking region (DFR) of *cooS*; *pyrE* (Tk<sub>v</sub>\_c14380), as a selection marker; *amp<sup>R</sup>*, ampicillin resistance cassette.

*T. kivui*  $\Delta pyrE$  was transformed with the plasmid pSJ006. *cooS* deletion was carried out through homologous recombination as described in Fig. 24. The plasmid contains *pyrE* gene as a selection marker, therefore, transformants can only grow in minimal medium if

the *pyrE* gene from pSJ006 was integrated. Subsequently, these transformants were subjected to second round of selection for the loss of the plasmid. It was forced by plating with the anti-metabolite 5-FOA (5 mM) on minimal media with uracil (50  $\mu$ M).

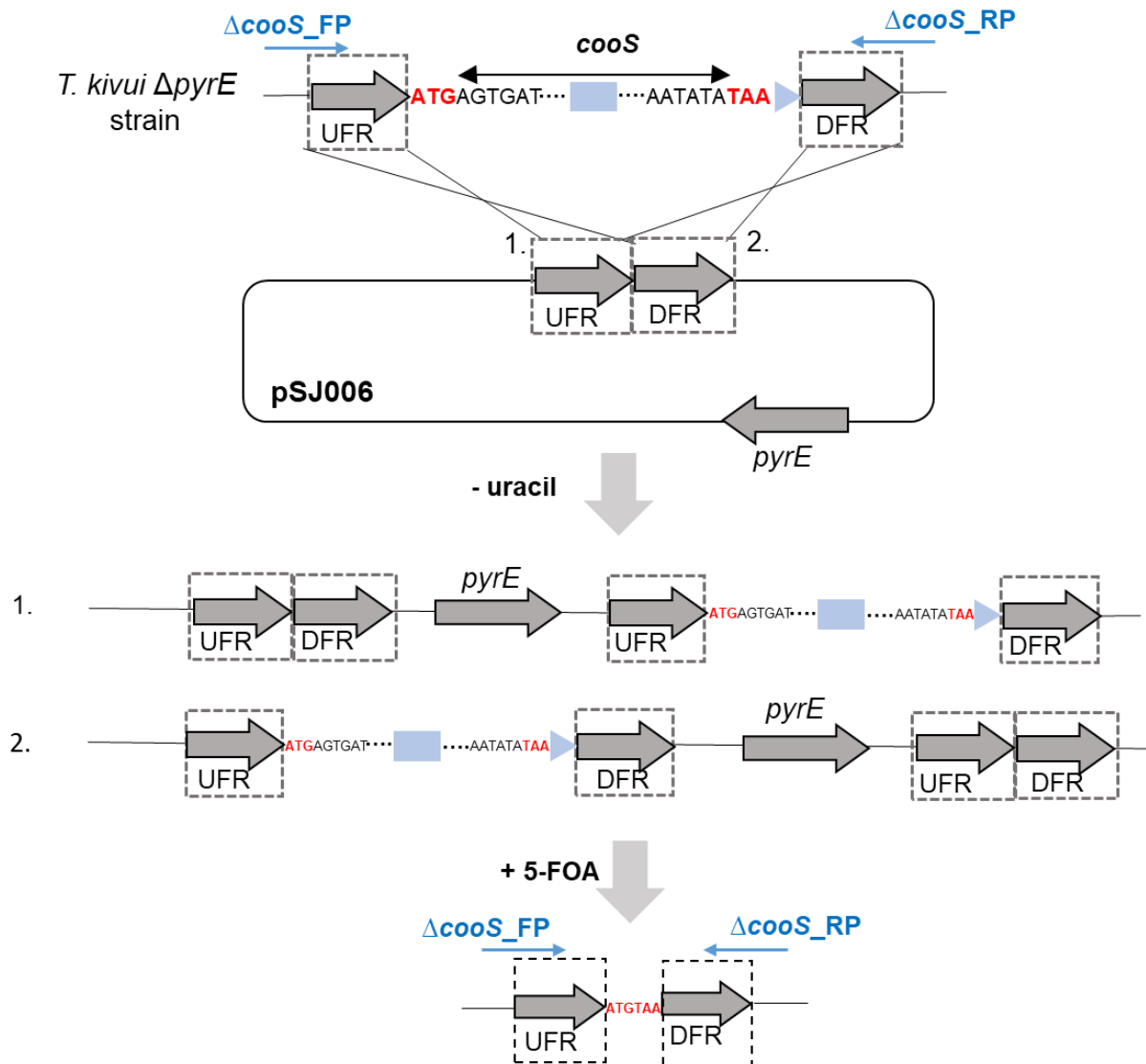


**Fig. 24. Scheme for deletion of *cooS* using plasmid pSJ006.** *T. kivui* was transformed with the plasmid (pSJ006) that contains a selection marker (*pyrE*), and the upstream flanking region (UFR) and downstream flanking region (DFR) of *cooS* gene. *cooS* gene deletion starts after 3 base pairs of UFR and ends before 3 base pairs of DFR. In the absence of uracil, isolates were selected which had integrated the plasmid in first round of selection by simple homologous recombination at the UFR or DFR region. After subsequent counter-selection with 5-FOA, the plasmid was disintegrated from the genome and the genotype obtained was  $\Delta pyrE$  mutant with the deletion of *cooS* genes, where 1,884 base pairs were deleted. Blue arrows marked are the primer binding sites of the oligonucleotides used for the detection of genotype with *cooS* deletion.

After the second round of selection colonies were obtained which was verified by PCR using primers  $\Delta cooS\_FP$  &  $\Delta cooS\_RP$  binding outside the *cooS* gene in the genome (Fig. 25A). The *cooS* gene of 1,884 base pairs were deleted, therefore, PCR of  $\Delta cooS$  isolates revealed the expected fragment size of 2 kb as seen in isolates 1 to 3 whereas the wild type had the fragment size of 3.9 kb (Fig. 25B).

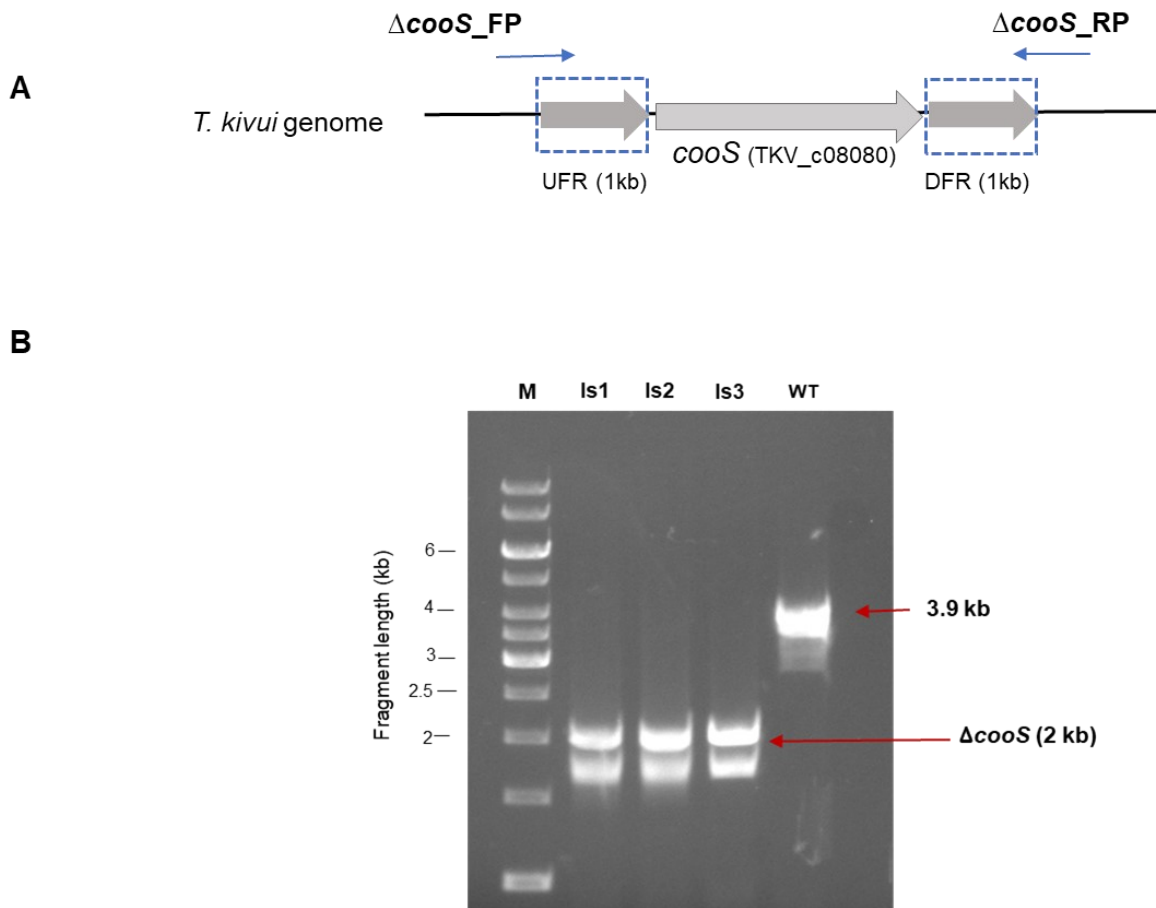


**Fig. 25. Genotypic analysis of *cooS* deletion in *T. kivui*.** The loss of *cooS* (1884 bp) was verified via PCR. A) Binding sites of the oligonucleotides  $\Delta cooS\_FP$  &  $\Delta cooS\_RP$ , used for the detection of genotype with *cooS* deletion. They bind outside the *cooS* gene in the genome. Expected sizes of PCR products, WT; 3884 bp,  $\Delta cooS$ ; 2000 bp B) DNA fragments amplified from the isolates were analyzed on a 1.0 % agarose gel showing PCR products of *T. kivui*  $\Delta cooS$  isolates (Is 1-3) and the wild type, WT. Is, isolates; M, Gene Ruler 1 kb DNA ladder (Thermo Fisher Scientific).

After verifying the genotype of the *T. kivui cooS* deletion mutant, the phenotype was examined. Growth experiments were conducted with CO as a sole carbon and energy

source. The control used for this study was  $\Delta pyrE$  (TKV\_MB002), the parental strain. As expected, the *T. kivui*  $\Delta cooS$  strain did not grow on CO. Nevertheless, it is important to note here that control strain, TKV\_MB002 also did not grow. This is expected since cells have to be sequentially adapted to grow on CO. Using the same procedure as described in Weghoff and Müller, (2016), we failed to adapt the strain on CO. This could have been due to the inability of  $\Delta cooS$  to grow on CO or due to the failure of adaptation of the cells to the toxic gas. To answer that, a different approach had to be used by deleting the *cooS* gene in a CO-adapted strain. Thus, *pyrE* was deleted first. The *pyrE* deletion mutant was prepared using the old plasmid pMBTkV002b (Basen et al., 2018). The plasmid was kindly prepared by Dr. Mirko Basen. The deletion strategy used was same as described in Basen et al., (2018) for deleting *pyrE*, but in the CO-adapted wild type *T. kivui*. In order to simplify the mutant preparation on solid media, we made sure that the CO-adapted strain would start to grow on CO immediately when cultivated on glucose in between.

After incubation at 65 °C for 4–5 days, few colonies were obtained that were resistant to 5-FOA and showed the genotype of deletion of *pyrE* (573 bp) which was confirmed by PCR with the primers MB\_IG\_0005 & MB\_IG\_0006 binding outside the *pyrE* gene in the *T. kivui* genome (Fig. 26A). PCR of the  $\Delta pyrE$  isolates revealed the expected fragment size of 2 kb as seen in isolates 1 to 3 whereas the wild type had the fragment size of 2.6 kb (Fig. 26B).

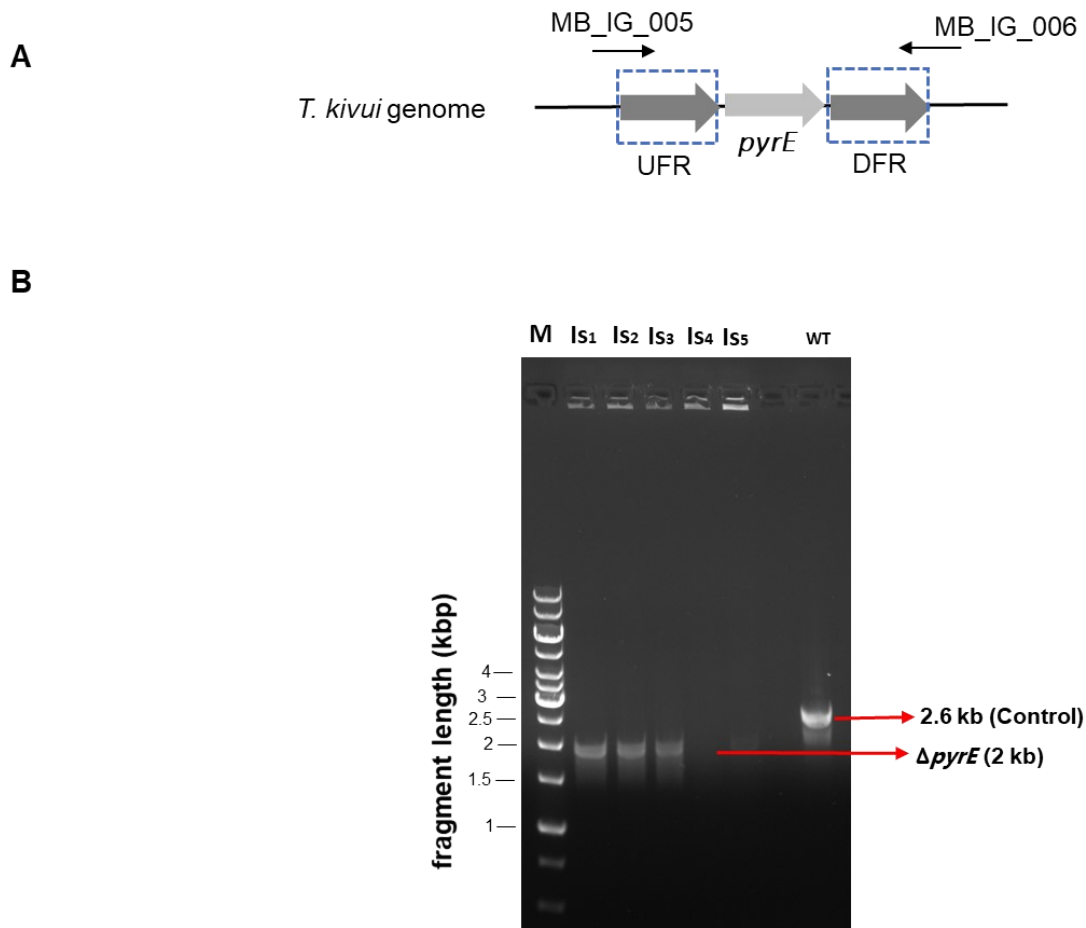


**Fig. 26. Genotypic analysis of *pyrE* deletion in CO-adapted *T. kivui*.** The loss of *pyrE* (573 bp) was verified *via* PCR. A) Binding sites of the oligonucleotides MB\_IG\_005 & MB\_IG\_006 used for the detection of genotype with *pyrE* deletion. They bind outside the *pyrE* gene in the genome. Expected sizes of PCR products, WT; 2573 bp,  $\Delta pyrE$ ; 2000 bp B) DNA fragments amplified from the isolates were analyzed on a 1.0 % agarose gel showing PCR products of *T. kivui*  $\Delta cooS$  isolates (Is 1-3) and the wild type, WT. Is, isolates; M, Gene Ruler 1 kb DNA ladder (Thermo Fisher Scientific).

The next step was to delete *cooS* from newly developed  $\Delta pyrE$  mutant. Again, the same strategy was used as described above (Fig. 24) but here, “CO adapted  $\Delta pyrE$ ” strain was transformed with the plasmid pSJ006. pSJ006 was integrated *via* homologous recombination at the UFR and DFR site. Transformants containing the *pyrE* gene were selected after growing in minimal media without uracil. After 2<sup>nd</sup> round of selection with 5-FOA, genotypic analysis was carried out using PCR with the primers  $\Delta cooS\_FP$  &  $\Delta cooS\_RP$  as shown in Fig. 25A. Substrate used for the preparation of mutant was 25 mM glucose.

The *cooS* gene of 1,884 base pairs were deleted again and PCR of  $\Delta cooS$  isolates revealed the expected fragment size of 2 kb as seen in isolates 1 to 3 whereas the wild type had the fragment size of 3.9 kb (Fig. 27A). Isolate 1 was also verified by internal primers binding inside the *cooS* gene, where no band was expected (Fig. 27B). Isolate 1 was further verified by DNA sequencing.

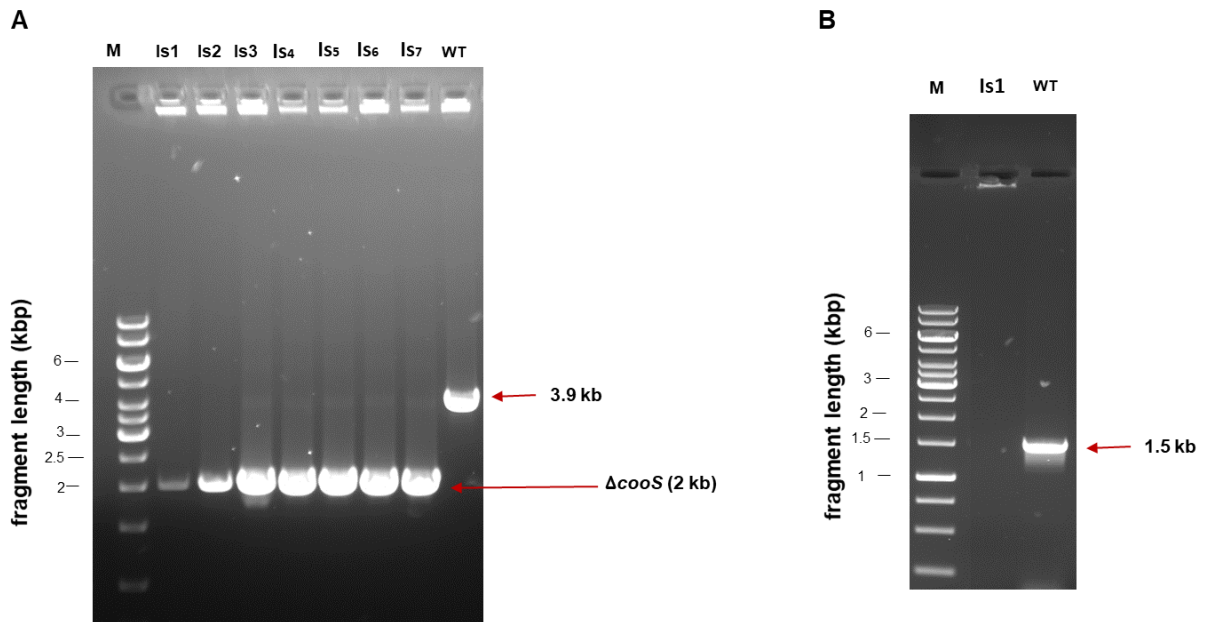


**Fig. 27. Genotypic analysis of *cooS* deletion in CO-adapted  $\Delta pyrE$ .** A) DNA fragments amplified from the isolates with *cooS* deletion (2 kb) and wild type (3.9 kb) using primers  $\Delta cooS\_FP$  &  $\Delta cooS\_RP$  which bind outside the *cooS* region in the genome. (B) Verification of  $\Delta cooS$  strain using primers *cooS* int\_ FP & RP, binding inside the *cooS* gene. Expected sizes of PCR products, WT; 1.5 kb,  $\Delta cooS$ ; no DNA fragment. Is, isolates; WT, *T. kivui*  $\Delta pyrE$ ; M, Gene Ruler 1 kb DNA ladder (Thermo Fisher Scientific).

### 3.3.3 Complementation of the *cooS* deletion mutant

For the reintegration of *cooS* gene back into the genome of the  $\Delta cooS$  mutant strain, plasmid pSJ008 was prepared (Fig. 28). The *cooS* gene (TKV\_c08080) was inserted between the convergent genes TKV\_c24500, encoding for general secretion pathway protein A (*exeA*) and TKV\_c24520, encoding for hydroxylamine reductase (*Hcp*). The *cooS* gene was not inserted at its original locus to avoid any polar effects. The area in the genome between the genes TKV\_c24500 and TKV\_c24520 contains no ORFs and



insertion of genes into that region is presumably not having any effect on neighboring genes. The plasmid contains the *cooS* gene under the control of the S-layer protein promoter from *T. kivui*, followed by *pyrE* under the regulation of the gyrase promoter from *Thermoanaerobacter* sp. strain X514. The plasmid has an ampicillin and a kanamycin resistance cassette for the selection in *E. coli*. To construct pSJ008, the backbone was amplified from pJM006 with the primers *cooS* BB compl. \_FP & *cooS* BB compl. \_RP, and *cooS* was amplified from the genomic DNA of wild type *T. kivui* with the primers *cooS* compl.\_FP & *cooS* compl.\_RP. The amplified fragments were assembled by Gibson Assembly.

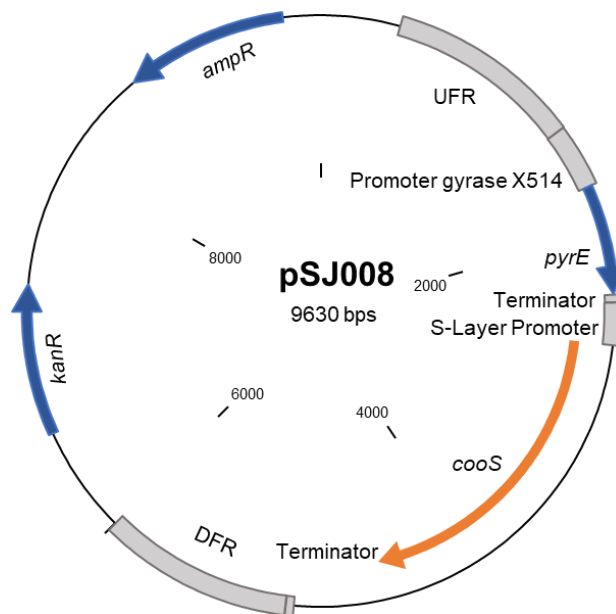


**Fig. 28. Physical map of plasmid pSJ008.** The plasmid was used for complementation of *cooS* gene back into the  $\Delta cooS$  mutant strain. The plasmid contains the upstream flanking region (UFR) and downstream flanking region (DFR) of the genome region between *Tkv\_c24500* and *Tkv\_24520*; between UFR and DFR is *pyrE* (*Tkv\_c14380*), under regulation of gyrase promoter from *Thermoanaerobacter* sp. strain X514; *cooS* gene under regulation of S-layer protein promoter from *T. kivui*; *amp<sup>R</sup>* & *kan<sup>R</sup>*, ampicillin and kanamycin resistance cassettes for selection in *E. coli*.

The gene integration was carried out through homologous recombination as shown in the scheme (Fig. 29). pSJ008 was transformed into the *T. kivui*  $\Delta cooS$ . This resulted into the *T. kivui* *cooS* complemented strain.

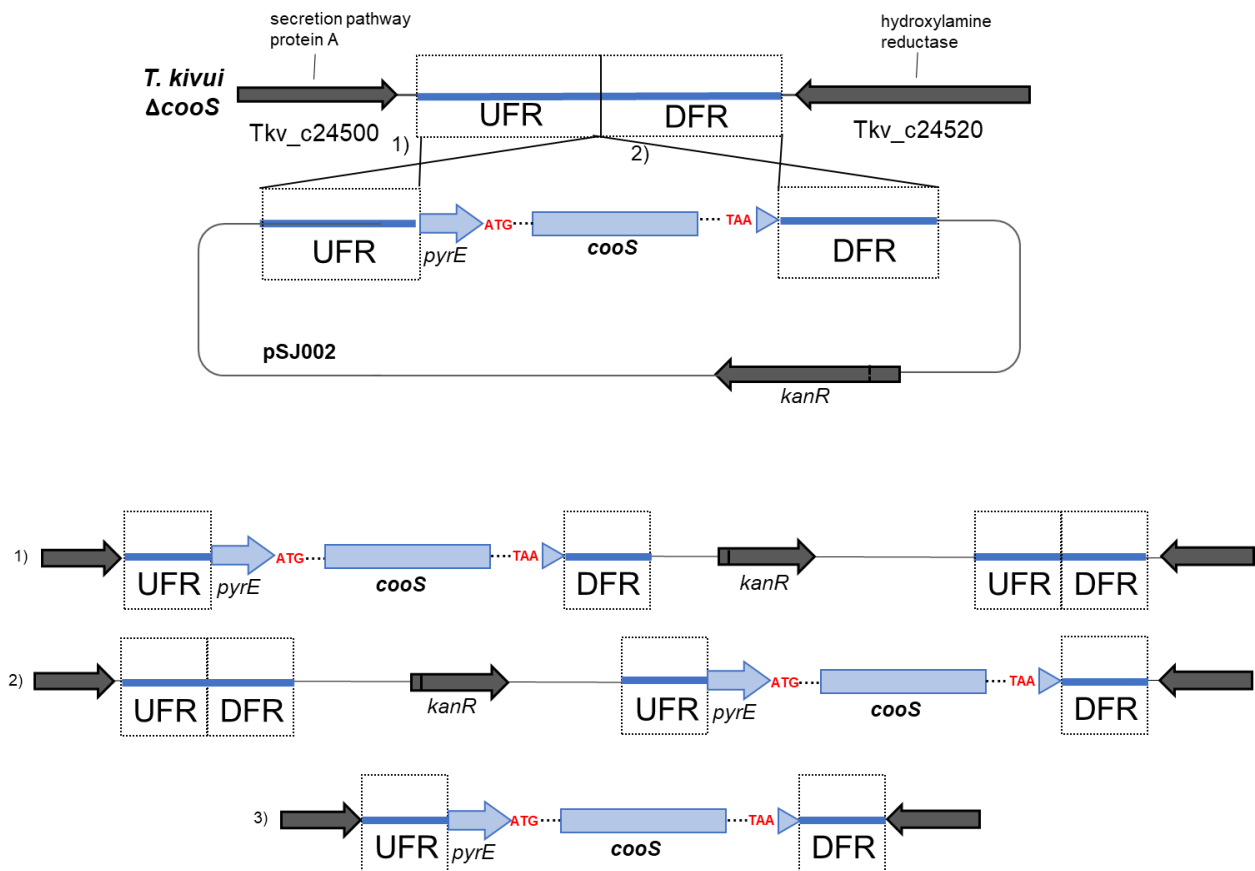


**Fig. 29. Scheme for the integration of *cooS* gene in *T. kivui*  $\Delta cooS$  genome.** *T. kivui* was transformed with the plasmid pSJ008 that contains a selection marker (*kanR*) and an upstream flanking region (UFR) and downstream flanking region (DFR). The selection for isolates, which integrated parts of pSJ008 through single- (1 and 2) or double (3) homologous recombination in chromosome, was carried out in minimal medium without uracil.

### 3.3.4 The *cooS* mutant does not grow on CO

Next, the growth phenotype of the *cooS* mutant was studied. Depending on the experiment, pre-cultures grown on glucose in complex or minimal medium were used to inoculate 120 ml serum bottles containing 20 ml of respective medium under a 100% CO atmosphere ( $2 \times 10^5$  Pa) to an initial OD<sub>600</sub> of 0.05. The control strain,  $\Delta pyrE$  (CO) grew to a maximal OD<sub>600</sub> of 0.6 after 5 days with a rate of 0.012 (h<sup>-1</sup>) whereas the *cooS* mutant did not grow in the same time frame (Fig. 30A). Notably, growth of the  $\Delta cooS$  mutant was

observed after 7 days, with a rate of  $0.0081 \text{ (h}^{-1}\text{)}$  to a final  $\text{OD}_{600}$  of 0.28. When the *cooS* gene was integrated back into the  $\Delta\text{cooS}$  genome, cells grew on CO with rates and final yields like the  $\Delta\text{pyrE (CO)}$ . To verify that cells actually grew on CO, growth in mineral medium was examined. After the first transfer, when the cells were transferred from glucose-mineral medium to CO-mineral medium, slow growth was again observed after 15 days, with a final OD of 0.2. But after a second transfer, growth was no longer observed, indicating that the  $\Delta\text{cooS}$  mutant did not grow on CO but on a component of the complex media. On the other hand, when the  $\Delta\text{pyrE (CO)}$  and *cooS* complemented strain were grown under similar conditions, they grew to an OD of 0.35 and 0.26 in 5 days, as shown in Fig. 30B.

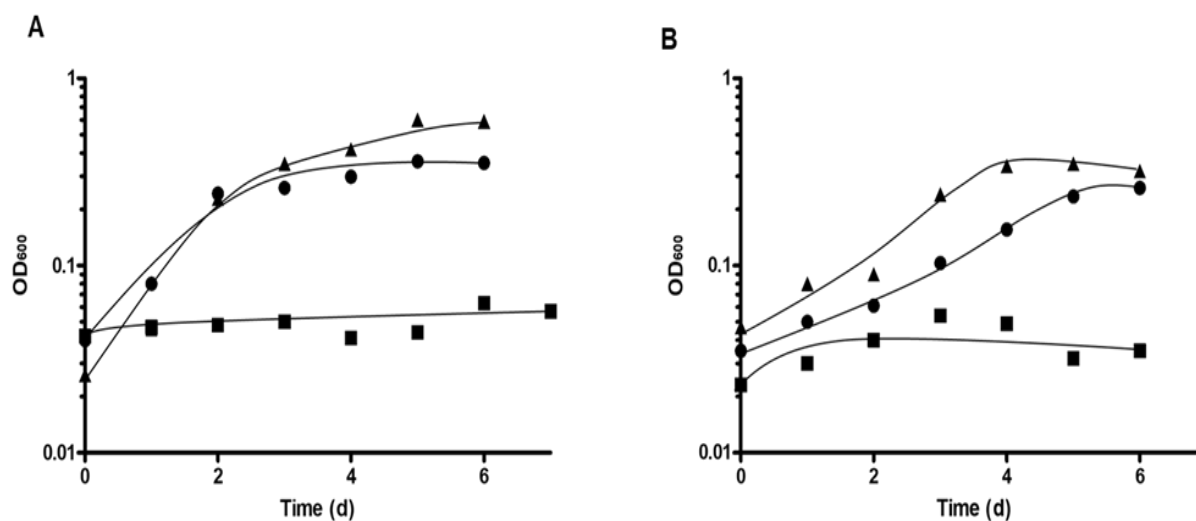


**Fig. 30. Growth of *T. kivui*  $\Delta\text{pyrE (CO)}$ ,  $\Delta\text{cooS}$  deletion mutant and *cooS* complemented strain on 100% CO.** Cells were grown at  $65^\circ\text{C}$  on 100% CO ( $2 \times 10^5 \text{ Pa}$ ) in 120 ml serum bottle containing 20 ml of complex media (A) or mineral media (B).  $\Delta\text{pyrE (CO)}$  (▲),  $\Delta\text{cooS}$  (■) and *cooS* complemented strain (●). Growth was measured by following the optical density at 600 nm. Shown growth curve is one representative experiment out of two independent replicates.

The  $\Delta\text{cooS}$  strain grew on  $\text{H}_2 + \text{CO}_2$  ( $2 \times 10^5$  Pa), 25 mM glucose, 25 mM mannitol or 100 mM formate, similar to the parent strain  $\Delta\text{pyrE}$  (CO) (Fig. 31).

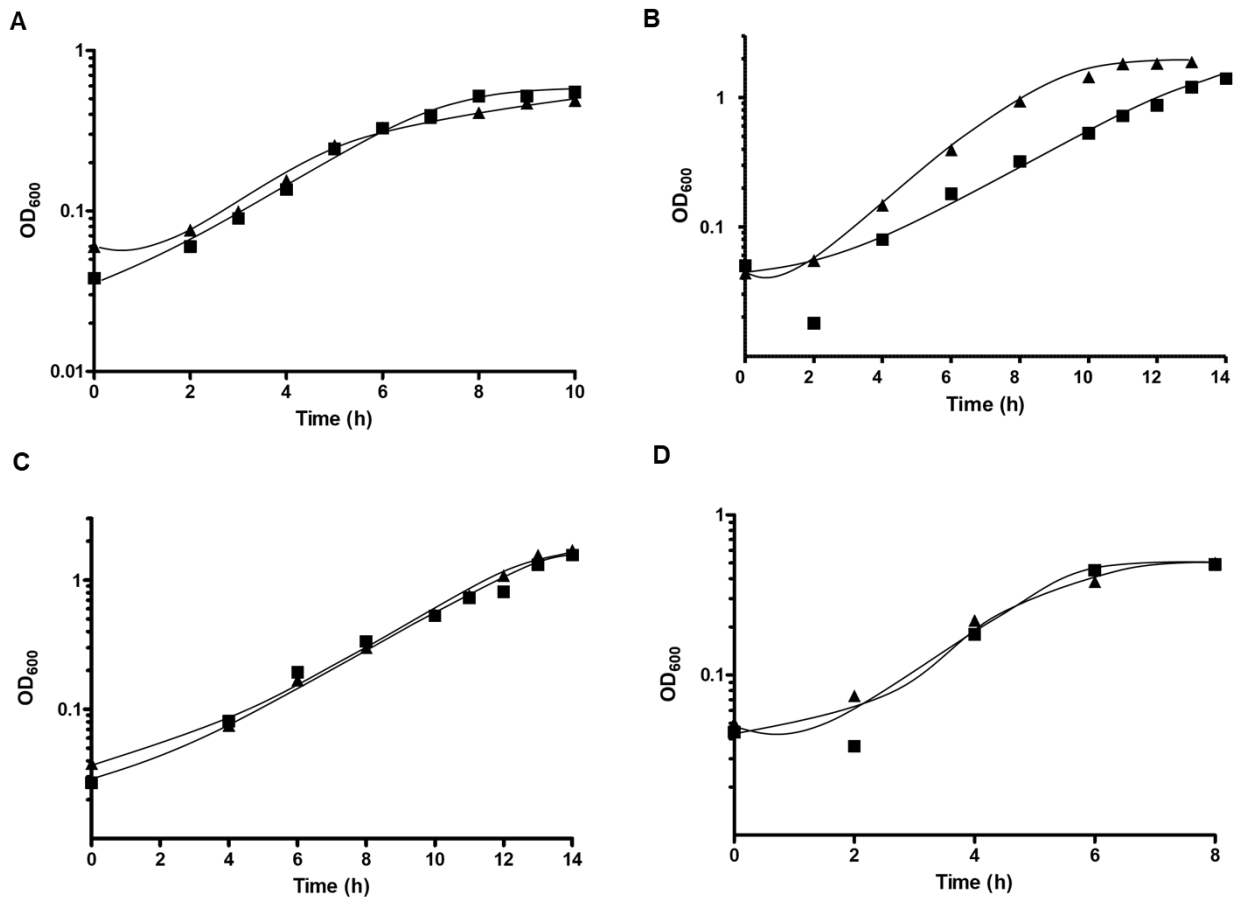


**Fig. 31. Growth of *T. kivui*  $\Delta\text{pyrE}$  (CO) and  $\Delta\text{cooS}$  deletion mutant.** Cells were grown in complex media at 65°C on (A)  $\text{H}_2 + \text{CO}_2$  (80/20 [v/v],  $2 \times 10^5$  Pa), (B) 25 mM glucose, (C) 25 mM mannitol (D) 100 mM formate.  $\Delta\text{pyrE}$  (CO) (▲) and  $\Delta\text{cooS}$  (■). Growth was measured by following the optical density at 600 nm. Shown growth curve is one representative experiment out of three independent replicates.

### 3.3.5 Measurement of CO-dehydrogenase activity in cell-free extracts of *T. kivui* $\Delta$ cooS

The carbon monoxide dehydrogenase activity was determined in cell-free extracts by measuring CO:MV oxidoreductase activity with CO as electron donor and methyl viologen (MV) as electron acceptor. The activity was measured in the  $\Delta$ cooS mutant and  $\Delta$ pyrE (CO) cells grown on 100% CO or 25 mM glucose in complex media. Cells were harvested in mid-exponential growth phase. The CO:MV oxidoreductase activity in CO-grown cells was  $178.6 \pm 12.8$  U/mg in wild type cells but only 8% ( $14.9 \pm 2.5$  U/mg) was observed in the  $\Delta$ cooS mutant. This finding clearly indicates the majority of CODH activity is catalyzed by CooS. In the strain complemented with cooS the activity increased by 41.6% to  $76.9 \pm 6.85$  U/mg.

In contrast, CODH activity measured in the cell-free extract of glucose-grown cells was in general lower but similar in the  $\Delta$ cooS mutant ( $50.6 \pm 6.1$  U/mg) and the  $\Delta$ pyrE (CO) ( $53.8 \pm 11.4$  U/mg). In contrast, the complemented strain had a higher activity of  $107 \pm 2.33$  U/mg.

### 3.3.6 Cell suspension experiments with *T. kivui* $\Delta$ cooS

Cell suspension experiments were performed in order to investigate acetate production by resting cells of *T. kivui*  $\Delta$ cooS compared to CO-adapted wild type strain. For preparation of resting cells, 500 ml of cultures in mid-exponential growth phase either grown on 25 mM glucose or on 25 mM glucose + 100% CO in the headspace harvested and resuspended in 5 ml imidazole buffer (50 mM imidazole, 20 mM MgSO<sub>4</sub>, 20 mM KCl, 20 mM NaCl, 4 mM DTE, 4  $\mu$ M resazurin, pH 7.0) in an anoxic chamber filled with N<sub>2</sub> and kept in 16 ml gas tight Hungate tubes. For the experiment, cells were resuspended with the same buffer in the presence of 50 mM of KHCO<sub>3</sub> in 120 ml serum bottles under N<sub>2</sub>/CO<sub>2</sub> (80/20 [v/v],  $2 \times 10^5$  Pa) atmosphere. Cells were added according to a protein concentration of 1 mg/ml and the final volume of the suspension was made 10 ml.

Substrate used was  $H_2 + CO_2$  (80/20 [v/v]) at  $2 \times 10^5$  Pa. The experiment was started after the resting cells were incubated at  $65^\circ C$  for 10 minutes in a pre-warmed water bath. 0.8 ml cells were taken every hour for the determination of product formation up to 9 hours.

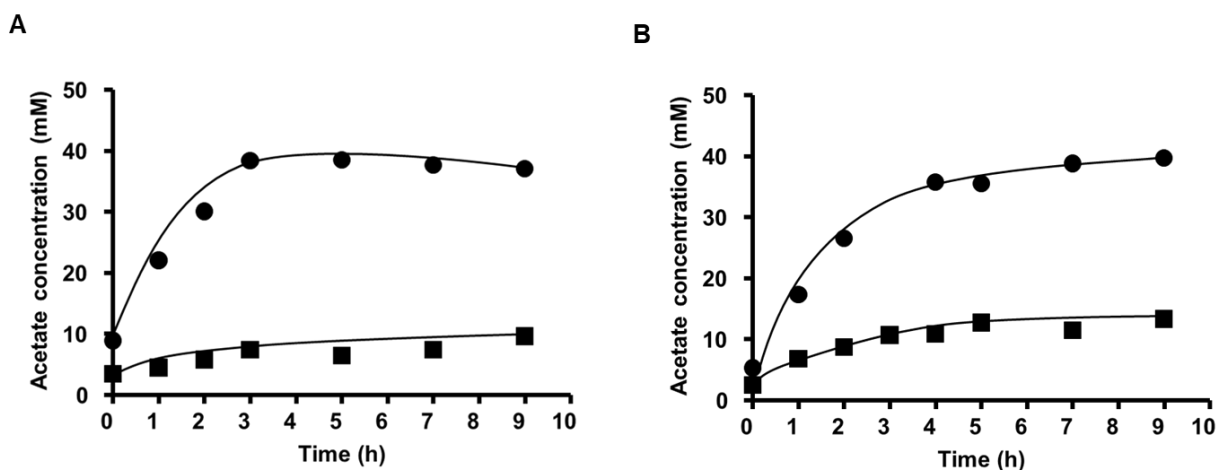


**Fig. 32. Acetate production from resting cells of *T. kivui*  $\Delta cooS$  in the presence of  $H_2 + CO_2$ .** Cells were grown on 25 mM glucose (A) or 25 mM glucose with 100%  $CO$  in the headspace (B) to the mid exponential phase and then harvested. The cells were washed and resuspended in imidazole buffer (50 mM imidazole, 20 mM  $MgSO_4$ , 20 mM  $KCl$ , 20 mM  $NaCl$ , 4 mM DTE, 4  $\mu M$  resazurin, pH 7.0) to a protein concentration of 1 mg/ml with the addition of 50 mM  $KHCO_3$  in 120 ml serum bottles. The resting cells were incubated with  $H_2 + CO_2$  (80/20 [v/v],  $2 \times 10^5$  Pa) as a substrate in pre-warmed water bath at  $65^\circ C$ . 0.8 ml of samples was collected for the determination of acetate over the time using gas chromatography. *T. kivui* wild type =  $CO$  adapted *T. kivui* strain (■) and *T. kivui*  $\Delta cooS$  (●).

Acetate formation from  $H_2 + CO_2$  was studied for 9 hours. 39 mM of acetate was formed by the  $\Delta cooS$  mutant, while  $CO$  adapted wild type produced only 10 mM of acetate (Fig. 32A) in glucose grown cells. Same pattern was observed with the glucose +  $CO$  grown cells. 40 mM of acetate was formed from  $\Delta cooS$  mutant, while  $CO$  adapted wild type produced only 13 mM of acetate (Fig. 33B). Unexpectedly, acetate formation was substantially higher in the  $\Delta cooS$  mutant.

### 3.4 Generation and characterization of a $\Delta hydAB$ mutant of *T. kivui*

#### 3.4.1 Identification and organization of electron bifurcating hydrogenase genes

In addition to the hydrogenase gene *hydA2* in the HDCR gene cluster, the *T. kivui* genome encodes an electron bifurcating hydrogenase HydABC, a key enzyme for H<sub>2</sub> oxidation (Schuchmann and Müller, 2012). The genome of *T. kivui* harbors *hydA1* (Tkv\_c19580) followed by *hydB* (Tkv\_c19590) and *hydC* (Tkv\_c19600), all transcribed in the same direction. Bifurcating hydrogenases also operate in reverse direction during heterotrophic metabolism, which is important for redox balancing to oxidize NAD(P)H and Fd<sup>2-</sup> and yielding hydrogen.

HydA1 shares 56, 49, 45 and 43% identity with the corresponding subunits of *M. thermoacetica* (Wang et al., 2013b), *A. woodii* (Schuchmann and Müller, 2012), *C. autoethanogenum* (Wang et al., 2013a) and *T. maritima* (Schut and Adams, 2009). HydB from *T. kivui* shares 59, 54, 53 and 51% identity with the corresponding subunit of *A. woodii*, *M. thermoacetica*, *C. autoethanogenum*, and *T. maritima*, respectively and HydC of *T. kivui* shares 52, 47, 44 and 42% identity with the corresponding subunit of *T. maritima*, *A. woodii*, *C. autoethanogenum* and *M. thermoacetica* (Fig. 33).

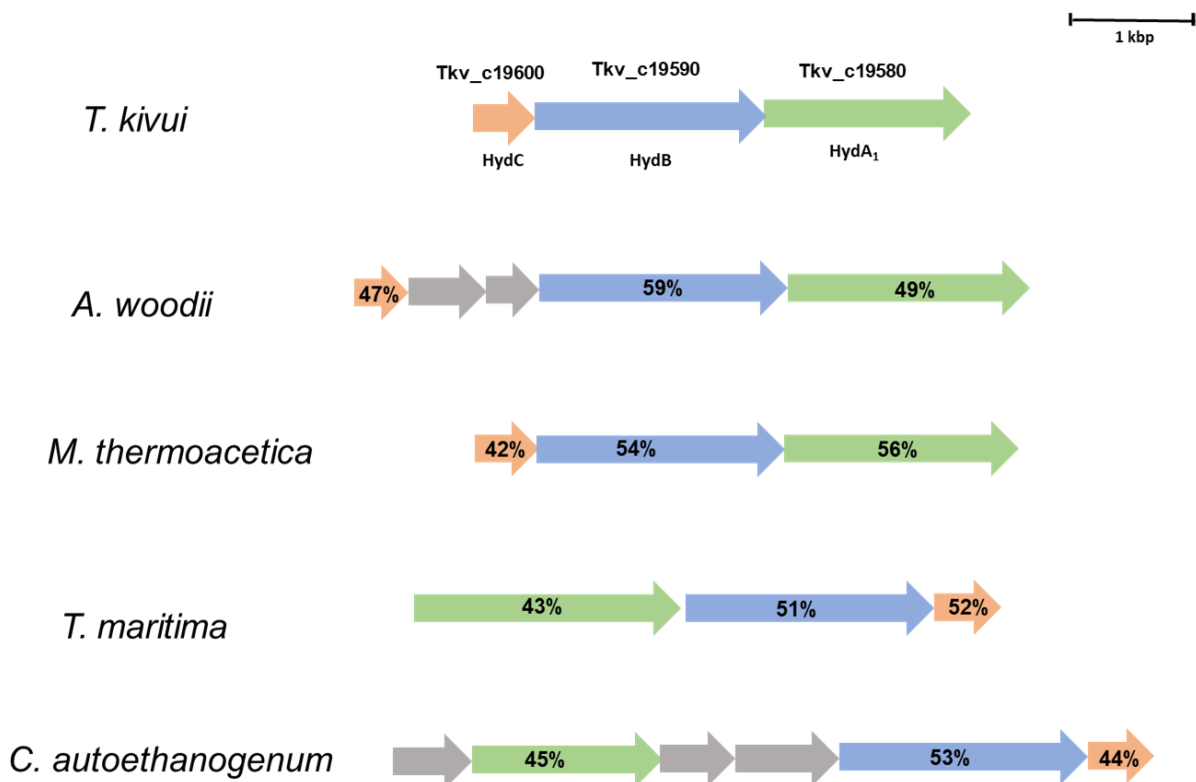


**Fig. 33. Genetic organization of electron-bifurcating hydrogenase genes in different bacteria.** The percentage represents the identity to the amino acid sequence to the respective gene in *T. kivui*. The identity determination was carried out by BlastP based on NCBI database. HydA (green), HydB (blue) and HydC (orange). *A. woodii*, *Acetobacterium woodii*; *C. autoethanogenum*, *Clostridium autoethanogenum*; *T. maritima*, *Thermotoga maritima*; *M. thermoacetica*, *Moorella thermoacetica*.

### 3.4.2 Deletion of the *hydA<sub>1</sub>B* genes in *T. kivui*

The deletion of complete *hydABC* cluster in *T. kivui* failed, therefore, we aimed to delete only *hydA<sub>1</sub>B* (Tk<sub>v</sub>\_c19580, Tk<sub>v</sub>\_c19590) genes in *T. kivui* since this had been proven successfully before in *A. woodii* (Wiechmann et al., 2020). To delete *hydA<sub>1</sub>B*, plasmid pSJ011 was generated by inserting 950 bp upstream (position: 1882425 - 1883375, see appendix 7.3.1) and 1000 bp downstream (position: 1887009 - 1888009, see appendix 7.3.2) of the *hydA<sub>1</sub>B* gene (Fig. 34). The backbone of pSJ011 was amplified from pMBTk<sub>v</sub>012 (Jain et al., 2020) containing an ampicillin resistance cassette and *pyrE* gene which served as a selectable marker for introducing into the *T. kivui*  $\Delta$ *pyrE* (Basen et al., 2018). Primers used for UFR and DFR of *hydA<sub>1</sub>B* amplification are  $\Delta$ *hydA<sub>1</sub>B*\_UFR\_FP & RP, respectively followed by ligation into pMBTk<sub>v</sub>012 using oligonucleotides



$\Delta hydA_1B\_BB\_FP$  &  $\Delta hydA_1B\_BB\_RP$ . The amplified fragments were fused by Gibson Assembly.

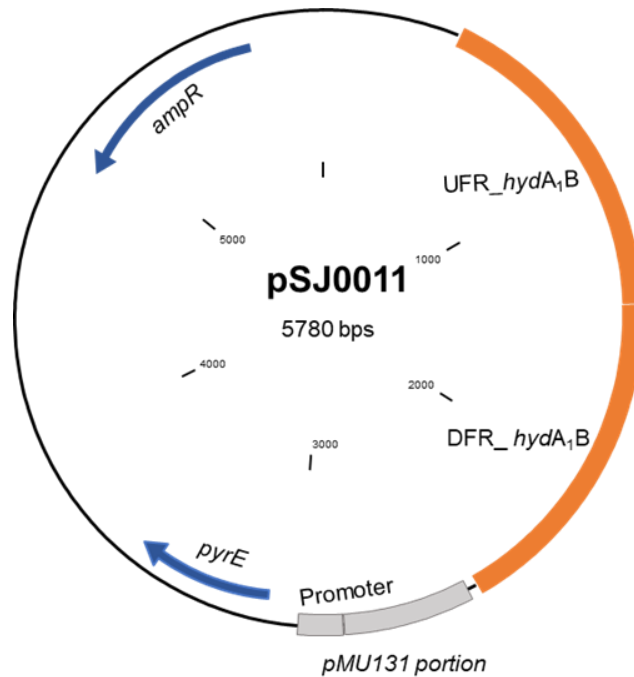


**Fig. 34. Physical map of plasmid pSJ0011.** The plasmid was used for the deletion of *hydA1B* (Tk<sub>v</sub>\_c19580, Tk<sub>v</sub>\_c19590) genes from *T. kivui* genome. The plasmid contains the upstream flanking region (DFR) and downstream flanking region (DFR) of *hydA1B*; *pyrE* (Tk<sub>v</sub>\_c14380), as a selection marker; *amp<sup>R</sup>*, ampicillin resistance cassette.

*T. kivui*  $\Delta pyrE$  was transformed with the plasmid pSJ0011. Since the plasmid has the *pyrE* gene as a selection marker, in the first round of selection, transformants were plated on agar plates in defined media without uracil in the presence of 25 mM glucose + 50 mM formate. The substrates used were in accordance with the *hydAB* deletion mutant preparation in *A. woodii* (Wiechmann et al., 2020). After selecting the transformants with the plasmid integration, they were subjected to a second round of selection for disintegration of plasmid in minimal media supplemented with same substrate, 50  $\mu$ M uracil and 5 mM 5-FOA (Fig. 35).

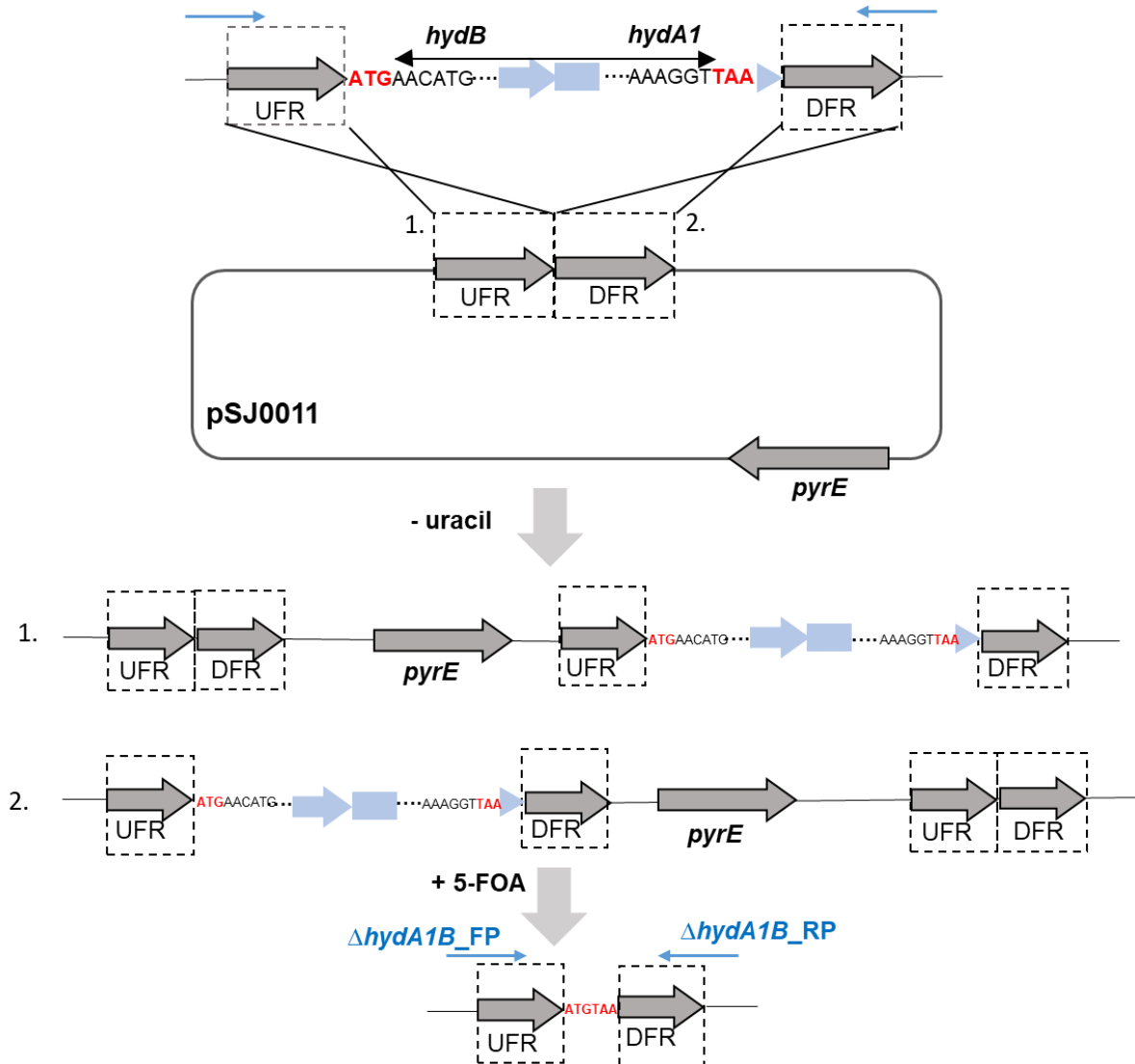


**Fig. 35. Scheme for deletion of *hydA1B* genes using plasmid pSJ0011.** *T. kivui* was transformed with the plasmid pSJ0011 that contains a selection marker (*pyrE*) and the upstream (UFR) and downstream (DFR) region of the *hydA1B* genes. *hydA1B* gene deletion starts after 3 base pairs of UFR and ends before 3 base pairs of DFR. In the absence of uracil, isolates were selected which had integrated the plasmid in first round of selection by simple homologous recombination at the UFR or DFR region. After subsequent counter-selection with 5-FOA, the plasmid was disintegrated from the genome and genotypes were obtained either  $\Delta pyrE$  mutant or  $\Delta pyrE$  mutant with the deletion of *hydA1B* genes where 3609 base pairs were deleted. Blue arrows marked are the primer binding sites of the oligonucleotides used for the detection of genotype with *hydA1B* deletion.

After incubation of plates at 65 °C for 4-5 days, few colonies were obtained. Genotype analysis was carried out by PCR with the primers  $\Delta hydA1B_{FP}$  &  $\Delta hydA1B_{RP}$  binding outside the *hydBA1* in the genome (Fig. 36A). The *hydA1B* genes of 3,609 base pairs were deleted, therefore, PCR of  $\Delta hydA1B$  isolates revealed the fragment size of 2 kb

whereas the wild type had the fragment size of 5.6 kb (Fig. 36B). For further verification, PCR was performed with the isolates 1-3 by using primers *hydA1B* int\_FP & *hydA1B* int\_RP, binding inside the *hydA1B* gene. No DNA fragment were observed in the isolates 1-3 but the wild type showed the band size of 3.5 kb (Fig. 36C). This verified the clean deletion of *hydA1B* genes. A single isolate was further confirmed by Sanger sequencing and used for further studies.

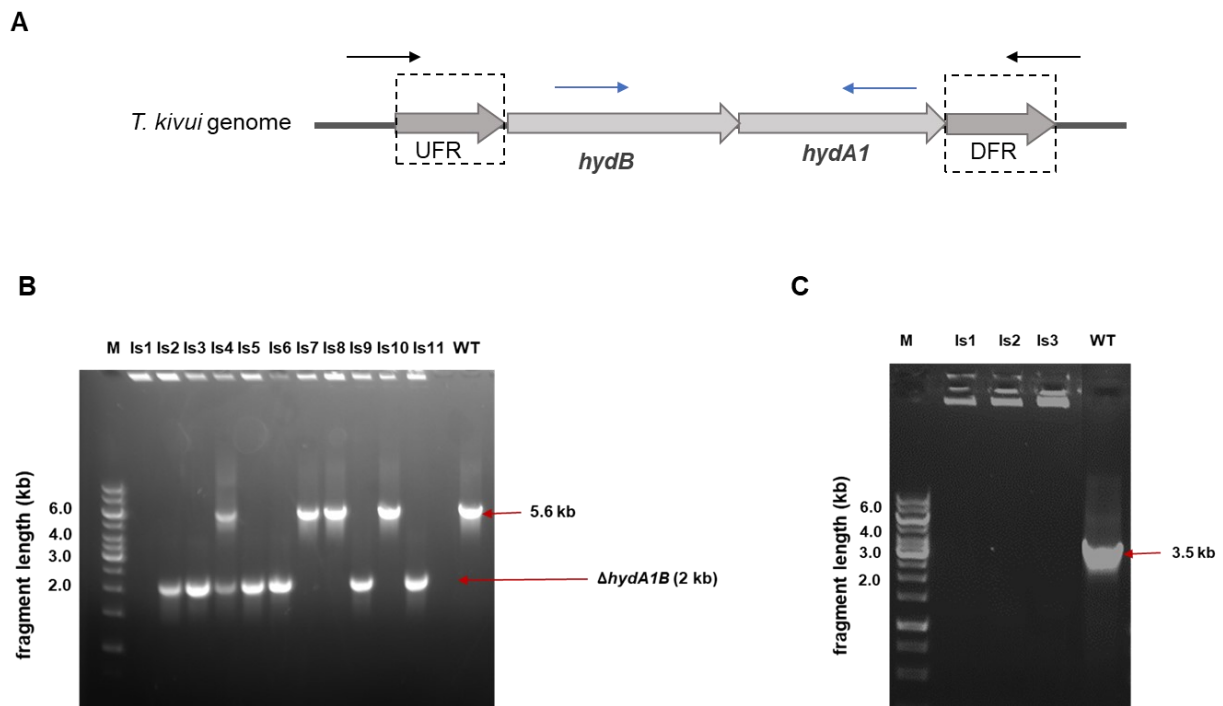


**Fig. 36. Genotypic analysis of the *hydA1B* deletion in *T. kivui*.** The loss of *hydA1B* (3609 bp) was verified *via* PCR. A) Oligonucleotides  $\Delta$ *hydA1B*\_FP &  $\Delta$ *hydA1B*\_RP (black), binding outside the *hydA1B*; oligonucleotides *hydA1B* int\_FP & *hydA1B* int\_RP (blue), binding inside the *hydA1B* genes. (B) DNA fragments amplified from the isolates with *hydA1B* deletion (2kb) and wild type (5.6 kb) using outside binding primers. (C) DNA fragments amplified from the isolates 1-3 for verification of  $\Delta$ *hydA1B* strain using internal binding primers. Expected sizes of PCR products, WT; 3.5 kb,  $\Delta$ *hydA1B*; no DNA fragment. Is, isolates; WT, wild type; M, Gene Ruler 1 kb DNA ladder (Thermo Fisher Scientific).

### 3.4.3 Growth experiments with *T. kivui* $\Delta hydA_1B$

For the growth experiment with the *hydA<sub>1</sub>B* deletion mutant, pre-cultures were grown on glucose (25 mM) + formate (50 mM) in complex medium. Controls used for the growth experiment were *T. kivui* wild type and *T. kivui*  $\Delta ech2$ . The *T. kivui*  $\Delta ech2$  deletion mutant was kindly provided by Dr. Mirko Basen, Rostock University.

First, the ability to grow on H<sub>2</sub> + CO<sub>2</sub> was examined. The wild type grew until an OD<sub>600</sub> of 0.67 was reached. The  $\Delta ech2$  mutant also grew but the maximum OD<sub>600</sub> was lowered to 0.42. In contrast, the *hydA<sub>1</sub>B* mutant did not grow on H<sub>2</sub> + CO<sub>2</sub> (Fig. 37A).

Next, heterotrophic growth on glucose (25 mM) or mannitol (25 mM) was tested. Surprisingly and in contrast to *A. woodii*, the mutant strain grew on both substrates. The growth rate was 0.36 h<sup>-1</sup> (doubling time of 2.5 hours) on glucose (Fig. 37B) and 0.27 h<sup>-1</sup> (doubling time of 1.9 hours) on mannitol (Fig. 37C). The maximum OD<sub>600</sub> was ~2.5 with both the substrates, which was comparable to wild type and  $\Delta ech2$ . This experiment demonstrated the dispensability of electron bifurcating hydrogenase in heterotrophic metabolism of *T. kivui*. Similar growth behavior was observed in the presence of glucose (25 mM) plus formate (50 mM).

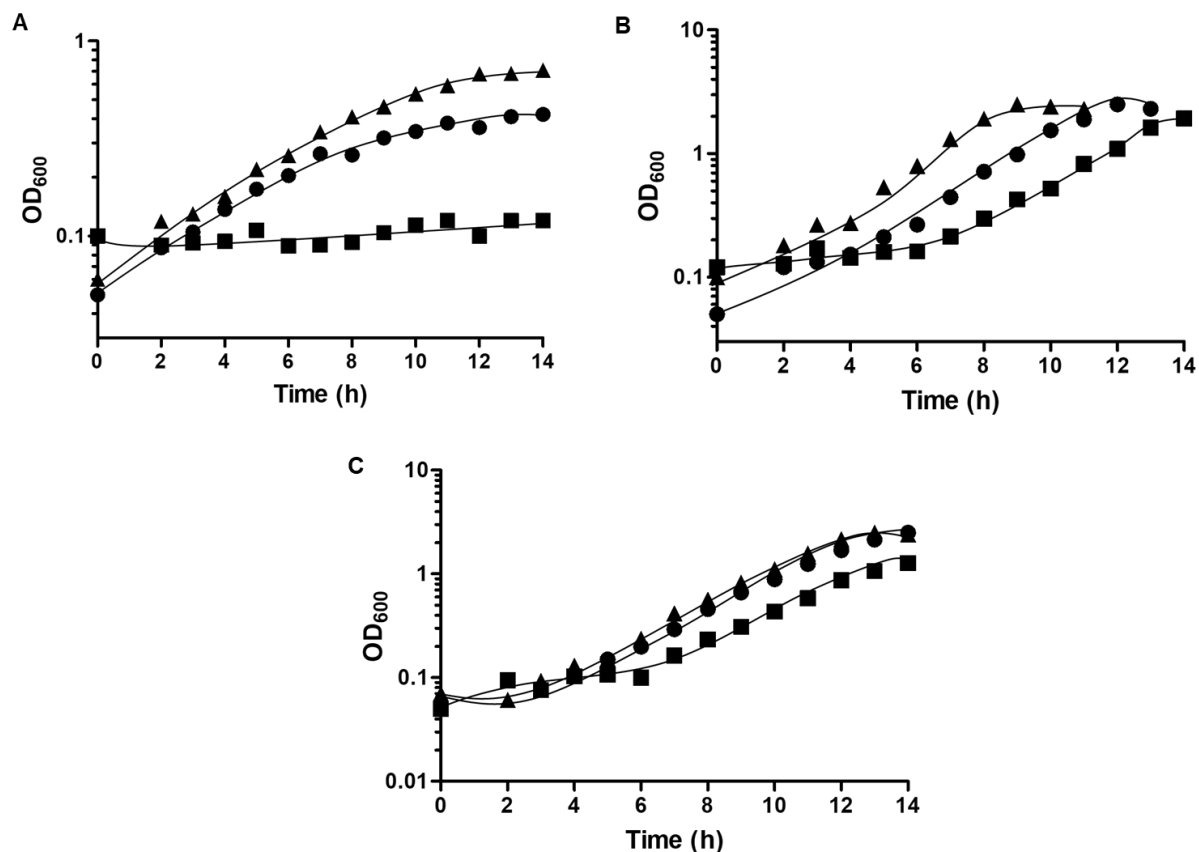


**Fig. 37. Growth of *T. kivui* strain  $\Delta hydA1B$  in complex media at 65 °C.** Growth on (A) H<sub>2</sub> + CO<sub>2</sub> (80/20 [v/v]) at 2 × 10<sup>5</sup> Pa, (B) 25 mM glucose or (C) 25 mM mannitol.  $\Delta hydA1B$  (■), wild type (▲) and  $\Delta ech2$  (●). Pre-cultures were grown on glucose (25 mM) + formate (50 mM) in complex medium. Growth was measured by following the optical density at 600 nm. The experiments were performed in biological triplicates and one representative growth curve was presented.

#### 3.4.4 Cell suspension experiments with *T. kivui* $\Delta hydA1B$

In order to investigate the influence of deletion of *hydAB* genes on acetate production, resting cell experiments were carried out with *T. kivui*  $\Delta hydAB$  and wild type cells. For resting cells preparation, 500 ml of cultures were grown till mid-exponential growth phase on 25 mM glucose only and then were resuspended in 5 ml imidazole buffer (50 mM imidazole, 20 mM MgSO<sub>4</sub>, 20 mM KCl, 20 mM NaCl, 4 mM DTE, 4 μM resazurin, pH 7.0) in an anoxic chamber filled with N<sub>2</sub> and kept in 16 ml gas tight Hungate tubes. For the experiment, cells were resuspended with the same buffer in the presence of 50 mM of

KHCO<sub>3</sub> in 60 ml serum bottles under a N<sub>2</sub>/CO<sub>2</sub> (80/20 [v/v], 2 × 10<sup>5</sup> Pa) atmosphere. Cells were added to a protein concentration of 2 mg/ml and the final volume of the suspension was made 10 ml. After the cells were incubated at 65 °C for 10 mins in a pre-warmed water bath, the experiment was started by addition of 10 mM glucose and 0.8 ml cell suspension were taken up to 4 hours for the determination of substrate consumption and product formation.

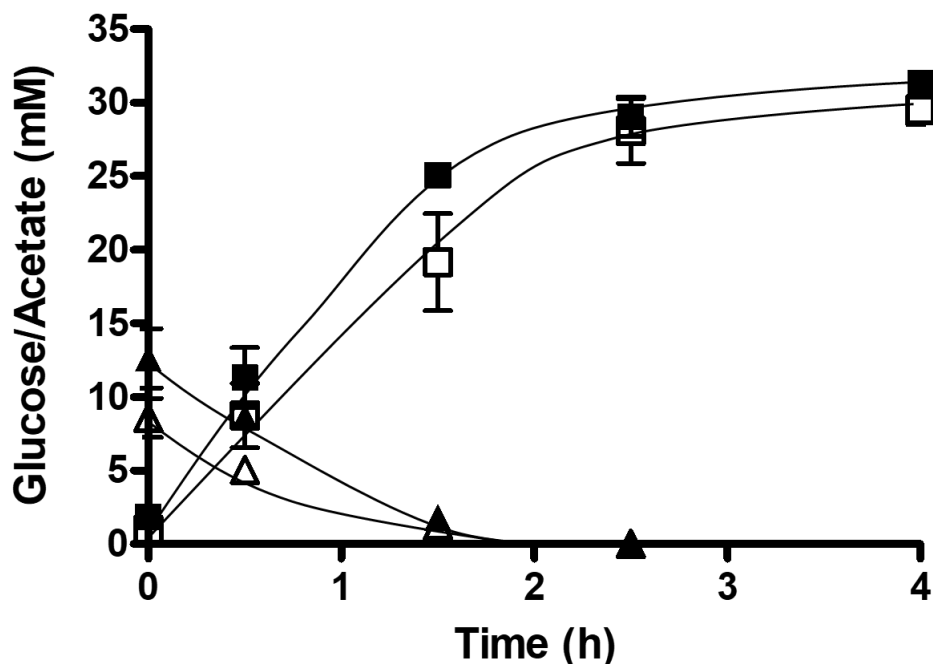


**Fig. 38. Acetate production and glucose consumption by resting cells of *T. kivui*  $\Delta$ *hydAB*.** Cells were grown on 25 mM glucose to the mid exponential phase and then harvested. The cells were washed and resuspended in imidazole buffer (50 mM imidazole, 20 mM MgSO<sub>4</sub>, 20 mM KCl, 20 mM NaCl, 4 mM DTE, 4  $\mu$ M resazurin, pH 7.0) to a protein concentration of 2 mg/ml. The resting cells were incubated with 10 mM glucose as substrate in pre-warmed water bath at 65 °C. 0.8 ml of samples were collected for the determination of glucose and acetate over the time. The concentrations of glucose was determined by high performance liquid chromatography. Acetate concentrations was determined using gas chromatography. *T. kivui*  $\Delta$ *hydAB* acetate (■), glucose (▲) and *T. kivui* wild type acetate (□), glucose (Δ). The experiments were carried out in biological triplicates.

Acetate formation was similar between the  $\Delta$ *hydAB* and wild type. 10 mM glucose was completely consumed within 2.5 hours, and at the same time 30 mM acetate was produced. (Fig. 38). The ratio of acetate/glucose was 3.

### 3.5 Electron carrier specificity of the methylene-THF dehydrogenase in crude extracts of *T. kivui*

In order to analyze the electron carrier specificity of the methylene-THF dehydrogenase, the enzyme was measured in cell-free extract. Therefore, the cells were grown on 25 mM glucose and the cell extract was prepared. The methylene THF-dependent reduction of NAD<sup>+</sup> or NADP<sup>+</sup> was determined using methylene-THF as an electron donor. The assay was performed in 50 mM MOPS buffer, 10 mM NaCl, 20 mM MgSO<sub>4</sub>, 2 mM DTE, pH 7. NADP<sup>+</sup> was reduced with the activity of  $24.4 \pm 1.2$  U/mg (Fig. 39A), NAD<sup>+</sup> was not reduced (Fig. 39B). This experiment demonstrated methylene-THF dehydrogenase in *T. kivui* is NADP<sup>+</sup>-specific.

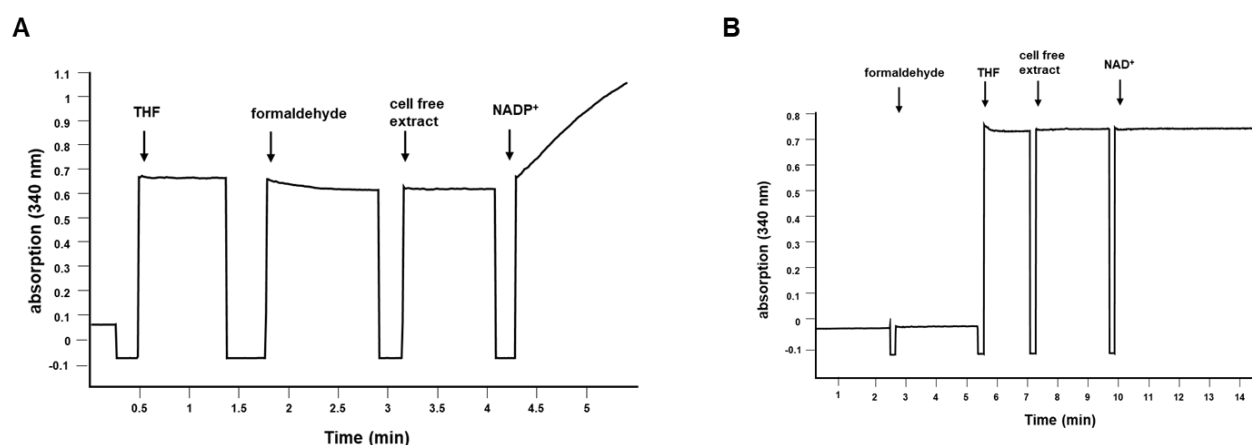


**Fig. 39. NADPH-dependent methylene-THF dehydrogenase activity in cell-free extracts of *T. kivui*.**

Cells were grown on glucose and harvested in the mid exponential growth phase. Methylene-THF dehydrogenase activity was measured in 1.8-ml anoxic cuvettes containing an overall liquid volume of 1 ml under 100% N<sub>2</sub> atmosphere at 60 °C. The assay buffer contained 50 mM MOPS buffer, 10 mM NaCl, 20 mM MgSO<sub>4</sub>, 2 mM DTE, pH 7 and 200 -500 µg of cell-free extract. Methylene-THF served as an electron donor. The reaction was started by addition of 1 mM NAD<sup>+</sup> (A) and 1 mM NADP<sup>+</sup> (B). Reduction of NAD<sup>+</sup> and NADP<sup>+</sup> was monitored at 340 nm ( $\epsilon=6.22$  mM<sup>-1</sup>·cm<sup>-1</sup>). The measurements were carried out in the biological triplicates.

## 4. Discussion

To study the genetics of *T. kivui*, understanding the basic physiology was primarily important. The heterotrophic growth with wild type *T. kivui* on glucose, pyruvate as well as autotrophic growth on  $H_2 + CO_2$  was obtained as reported in previous studies (Leigh et al., 1981). Growth of *T. kivui* was also obtained in minimal media without yeast extract demonstrating that growth was solely dependent on the supplied energy and carbon source. However, the growth rate obtained was 1.3 times lower in minimal media (Fig. 9). Most of the *Thermoanaerobacter* species require yeast extract when grown chemorganotrophically (Onyenwoke and Wiegel, 2015; Shao et al., 2016). There are only a few species known to grow without the addition of yeast extract, such as *Thermoanaerobacter wiegelii* (Cook et al., 1996), *Thermoanaerobacter kivui* (Leigh et al., 1981) and *Thermoanaerobacter siderophilus* (Slobodkin et al., 1999). It is known that yeast extract contains a large amount of proteins, amino acids, nucleotides, and vitamins (Eisenbrand, 2006). Other than the growth studies, minimal media was also used for mutagenesis studies of *T. kivui* for the selection of uracil-auxotrophic transformants. Physiological experiments and the genome sequence (Hess et al., 2014) enhanced the metabolic capabilities of *T. kivui*.

The genome of *T. kivui* contains genes for a potential trehalose/maltose transport system (MalF), an ABC transporter for the uptake of trehalose or maltose. To date, maltose or trehalose were not known as the carbon source for *T. kivui*. Consistent with the original publication (Leigh et al., 1981), first attempts to grow *T. kivui* on 25 mM maltose or 25 mM trehalose as carbon and electron source failed. However, when glucose-grown cells are transferred to higher concentration (50 mM) maltose or trehalose, cultures were adapted. Interestingly, re-inoculation of adapted cultures to 25 mM maltose or 25 mM trehalose grew to a maximum  $OD_{600}$  of 1.12 and 0.73, respectively (Fig. 11). Apparently, the organism needs higher concentration of these carbon sources to adapt its metabolism. Maltose or trehalose utilization has been reported in other thermophilic organisms as well. *Pyrococcus furiosus*, a hyperthermophilic archaeon grows on mannitol



(Fiala and Stetter, 1986) and the metabolically engineered strain is reported to produce 3-hydroxypropionate (3HP) from maltose (Hawkins et al., 2015). Trehalose utilization has been reported in an aerobic marine thermophilic bacterium, *Rhodothermus marinus*, where trehalose plays a minor role in osmo- or thermo-adaptation of this organism (Jorge et al., 2008). In addition to the transport system, trehalose and maltose hydrolase genes are also found in the *T. kivui* genome, annotated as kojibiose phosphorylase. Kojibiose phosphorylase has also been reported in *Thermoanaerobacter brockii* ATCC35047 to catalyze the reversible phosphorolysis of kojibiose (disaccharide that occurs in koji extract) into  $\beta$ -D-glucose 1-phosphate and D-glucose (Yamamoto et al., 2004). Growth on maltose and trehalose expands the substrates spectrum of *T. kivui*. In fact, acetogens are well known for their metabolic flexibility and are still evolving in terms of their substrate range utilization, which would otherwise be outcompeted by their relative organisms on thermodynamic grounds.

Recently, it was shown that *T. kivui* grows on mannitol (Moon et al., 2019). The growth was reported with and without  $\text{HCO}_3^-$  (or external  $\text{CO}_2$ ) in minimal media. Mannitol uptake is through a mannitol-specific PTS (Hess et al., 2014), where mannitol is phosphorylated and oxidized to fructose-6-phosphate, generating one additional NADH compared to glucose (Moon et al., 2019). Mannitol utilization has also been reported in other acetogens such as *Clostridium huakuii* and *Sporomusa termitida* (Ruan et al., 2014; Breznak et al., 1988). Since *T. kivui* has been reported to grow much slower on mannitol in the absence of  $\text{HCO}_3^-$ , therefore, an addition of formate was tested in this study to compensate for the “missing”  $\text{CO}_2$ . Interestingly, when formate was added, the maximal  $\text{OD}_{600}$  stimulated to 2.5 with the doubling time to 2.0 h (Fig. 12), implying that the external formate can serve as an electron acceptor in the absence of  $\text{CO}_2/\text{HCO}_3^-$ . These results correspond to the function of formate as an electron acceptor as described for the stimulated growth of *T. kivui*  $\Delta h d c r$  mutant on glucose (Jain et al., 2020).

#### 4.1 Effect of deletion of hydrogen-dependent CO<sub>2</sub> reductase (*hdcr*) in *T. kivui*

Acetogens utilize H<sub>2</sub> + CO<sub>2</sub> or C1 compounds such as formate or the methyl groups of methanol, methylamines or methoxylated compounds as the sole source of energy and carbon *via* WLP (Fischer et al., 1932; Wood and Ljungdahl, 1991; Kerby et al., 1983; Schuchmann et al., 2016). Formate also serves as an intermediate in the WLP, which is provided by formate dehydrogenase (FDH). Formate dehydrogenases are a group of enzymes found in all three domains of life. Based on their catalytic strategies and their redox cofactors at the active site of the enzyme, they are classified into "metal-independent" and "metal-containing". FDH's containing molybdenum or tungsten at the active site are found in anaerobic bacteria and archaea (Crale et al., 2011; Ferry, 1990; Maia et al., 2015). In contrast to the classical formate dehydrogenases, some acetogenic bacteria have an enzyme complex of molybdenum or tungsten containing FDH bounded to hydrogenase and two electron transfer subunits that directly uses molecular hydrogen for CO<sub>2</sub> reduction in the first step of the WLP. This soluble enzyme complex has been first characterized from a mesophilic bacterium, *A. woodii* (Schuchmann and Müller, 2013) and then later from the thermophilic bacterium, *T. kivui* (Schwarz et al., 2018). *hdcr* gene cluster is also present in thermophilic organisms *Symbiobacterium thermophilum*, which grows in coculture with *Geobacillus* sp. (Ohno et al., 2000). Direct hydrogenation of CO<sub>2</sub> to formate or to other chemicals is of great biotechnological interest due to the rise in CO<sub>2</sub> concentration.

The genome of *T. kivui* has *fdhF*, *hycB<sub>3</sub>*, *hycB<sub>4</sub>*, *hydA<sub>2</sub>* and *fdhD* (*hdcr*) (Hess et al., 2014). The genome of *T. kivui* consists only one *fdhF* (TKV\_c19990), which is different in other acetogens such as *A. woodii* which has *fdhF2* in addition to *fdhF1* (Poehlein et al., 2015) or *Treponema primitia* that has several *fdh* copies, or genes encoding formate:H<sub>2</sub> lyase (FHL) in addition to *fdh* genes (Matson et al., 2010). In *Escherichia coli*, FHL catalyzes the formate-H<sub>2</sub> interconversion (McDowall et al., 2014); (Trchounian and Trchounian, 2014; Pinske and Sargent, 2016). The deletion of the *hdcr* gene cluster from *T. kivui* completely eliminated its ability to grow on formate as sole substrate and electron donor.

*fdhD* was not deleted, since the function of *fdhD* is unknown and it was not identified as part of the enzyme complex (Schwarz et al., 2018). In principle, the overall balance of formate metabolism of the wild type is:



In this study, the *hdcr* gene cluster was deleted to gain insights into the physiological function of HDCR in the metabolism of *T. kivui*. The deletion of genes were carried out using the recently developed genetic system based on uracil auxotrophy (Basen et al., 2018). Initially glucose was used as substrate for screening the mutants which always resulted in a mixed culture with wild type and the isolation of clean *hdcr* deletion mutant failed even after screening >50 colonies. Since formate is the product of HDCR, we used the approach of adding formate (50 mM) with glucose during the selection process. This indeed resulted in the “clean” *hdcr* deletion mutants. The deletion of *hdcr* genes was detected by PCR using primers which binds outside the *hdcr* gene cluster, whereby due to the gene deletion, a significantly shortened PCR product was amplified compared to the wild type (Fig. 16B). Out of the screened colonies as verified by PCR analysis after the second round of selection, one of the colony reverted back to the wild type. Furthermore, PCR was performed with primers binding inside the *hdcr* gene cluster where an amplicate was no longer observed, verified the deletion of genes (Fig. 17). In order to finally ensure the physiology of *T. kivui*  $\Delta$ *hdcr* mutant, the deleted genes were complemented in the mutant strain. The complementation of the *hdcr* genes was controlled by the strong promoter of the S-layer protein of *T. kivui*.

#### 4.1.1 The physiological role of HDCR in the metabolism of *T. kivui*

Growth of the  $\Delta$ *hdcr* mutant was not observed on formate or H<sub>2</sub> + CO<sub>2</sub>, which demonstrates the essentiality of gene in the CO<sub>2</sub> reduction to formate as well as formate oxidation (Tab. 10). In comparison to the membrane bound FHL that primarily oxidizes formate to CO<sub>2</sub> in mixed acid fermentation (Pinske and Sargent, 2016), the metabolic function of HDCR is not only formate oxidation but also formate production from CO<sub>2</sub> in

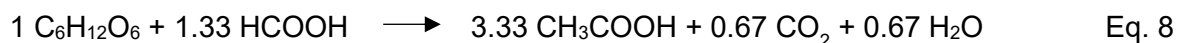
the WLP. Therefore, the ability to use CO<sub>2</sub> as an electron acceptor was abolished due to the deletion of *hdcr* genes. A possibility to grow the mutants on H<sub>2</sub> + CO<sub>2</sub> was obtained by the addition of formate (Fig. 20D), since formate is an intermediate in the methyl branch of the WLP. Indeed, formate served as the electron acceptor to run the WLP normally and the growth of mutant strain was supported, with the comparable growth rate to wild type. After the complementation, the growth was restored and the final optical density was comparable to the *T. kivui* wild type (Fig. 20C).

Interestingly, also the growth of  $\Delta$ *hdcr* mutant on glucose was abolished (Fig. 20A), which proves that HDCR is essential for complete glucose oxidation in the acetogen *T. kivui*. Growth on glucose may be impaired due to the non-functional C1 metabolism or disturbed redox balancing. The disturbance in redox balancing was observed for *A. woodii*, where a functional Rnf complex was essential for providing Fd<sup>2-</sup> to support the growth on low-energy heterotrophic substrates such as lactate or ethanol (Westphal et al., 2018). Again, the extracellularly added formate complemented the growth deficiency on glucose (Fig. 20B). Similarly, the  $\Delta$ *hdcr* mutant also did not grow with mannitol or pyruvate as depicted in table 1. If the *hdcr* is missing, cells were unable to grow on glucose or pyruvate or mannitol except when they grow mixotrophically with formate. This shows the tight coupling of multi-carbon substrate oxidation to the WLP where WLP act as an electron sink. As some anaerobes can grow by oxidation of sugars to 2 mol acetate, 2 mol CO<sub>2</sub> and 4 mol H<sub>2</sub> (Drake et al., 2008), we initially hypothesized the dispensability of HDCR in *T. kivui* for growth on sugars, however this was not the case.

With the observation of the mutational studies, we have described the function of formate as an electron acceptor which has also been reported for the growth of wild type *A. woodii* on CO with formate as a co-substrate (Bertsch and Müller, 2015), although, that study had a different focus of showing utilization of CO in the presence of formate. *Butyrivacterium methylotrophicum* has been reported to utilize CO or H<sub>2</sub> + CO<sub>2</sub> and formate simultaneously (Kerby et al., 1983; Kerby and Zeikus, 1987). Similarly, *A. woodii* in the absence of CO<sub>2</sub>, grows with caffeate as an electron acceptor, forming hydrocaffeate as reduced product (Tschech and Pfennig, 1984). In the environment, where there is no

or little CO<sub>2</sub> present, acetogens potentially have the metabolic advantage to utilize electron acceptors other than CO<sub>2</sub>. It is speculated that utilization of formate as an electron acceptor might be an Early Earth metabolic trait as acetogenesis itself is also considered as one of the ancient metabolic pathways (Weiss et al., 2016) and the coupled formate + CO<sub>2</sub> respiration, as described here, might be the mode to conserve energy in a primordial environment.

When the electron accepting pathway is impaired then theoretically reducing equivalents from sugar oxidation may have a possibility of taking alternative route by channeling electron towards hydrogen production. This was observed in the hyperthermophilic anaerobic bacterium *Thermotoga maritima*. The generated NADH and Fd<sub>red</sub> from glycolysis is oxidized *via* electron-bifurcating [FeFe] hydrogenase to produce hydrogen (Schut and Adams, 2009). In the resting cell experiment, rate of glucose oxidation was impaired in *T. kivui*  $\Delta h d c r$  mutant when formate was not added as a co-substrate (Fig. 21B). The amount of hydrogen produced was only 7 mM. This represents the dispensability of electron- bifurcating hydrogenase towards hydrogen production in *T. kivui*. In contrast to this, glucose was completely consumed in the presence of formate (Fig. 21A) and the acetate production to substrate consumption was slightly higher than 3.



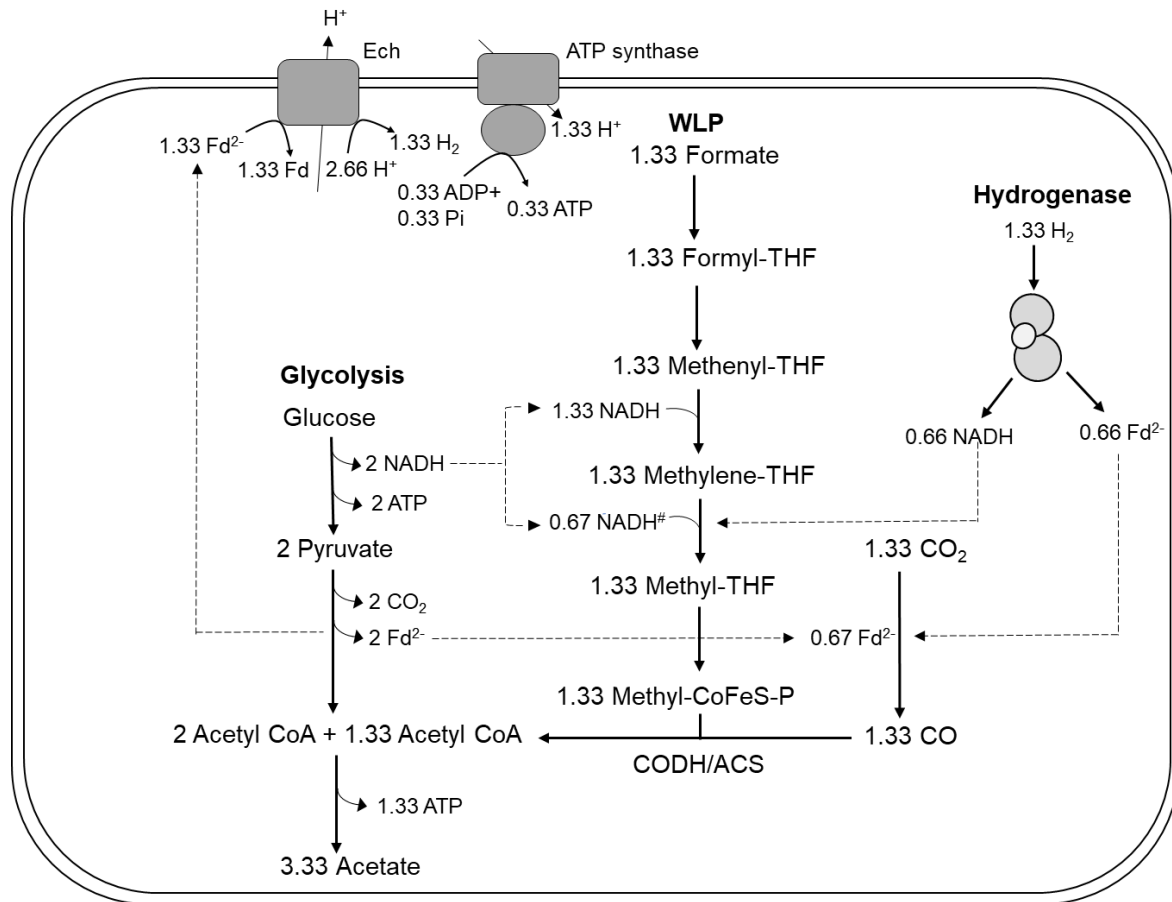
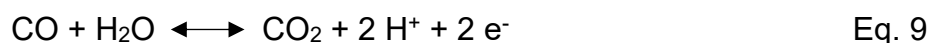


**Fig. 40. Putative model of acetogenesis from glucose with formate + CO<sub>2</sub> as electron acceptors in *T. kivui*  $\Delta$ hdcr.** WLP, Wood-Ljungdahl-pathway; Fd<sup>2-</sup>, reduced ferredoxin; Ech, electron-converting hydrogenase; CoFeS-P, corronoid iron-sulfur protein; CODH/ACS, carbon monoxide dehydrogenase/ acetyl-CoA synthase; NfnAB, transhydrogenase.

## 4.2 Effect of deletion of *cooS* in *T. kivui*

CO is a toxic gas for many organisms originating from natural and anthropogenic sources. One of the ways to remove atmospheric CO is by microbial oxidation, for example to CO<sub>2</sub> and H<sub>2</sub>, which can serve as the intermediates for acetogenesis, methanogenesis and sulphate reduction (Bertsch and Müller, 2015; Matson et al., 2010; Diender et al., 2015). Many life forms use CO as a feedstock for their carbon and energy source (Henstra et al., 2007; Sokolova et al., 2009; Robb and Techtmann, 2018). The low redox potential of CO (E<sup>0</sup> [CO/CO<sub>2</sub>] = -520 mV), makes it an excellent electron donor for biological processes (Thauer et al., 1977). These carboxydrotrophs have a common key enzyme, carbon monoxide dehydrogenase (CODH), in anaerobic as well as aerobic microbial CO utilization (Ragsdale, 2000; Dobbek et al., 2001). This enzyme catalyzes the oxidation of CO to CO<sub>2</sub> and protons/electrons according to:



*T. kivui* is one of the few acetogens which utilizes CO and produces acetate, although it had been described previously, to not use CO as a sole carbon and energy source (Daniel et al., 1990) but recently, it was adapted to grow solely on CO. Using a preculture grown on H<sub>2</sub> + CO<sub>2</sub>, cells started to grow in the presence of 10% CO by subsequent transfer to media with increasing CO concentrations since it finally grew at 100% CO (Weghoff and Müller, 2016), which indicates the organism has adapted its metabolism during the course of time and undergone metabolic changes during autotrophic growth on H<sub>2</sub> + CO<sub>2</sub>. *T. kivui* also grows on syngas in mineral media without additional vitamins and yeast extract. The dispensability of these components for growth is an economically very valuable asset for biotechnological applications of *T. kivui* (Müller, 2019). *Rubrivivax gelatinosus* (formerly *Rhodopseudomonas gelatinosus*) was the first bacterium known for CO utilization under anoxic conditions where CO is oxidized to CO<sub>2</sub> and H<sub>2</sub> in the dark (Uffen, 1976; Uffen, 1983). Similar observation was made in the methanogen *Methanobacterium thermoautotrophicum* where CO uptake is coupled to methane production (Daniels et al., 1977). Later, the physiology of anaerobic CO oxidation in phototrophic bacterium

*Rhodospirillum rubrum* was solved (Bonam et al., 1989; Kerby et al., 1995; Fox et al., 1996a; Fox et al., 1996b; Shelver et al., 1997). To date, various anaerobic bacteria and archaea have been known to conserve energy from anaerobic CO oxidation.

The ability to tolerate CO and proper adaptation is the key for CO metabolization for example, *Acetobacterium woodii* can utilize CO only in combination with  $H_2 + CO_2$  (Bertsch and Müller, 2015). One of the major constraints for CO utilization is the sensitivity of hydrogenase towards CO (Ragsdale, 2000). Hydrogenases are generally known to be inhibited by CO, where CO binds at the active site of the enzyme. This also supports the inability of *A. woodii* to use CO as sole energy source (Bertsch and Müller, 2015), since the electron-bifurcating hydrogenase and the HDCR is reported to be highly sensitive towards CO (Schuchmann and Müller, 2012; Schuchmann and Müller, 2013).  $H_2$  evolution from CO has been seen in the organisms containing CO-tolerant hydrogenase. CO-oxidizing,  $H_2$ -forming enzyme systems (Coo) is known in *Methanosarcina barkeri* (Bott and Thauer, 1987), *Rhodospirillum rubrum* (Kerby et al., 1995), *Carboxydotherrmus hydrogenoformans* (Svetlitchnyi et al., 1991) and *Thermococcus onnurineus* NA1 (Lee et al., 2008). *C. hydrogenogens* is specialized for CO metabolism. CO-oxidizing,  $H_2$ -forming enzyme purified from this organism has 6-subunit [NiFe]-hydrogenase which forms a complex with CooS (Ni-containing CODH) and CooF (an electron transfer protein) (Soboh et al., 2002). Similarly, *T. kivui* has the potential to grow on CO and resting cell experiments exhibited higher  $H_2$  evolution after addition of CO as compared to cells grown on glucose, indicating the hydrogenase activity is elevated in CO-grown cells (Schoelmerich and Müller, 2019). Genome of *T. kivui* encodes for monofunctional CO dehydrogenase (*cooS*) as well as for the bifunctional CODH/ACS (*acsA*) (Hess et al., 2014). The monofunctional CO dehydrogenase, CooS likely oxidizes CO and generates reduced ferredoxin which is used by the Ech complex to make hydrogen. The bifunctional CODH, AcsAB, catalyzes *in vivo* the reversal of the aforementioned reaction, the reduction of  $CO_2$  to CO, which is then condensed with a methyl group and CoA to give acetyl-CoA *via* WLP (Fig. 41). *In vitro*, it also oxidizes CO to  $CO_2$  and in some species also *in vivo*.



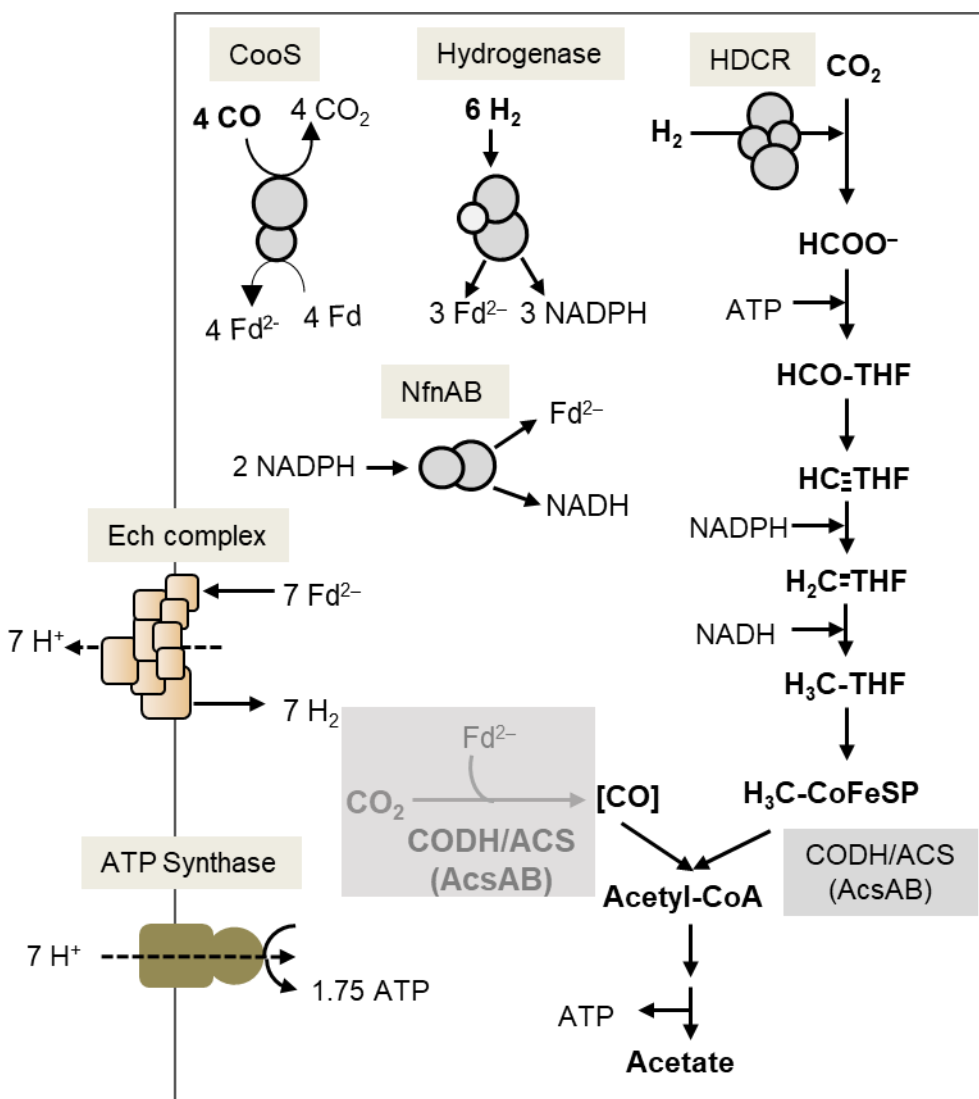


**Fig. 41. Model of electron and carbon flow in *T. kivui* from CO.** Oxidation of CO is catalysed by monofunctional CO dehydrogenase, CooS. Oxidation of CO reduces Fd<sup>2-</sup> which is utilised by energy converting hydrogenase, Ech complex in combination with the excess Fd<sup>2-</sup> produced from electron bifurcating hydrogenase, HydABC. Reversal of this reaction is catalyzed by bifunctional CODH, AcsAB to reduce CO<sub>2</sub> to CO that combines with methyl group and CoA to give acetyl-CoA. Reducing equivalents for WLP is provided by HydABC and transhydrogenase, NfnAB. Fd<sup>2-</sup>, Ferredoxin; THF, tetrahydrofolate; CODH/ACS, carbon monoxide dehydrogenase / acetyl-CoA synthase.

Lately, the focus is moving towards genetic approaches to understand acetogens on molecular level. For deletion of the *cooS* gene,  $\Delta pyrE$  (TKV\_MB002) was used as the parental strain according to the developed genetic system (Basen et al., 2018) using the usual substrate, glucose, for isolating mutants on solid media and indeed the *cooS* deletion mutants was obtained, as verified by PCR (Fig. 25). Later, when the phenotype

was examined *T. kivui*  $\Delta$ *cooS* strain did not grow on CO, which did fit the expectation. However, the parental strain  $\Delta$ *pyrE* (TKV\_MB002) also did not grow using the procedure as described in Weghoff and Müller, (2016), since this organism needs proper adaptation and metabolic changes to grow on CO. Thus, the actual phenotype of *T. kivui*  $\Delta$ *cooS* strain was inconclusive, since the parental strain also did not grow on CO. However, we could answer that by using a different approach by first deleting *pyrE* gene in “CO-adapted” wild type *T. kivui* and successfully *T. kivui*  $\Delta$ *pyrE* (CO-adapted) was obtained, as verified by PCR (Fig. 26). Later, the *cooS* gene was deleted again but using the new parental strain (CO-adapted  $\Delta$ *pyrE*), the mutant was genotypically analyzed and verified by sequencing (Fig. 27). When the *T. kivui*  $\Delta$ *cooS* mutant was incubated under 100% CO, growth was no longer observed whereas  $\Delta$ *pyrE* (CO) grew to the maximal OD<sub>600</sub> of 0.6 in the time frame of 5 days (Fig. 30A). However, growth was observed in the  $\Delta$ *cooS* mutant after 7 days, with 1.5 times lower growth rate as well as a lower final optical density. The complementation of the *cooS* gene in *T. kivui*  $\Delta$ *cooS* restored growth and the final optical density was comparable to the *T. kivui* wild type. Interestingly, this was not the case in minimal media, indicating that cells of the  $\Delta$ *cooS* mutant did not grow on CO but on a component of the complex media. Here, by markerless deletion of monofunctional CO-dehydrogenase, *cooS*, we have observed complete loss of growth on 100% CO in minimal media (Fig. 30B). This supports the previous data reported in Weghoff and Müller, (2016), where it was speculated based on expression analyses that *CooS* is involved in CO utilization. This consolidates the superiority of *CooS* during CO metabolism in *T. kivui*. In contrast to this, the dispensability of *cooS* was shown in the acetogen *Clostridium autoethanogenum* by mutational studies. This acetogen has two *cooS* genes. Deletion of *cooS2* had no significant effect on autotrophic growth, whereas deletion of *cooS1* led to a long lag phase, slower growth and lower optical density whereas the knockout of *acsA* (bifunctional CODH/ACS) led to a complete loss of growth on H<sub>2</sub> + CO<sub>2</sub> or CO (Liew et al., 2016a). Similar observation has been shown for the monofunctional CODH's in *Methanosarcina acetivorans* (Rother and Metcalf, 2004). Attempts to generate *acsA* deletion mutant in *T. kivui* failed so far, which is likely due to

its essentiality for WLP. However, deletion of *cooS* in *T. kivui* led to the complete loss of growth on CO, demonstrating that *AcsA* cannot compensate for a loss of *CooS*. Furthermore, the CODH activity was determined in cell-free extracts from  $\Delta cooS$  mutant compared to  $\Delta pyrE$  (CO) and the complemented strain. In CO-grown cells, the activity of  $\Delta cooS$  mutant was just 8% compared to the  $\Delta pyrE$  (CO), which indicates the majority of CODH activity is catalyzed by *CooS* in CO-growing cells. The CODH activity determined in the cell-free extract of glucose-grown cells in  $\Delta cooS$  mutant and the  $\Delta pyrE$  (CO) was quite similar. Interestingly, the complemented *cooS* strain had almost double the enzymatic activity, which could be due to the fact that expression of *cooS* was controlled by the strong promoter of the S-layer protein of *T. kivui*.

Since CO is an intermediate in the carbonyl branch of the WLP, we analyzed acetogenesis from  $H_2 + CO_2$  by resting cells and interestingly, deletion of *cooS* in *T. kivui* increased acetate formation from  $H_2 + CO_2$  in glucose-grown cells as well as in glucose + CO-grown cells (Fig. 32). Acetate formation was 3.9 times higher in the  $\Delta cooS$  mutant compared to wild type in glucose-grown cells. Similarly, in the glucose + CO-grown cells, the  $\Delta cooS$  mutant had 3.1 times higher acetate formation as compared to wild type. The resting cells of the *T. kivui*  $\Delta cooS$  mutant has also been reported to produce higher amounts of acetate from CO but the formate production was almost abolished, when cells were uncoupled (Schwarz et al., 2020). This demonstrates the essentiality of *CooS* for CO-coupled ferredoxin reduction to make hydrogen required for HDCR. It is conceivable that few acetogens utilize *CooS* to oxidize CO (+  $H_2O$ ) to  $CO_2 + H_2$ . It is estimated  $10^8$  tons of atmospheric CO can be removed from by microbial oxidation (Bartholomew and Alexander, 1979). Thus, introducing a cycle to minimize free CO concentrations (Liew et al., 2016b; Robb and Techtmann, 2018).

## Sources of carbon monoxide

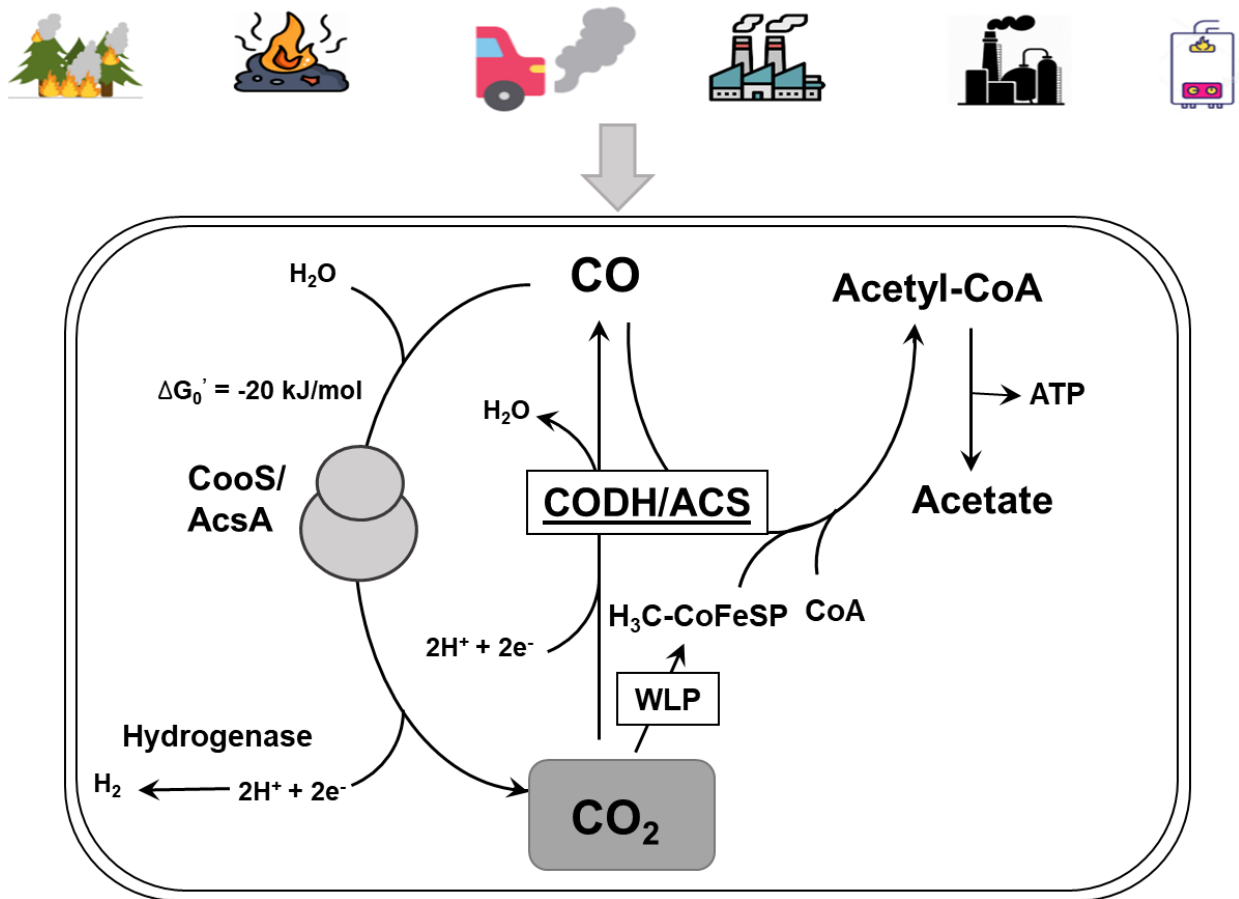


**Fig. 42. General model for CO cycle in acetogens (modified after Kung and Drennan, 2011).** The oxidation of CO generates CO<sub>2</sub> via monofunctional CO dehydrogenase (CooS/AcsA). Bifunctional CODH (CODH/ACS) complex catalyzes reduction of CO<sub>2</sub> to CO. This happens in the enzyme that has a tunnel to avoid escape of CO to the environment. CO is coupled to generate acetate by carbonyl branch of Wood-Ljungdahl pathway, WLP.

### 4.3 Effect of deletion of electron bifurcating hydrogenase (*hydAB*) in *T. kivui*

Alongside membrane-bound enzyme complexes, an electron bifurcating hydrogenase is involved in producing  $Fd_{red}$  required for energy conservation. Electrons for autotrophic growth on hydrogen and carbon dioxide are derived from the oxidation of  $H_2$ . *A. woodii* possesses a soluble hydrogenase HydABCD (Fig. 4), containing Fe-S centers and a flavin that couples the reduction of ferredoxin and NAD with oxidation of  $H_2$  (Schuchmann et al., 2018; Schuchmann and Müller, 2012). In *C. autoethanogenum*, the putative hydrogenase enzyme uses Fd and NADP as electron acceptor (Wang et al., 2013a). The genome of *T. kivui* has *hydA1* (Tkv\_c19580) followed by *hydB* (Tkv\_c19590) and *hydC* (Tkv\_c19600) (Hess et al., 2014) providing NADPH and  $Fd_{red}$  for the WLP (Katsyv et al., 2021, submitted). The bifurcating hydrogenase is also known to work in opposite direction during heterotrophic growth for example, in *Thermotoga maritima*, it has been described as hydrogen evolving enzyme where it utilizes ferredoxin and NADH synergistically to produce  $H_2$  (Schut and Adams, 2009).

With the markerless deletion of *hydA1B* genes of *T. kivui*, we were able to gain insights into the physiological function of the electron bifurcating hydrogenase. The deletion of the complete gene cluster of electron-bifurcating hydrogenase encoded by HydABC failed. Therefore, the two major subunits, encoded by *hydAB* were deleted. For deletion preparation, glucose plus formate was used as a substrate since the deletion of *hdcr* genes in *T. kivui* was prepared under similar conditions (Jain et al., 2020). Similarly, isolation of *hydA1B* mutant in *A. woodii* was successful when fructose was supplemented with  $H_2$  gas atmosphere (Wiechmann et al., 2020), therefore, it was hypothesized that for deletion of *hydAB* genes the addition of formate is essential for the organism to grow. Clean *hydAB* deletion mutants were obtained. The deletion of *hydAB* genes was detected by PCR using primers which binds outside the *hydAB* gene cluster whereby due to the gene deletion, a significantly shortened PCR product was amplified compared to the wild type. Half of the isolates showed the genotype of wild type since theoretically the chances of the loss of *hydA1B* gene was 50% (Fig. 36B). For the verification, an additional PCR

was performed with primers binding inside the *hydA1B* genes where no amplificate was observed, as expected (Fig. 36C).

#### 4.3.1 The physiological role of hydrogenase in the metabolism of *T. kivui*

Growth of the *T. kivui*  $\Delta$ *hydA1B* mutant was not observed when grown in the presence of  $H_2 + CO_2$  (Fig. 37A), since the ultimate source of electrons is molecular hydrogen which is oxidized by electron-bifurcating hydrogenases (Schuchmann and Müller 2012; Wang et al. 2013) to generate NADPH and  $Fd_{red}$  in *T. kivui* (Katsyv et al., 2021, submitted) which are then consumed in the WLP for acetate production as well as for energy conservation. Under autotrophic growth, deletion of electron bifurcating hydrogenase impaired the WLP. Interestingly and surprisingly, *T. kivui*  $\Delta$ *hydA1B* mutant grew in the presence of glucose as well as on mannitol (Fig. 37B&C) when used as a sole carbon source. This was completely opposite to what was observed in *A. woodii*, regardless of sharing high sequence identity to HydAB of *T. kivui*. Deletion of *hydAB* genes in *A. woodii* abolished the growth on sugars (Wiechmann et al., 2020), since *A. woodii* has only one hydrogen providing source (Schuchmann and Müller, 2012). The cell suspension experiments with the *T. kivui*  $\Delta$ *hydA1B* mutant showed no difference in acetate production with wild type. The ratio of 1:3 was obtained after 2.5 hours (Fig. 38).

The growth of *T. kivui*  $\Delta$ *hydA1B* on heterotrophic substrates was obtained, which implies the dispensability of electron-bifurcating hydrogenase in the heterotrophic metabolism of *T. kivui*. This raised the question how HDCR is fueled in *T. kivui* metabolism under heterotrophic conditions. Furthermore, the electron donor of methylene-THF dehydrogenase was determined in the cell-free extract of wild type *T. kivui* to understand the redox balancing. *T. kivui* catalyzed the reduction of  $NADP^+$  with methylene-THF as electron donor whereas,  $NAD^+$  was not reduced (Fig. 39), demonstrating the NADPH-specific methylene-THF dehydrogenase, which was assumed to be NADH, till now (Basen and Müller, 2017). In *M. thermoacetica*, Methylene-THF dehydrogenase is reported to be NADPH-specific where NADPH likely comes from NADH-dependent

reduced ferredoxin:NADP oxidoreductase (NfnAB) (Huang et al., 2012). An inspection of the genome sequence revealed genes for a NfnAB type transhydrogenase (Tkv\_c22270 and Tkv\_c22280) in *T. kivui*. NfnAB shares 57% and 69% identity to NfnA (Moth\_1518) and NfnB (Moth\_1517) of *M. thermoacetica*. This consolidates the presence of NfnAB that could provide NADPH as an electron donor to methylene-THF dehydrogenase in *T. kivui*. Conversion of NADP<sup>+</sup> or NAD<sup>+</sup> with reduced ferredoxin is catalyzed *via* Nfn or Stn-type transhydrogenases has been found in *Pyrococcus furiosus* and *Sporomusa ovata* (Nguyen et al., 2017; Kremp et al., 2020). Thus, the revised putative scheme during glucose oxidation in *T. kivui* has been demonstrated in Fig. 43. Reducing equivalents generated from the glycolysis are carried over to the reductive branch of WLP in which 2 mol of CO<sub>2</sub> are reduced to acetate whereby, a molecule of reduced ferredoxin, NADH and NADPH are needed.

Now that we know the HydABC of *T. kivui* is NADPH dependent and this NADPH is being provided by the NfnAB transhydrogenase (Katsyv et al., 2021, submitted) which together with the excess ferredoxin (supplied by glycolysis) produces hydrogen from electron bifurcating hydrogenase. In some organisms, hydrogenase is only responsible only for hydrogen oxidation rather than hydrogen formation as observed in the hyperthermophilic archaeon *Pyrococcus furiosus* (McTernan et al., 2014). This H<sub>2</sub> can be utilized via the Ech complex (Katsyv et al., 2021, submitted). Fig. 43 shows a hypothetical model of hydrogen cycling in *T. kivui* by coupling H<sub>2</sub> production by HydABC and H<sub>2</sub> consumption by Ech. The H<sub>2</sub> cycling mechanism for energy conservation has been postulated in various anaerobic organisms such as *Desulfovibrio* sp. (Odom and Peck Jr., 1981; Odom and Peck, 1984), *Methanosarcina* sp. (Lovley and Ferry, 1985; Kulkarni et al., 2018), *Geobacter* sp. (Coppi, 2005), and *Methanococcus* sp. (Lupa et al., 2008). However, the energy conservation in form of H<sub>2</sub> is not possible in *A. woodii*, since it lacks the membrane-bound hydrogenase. Recently, in *A. woodii* a novel type of hydrogen cycling has been described, referred as “intracellular syntrophy” (Wiechmann et al., 2020), where it combines the metabolic features of two syntrophic partners by connecting an oxidative and reductive metabolic module in one bacterial cell. It is still not clear how deletion of

*hydA1B* or *ech2* had no effect on the heterotrophic growth of *T. kivui* and needs to be further investigated.

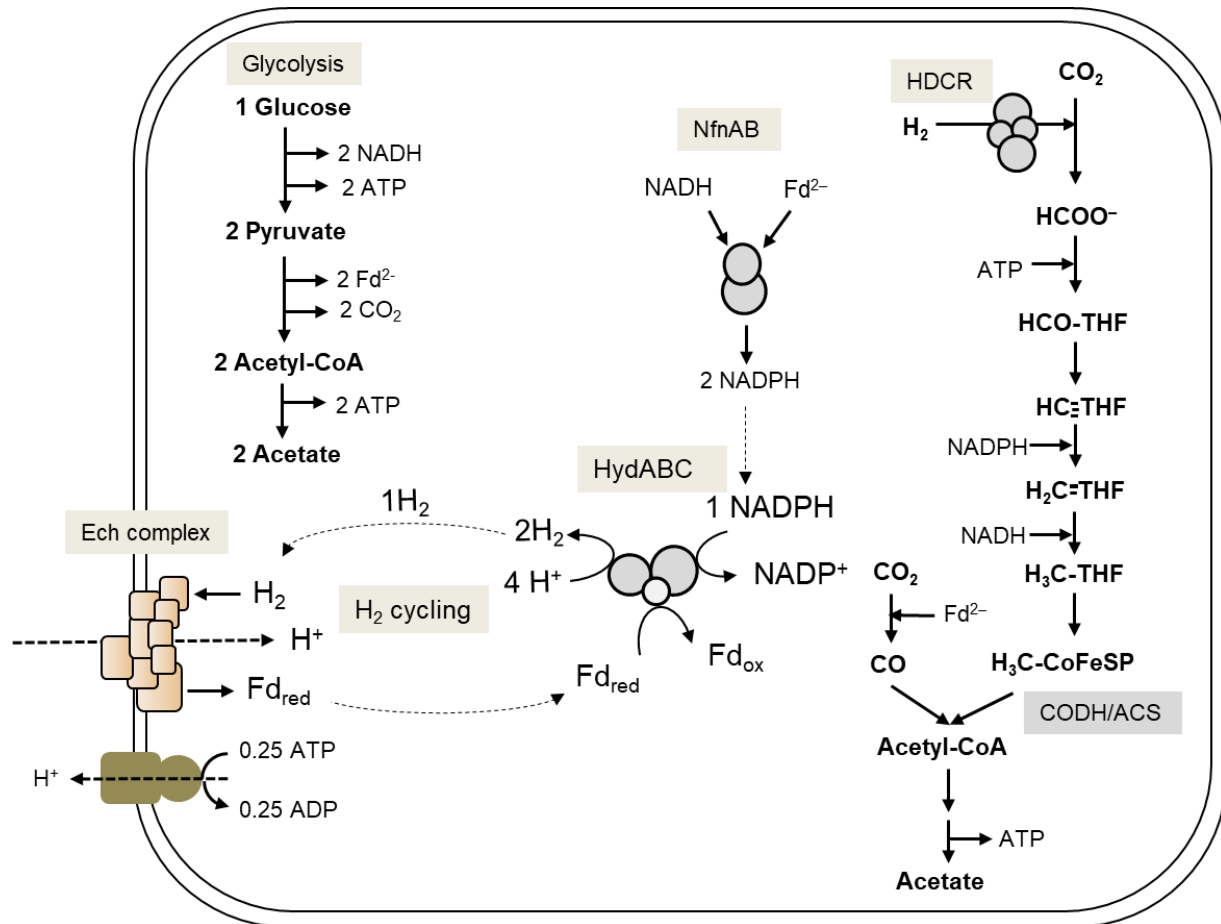


**Fig. 43. Model of electron and carbon flow in *T. kivui* when growing heterotrophically on glucose, involving the putative H<sub>2</sub> cycling.** The oxidation of NADPH and Fd<sub>red</sub> is coupled to generate H<sub>2</sub> via electron bifurcating hydrogenase (HydABC). H<sub>2</sub> can be used to reduce ferredoxin *via* Ech.



## 5. Conclusion

1. *Thermoanaerobacter kivui* was adapted to use maltose or trehalose as carbon and energy source with a maximal OD<sub>600</sub> of 1.12 and 0.73, respectively. Genes responsible for an ABC-type trehalose and maltose transport system and the hydrolase genes were found in the genome.
2. Formate served as an external electron acceptor for growth of *T. kivui* on mannitol in the absence of CO<sub>2</sub>. The doubling time was 2.0 h and the final OD<sub>600</sub> was 2.5, while in the absence of formate (or CO<sub>2</sub>) the maximal OD<sub>600</sub> observed was only 0.7 with the prolonged doubling time of 5.2 h. This experiment demonstrated CO<sub>2</sub>/bicarbonate can be replaced by formate.
3. The genes *fdhF*, *hycB3*, *hycB4*, *hydA2* and *fdhD* encoding for HDCR were deleted from *T. kivui*. The  $\Delta hdcr$  deletion mutant showed no growth on formate or H<sub>2</sub> + CO<sub>2</sub>, demonstrating the essentiality of HDCR for the CO<sub>2</sub> reduction to formate as well as formate oxidation. The complementation of the *hdcr* gene cluster in *T. kivui*  $\Delta hdcr$  strain restored the growth similar to wild type. The  $\Delta hdcr$  deletion mutant was no longer able to grow with glucose or mannitol or pyruvate, but growth on these substrates was restored by addition of formate to the medium.
4. The genome of *T. kivui* encodes a putative monofunctional CODH (CooS) and a bifunctional CODH (AcsAB) for CO metabolism. Deletion of *cooS* gene led to a complete loss of growth on CO. CO:MV oxidoreductase activity was almost abolished in the  $\Delta cooS$  mutant ( $14.9 \pm 2.5$  U/mg) when compared to the parental strain, CO-adapted  $\Delta pyrE$  ( $178.6 \pm 12.8$  U/mg), demonstrating that the majority of CODH activity is catalyzed by CooS in CO-grown cells. In contrast, CO:MV oxidoreductase activity measured in the cell-free extract of glucose-grown cells was similar in the  $\Delta cooS$  mutant ( $50.6 \pm 6.1$  U/mg) and the wild type ( $53.8 \pm 11.4$

U/mg), indicating that the monofunctional CODH CooS plays a superior role only during growth on CO.

5. The *hydA1B* genes encoding the electron bifurcating hydrogenase from *T. kivui* were deleted. The  $\Delta$ *hydA1B* mutant did not grow on H<sub>2</sub> + CO<sub>2</sub>. The provision of reducing equivalents by the electron bifurcating hydrogenase is therefore essential for autotrophic growth on H<sub>2</sub> + CO<sub>2</sub>. In contrast, the mutant was able to grow on glucose or mannitol demonstrating the dispensibility of HydABC in heterotrophic metabolism of *T. kivui*.
6. The electron donor of methylene-THF dehydrogenase was determined in the cell-free extract of wild type *T. kivui* using methylene-THF as an electron donor. *T. kivui* catalyzed the reduction of NADP<sup>+</sup> with a activity of  $24.4 \pm 1.2$  U/mg whereas, NAD<sup>+</sup> was not reduced. This experiment demonstrated that methylene-THF dehydrogenase in *T. kivui* is NADPH-specific.

## 6. Zusammenfassung

*Thermoanaerobacter kivui* ist ein thermophiles acetogenes Bakterium, das chemolithoautotroph auf  $\text{CO}_2$  unter Verwendung von molekularem  $\text{H}_2$  als Elektronendonator wächst und Acetat als Produkt über den Wood-Ljungdahl-Weg (WLP) bildet. Im WLP werden 2 Mol  $\text{CO}_2$  reduziert, um ein Mol Acetyl-CoA zu bilden. Erste Studien wurden durchgeführt, um die Physiologie von *T. kivui* zu verstehen. *T. kivui* wächst autotroph auf  $\text{H}_2 + \text{CO}_2$  und nach Adaptation auch auf CO oder Syngas. *T. kivui* wächst ebenfalls auch in Minimalmedium ohne weitere Zugabe von Vitaminen, was es zu einem Biokatalysator mit hohem Potenzial für die Produktion von Chemikalien mit hohem Mehrwert macht. Heterotroph wächst *T. kivui* auf Glucose, Fructose, Mannose, Pyruvat oder Formiat. Kürzlich wurde beschrieben, dass *T. kivui* in der Lage ist, auf dem Zuckeralkohol Mannitol in Gegenwart und Abwesenheit von  $\text{HCO}_3^-$  (oder externem  $\text{CO}_2$ ) zu wachsen. Allerdings war das Wachstum in Abwesenheit von externem  $\text{CO}_2$  deutlich verlangsamt. Daher wurde in dieser Studie getestet, ob eine Zugabe von externem Formiat das "fehlende"  $\text{CO}_2$  kompensieren kann. In Kombination mit Formiat wurde das Wachstum auf Mannitol in  $\text{CO}_2$  und  $\text{HCO}_3^-$  freien definierten Medien bis zu einer maximalen  $\text{OD}_{600}$  von 2,34 und mit einer Verdopplungszeit von  $2,0 \pm 0,0$  stimuliert, was dem Wachstumsverhalten auf Mannitol in Anwesenheit von  $\text{CO}_2/\text{HCO}_3^-$  entsprach. In Abwesenheit von Formiat (oder  $\text{CO}_2$ ) erreichte *T. kivui* nur eine endgültige optische Dichte von bis zu 0,7 mit einer verlängerten Verdoppelungszeit von  $5,2 \pm 0,2$  Stunden. Dieses Experiment zeigte die hohe metabolische Flexibilität von *T. kivui* durch die Nutzung von Formiat als Elektronenakzeptor, wenn kein oder nur wenig  $\text{CO}_2$  vorhanden ist.

Genomanalysen ergaben, dass *T. kivui* ein Trehalose- und Maltose-Transportsystem-Permeaseprotein (MalF) besitzt. Darüber hinaus verfügt *T. kivui* über Trehalose- und Maltosehydrolase-Gene, die als Kojibiose-Phosphorylase annotiert sind. Obwohl in der Originalveröffentlichung beschrieben wurde, dass der Organismus nicht auf Maltose oder Trehalose wachsen kann, konnte *T. kivui* im Laufe dieser Arbeit an das Wachstum auf

Maltose und Trehalose adaptiert werden. Nach dem Transfer von einer Glukose-Vorkultur auf ein Medium mit 25 mM Maltose oder 25 mM Trehalose als alleinige C-Quelle wurde kein Wachstum erzielt. Bei Verwendung der gleichen Vorkultur in einem Medium mit höherer Konzentration (50 mM) Maltose oder Trehalose, begannen die Zellen zu wachsen. Bei Verwendung dieser adaptierten kulturen als Vorkultur wuchsen die Zellen in Gegenwart von in 25 mM Maltose oder Trehalose bis zu einer maximalen OD<sub>600</sub> von 1,12 bzw. 0,73. Die Adaptation hing mit der Tatsache zusammen, dass der Organismus eine höhere Konzentration benötigt, um sich an diese Kohlenstoffquellen zu gewöhnen. Durch diese Daten wird das heterotrophe Potenzial von *T. kivui* erhöht.

Um die Bedeutung der wasserstoffabhängigen Kohlendioxidreduktase (HDCR) während des Wachstums auf Formiat oder auf H<sub>2</sub> + CO<sub>2</sub> im Stoffwechsel von *T. kivui* zu verstehen, wurden Studien auf molekularer Ebene durchgeführt. Die HDCR nutzt H<sub>2</sub> direkt für die Reduktion von CO<sub>2</sub> zu Formiat im ersten Schritt des Wood-Ljungdahl-Wegs (WLP). Um die Rolle der HDCR in dieser Reaktion zu untersuchen, wurde das *hdcr*-Gencluster mit Hilfe des kürzlich entwickelten Mutagenesytems für *T. kivui* deletiert. In Wachstumstudien konnte anschliessend gezeigt werden, dass die  $\Delta$ *hdcr*-Deletionsmutante nicht mehr auf Formiat oder H<sub>2</sub> + CO<sub>2</sub> als alleiniger Kohlenstoffquelle wachsen konnte. Nach Komplementation der Mutante mit dem *hdcr*-Gene *in cis* wuchsen die Kulture wieder auf Formiat oder H<sub>2</sub> + CO<sub>2</sub>. Diese Experimente zeigten, dass die HDCR für das Wachstum auf H<sub>2</sub> + CO<sub>2</sub> oder Formiat essentiell ist. Interessanterweise konnte in der  $\Delta$ *hdcr*-Mutante ebenfalls ein verändertes Wachstum auf Glukose als alleiniger C-Quelle festgestellt werden. Die *T. kivui*  $\Delta$ *hdcr*-Mutante wuchs nur bis zu einer OD<sub>600</sub> von 0,2, während der Wildtyp und der *hdcr*-komplementierte Stamm bis zu einer OD<sub>600</sub> von 2,64 bzw. 2,4 wuchsen. Damit wurde bewiesen, dass die HDCR auch für die vollständige Glukoseoxidation in *T. kivui* erforderlich ist. Durch die Zugabe von Formiat wurde das Wachstum vollständig wiederhergestellt, ähnlich wie beim Wildtyp. Dies belegt wieder die Nutzung Formiat als terminalen Elektronenakzeptor. Auch auf Mannitol oder Pyruvat konnte die Mutanten nur in Gegenwart von Formiat wachsen. Der Substratverbrauch und die Produktbildung der *T. kivui*  $\Delta$ *hdcr*-Mutante wurden in einem

Zellsuspensionsexperiment untersucht. Die Zellen verbrauchten Formiat nur in Gegenwart von Glukose und produzierten Acetat mit einem Acetat/Substrat-Verhältnis von etwas mehr als 3,0, während die Acetatproduktion nur 12 mM betrug, wenn Glukose als alleiniges Substrat verwendet wurde. Diese Ergebnisse zeigen eine enge Kopplung der Oxidation von Multikohlenstoffsubstraten an den WLP.

*T. kivui* ist eines der wenigen Acetogenen, die CO als einzige Kohlenstoff- und Energiequelle nutzen können. Die Entschlüsselung der Genomsequenz von *T. kivui* ermöglichte die Identifizierung von zwei Genen, die möglicherweise für eine Kohlenmonoxid-Dehydrogenasen (CODH) kodieren, die an der CO-Verwertung beteiligt sind. Das Gen *cooS*, das für die monofunktionale CO-Dehydrogenase kodiert und das Gen, *acsA*, welches für die CODH-Komponente des bifunktionalen CODH/ACS-Komplexes kodiert. Beide Gene werden von dem Gen *cooF* flankiert, das möglicherweise für die Übertragung von Elektronen auf eine membrangebundene Hydrogenase verantwortlich ist. *cooS* wurde in dem an CO angepassten Wildtyp von *T. kivui* genetisch deletiert, was dazu führte, dass die Mutante nicht mehr in der Lage war, auf CO in Minimalmedien zu wachsen. Um zu überprüfen, ob die Deletion von *cooS* das Wachstum auf CO beeinträchtigt, wurde das Gen in der  $\Delta cooS$ -Mutante wieder komplementiert. Der komplementierte Stamm wuchs wieder auf CO und erreichten eine ähnlich finale OD wie der Wildtyp. Dieser Wachstumphänotyp der  $\Delta cooS$ -Mutante, die aus dem CO-adaptierten Stamm generiert wurde, zeigt, dass *CooS* für den CO-Stoffwechsel essentiell ist. Bei der  $\Delta cooS$ -Mutante wurden keine wesentlichen Auswirkungen auf das Wachstum auf  $H_2 + CO_2$ , Glukose, Mannitol, Formiat auf  $H_2 + Formiat$  beobachtet. Eine genauere Untersuchung der CO:MV-Oxidoreduktase-Aktivität im zellfreien Extrakt ergab eine signifikant niedrigere Aktivität in der  $\Delta cooS$ -Mutante (8 %) im Vergleich zum Wildtyp bei Wachstum mit CO. Damit wurde die Hypothese unterstützt, dass der Großteil der CODH-Aktivität auf CO-gewachsenen Zellen durch die monofunktionale *CooS* katalysiert wird. Allerdings war die CODH-Aktivität im zellfreien Extrakt von auf Glukose gewachsenen Zellen in der  $\Delta cooS$ -Mutante und im Wildtyp ähnlich, während der komplementierte *cooS*-Stamm fast die doppelte enzymatische Aktivität aufwies, was darauf zurückzuführen sein

könnte, dass das zusätzliche *cooS*-Gen im Plasmid durch den starken Promotor des S-layer-Proteins von *T. kivui* kontrolliert wurde. Das Zellsuspensionsexperiment wurde durchgeführt, um die Acetogenese aus  $H_2 + CO_2$  zu verstehen, wobei CO ein Zwischenprodukt des Stoffwechsels über WLP ist. Die Acetatbildung durch die ruhenden Zellen der  $\Delta cooS$ -Deletionsmutante führte zu einer 4-fach höheren Acetatmenge im Vergleich zum Wildtyp in auf Glukose gewachsenen Zellen bzw. zu einer etwas mehr als 3-fach höheren Acetatmenge in auf Glukose und CO gewachsenen Zellen. Offensichtlich steht in der *cooS*-Mutante mehr Kohlenstoff für die Synthese von Acetat zur Verfügung.

Ein weiterer Schwerpunkt dieser Arbeit war es, die Rolle der bifurkierenden Hydrogenase (HydABC) im Stoffwechsel von *T. kivui* auf molekularer Ebene zu verstehen. Die Elektronen für das lithoautotrophe Wachstum auf Wasserstoff und Kohlendioxid stammen aus der Oxidation von  $H_2$ , katalysiert durch die HydABC-Hydrogenase. Die *hydAB*-Gene, die für die Hauptuntereinheiten des Enzyms kodieren, wurden genetisch deletiert. Nach der Deletion der *hydAB*-Gene zeigte die Deletionmutante kein Wachstum mehr auf  $H_2 + CO_2$  als alleiniger Energiequelle. Dieser Phänotyp bestätigte eindeutig, dass die bifurkierende Hydrogenase essentiell für die Bereitstellung von Elektronendonoren im WLP ist. Um die Rolle dieser bifurkierenden Hydrogenase im heterotrophen Stoffwechsel von *T. kivui* zu untersuchen, wurden physiologische Studien mit Glukose oder Mannitol in kohlenstoffhaltigen Medien durchgeführt. Die Deletion von *hydA1B* hatte keine Auswirkung auf das Wachstum in Gegenwart von Glukose oder Mannitol in kohlenstoffhaltigen komplexen Medien und die beobachtete optische Enddichte ( $\sim 2,5$ ) war mit der des Wildtyps vergleichbar, was auf die Entbehrlichkeit der bifurkierenden Hydrogenase im heterotrophen Stoffwechsel von *T. kivui* schließen lässt. Die vorläufigen Ergebnisse des Wachstumsverhaltens der  $\Delta hydA1B$ -Mutante auf Glukose in kohlenstofffreien Minimalmedien zeigten ein beeinträchtigtes Wachstum. Während der Wildtyp nach 3 Tagen die endgültige optische Dichte von 2,0 erreichte die Mutante nach 3 Tagen eine OD von 0,13. Es ist unklar, wie das Redox-Gleichgewicht in Abwesenheit von Carbonat gestört wird, dass muss in Folgestudie untersucht werden. Die Zellsuspensionsexperimente von *T. kivui*  $\Delta hydAB$  in Gegenwart von 10 mM Glukose

zeigten ein ähnliches Acetatproduktionsprofil wie beim Wildtyp. Nach 3 Stunden wurde das Acetat/Glukose-Verhältnis von 3 erhalten.

Aus den obigen Ergebnissen wurde abgeleitet, dass die Versorgung mit Elektronendonoren im heterotrophen Stoffwechsel von *T. kivui* durch den NfnAB-Transhydrogenase Komplex erfolgt, welcher in Genomanalysen bereits identifiziert werden konnte. Zu diesem Zweck wurde der Elektronendonator der Methylen-THF-Dehydrogenase im zellfreien Extrakt des Wildtyps von *T. kivui* bestimmt. *T. kivui* katalysierte die Reduktion von NADP<sup>+</sup> mit einer Aktivität von  $24,4 \pm 1,2$  U/mg, während NAD<sup>+</sup> unter Verwendung von Methyl-THF als Elektronendonator nicht reduziert wurde. Diese Ergebnisse belegen, dass die Methylen-THF-Dehydrogenase NADP spezifisch ist. Das NADPH wird aus dem im stoffwechsel wahrscheinlich über die NfnAB-Komplex aus NADH und reduzierten Ferredoxin generiert

## 7. Appendix

### 7.1 Deletion of the *hdcr* gene cluster in *T. kivui*

#### 7.1.1 UFR of *hdcr* gene cluster

TAAAGTTTAGTGCATTACCCCTAAAATAATGGTAGTTTTGCAGAAGAAAGGGTGGACTTTTTCTCTTGG  
AATTGTTTAAAACGGCTGTAATGCTGGCAGGCGGTAAGAGCAAACGAATGGGTTTTGACAAATGTAT  
GCTTAAAGTTCAAAATTGTTTTTAAAGTAAAATGATTATCAAAAATCTTAGAAAAGTTTTCGATGACAT  
AGTGGTGGTTACATGGAATAAGGAATTTTATCAGAATTTCAATGTAAGGGTGGTACATGATGAACTT  
CAAGGGATAGGACCTTTAGGGGGTATTCATGCAGGATTAAGCCTCTTTAAGCCACTATGCCTTTT  
TTATTGCCTGCGATATGCCTTTTATTTCCATACCGTACATAGAATATATGATGGAGCTTTTGAAAAG  
TTTAAAAAGATGTCATTATCTCTGAAAACAGAGGCTTCATTGAGCCCTTTTCATGCCTTTTATTCAA  
AGCTACTATTGACAAAATTGAAGAGTGTTATAAAGAAAACAACTGAAGATCGCAGATTTTTTAAAGA  
AGGTAGATGTGATAAAAGTAAAAGAAGAAAATGTGCGAAAATTTTCATCTGAGCTTGAAATATTTATA  
AACTTAAATAATCCCGAAGATGTTGTTAGATTTGAAGCAATAATCAAAAGTGCAGAAAAGTATAATTC  
ATAAGTAAAAAATTTAAAAGGCTTTTGAAATCAAATTGGTTCCTAAAACCTTTCTACTAAAGAGGTTTT  
ATACCATGTTTTTTTTGTGTAATTAACCTAAAATATGATATTTACTTGACCTAATTTTTATGATAAAATGT  
TAAAAAGTATACCTTGATAAATATTATTTTAGCAAGTAAAATAATATAAAATGCATTTCTTTTAATAG  
CCTCTTAAGATGTGTTAATCTAATTTGCAAAGAATCTTCAAATTCAGGCAATAAGCCCCACAAATAT  
GGTAAATATTTGCCTTTCTGCTTTGTTATAAGAGGAGGTTTTGTT

#### 7.1.2 DFR of *hdcr* gene cluster

AAATTTTGTGGTAGTGGGTTGTAAACAATCCTGTGAGAATAAGGCATGGCGTAAAGCTACCAAACCTT  
CTCACGAAGTCTCAACCTTTGAAGGTGGGAGTAGTTCACGAAATCTCTTAAGGAGGAAGTGAATGGA  
ATCATTAAAAGTATTAATATTTTAAAATACAAAATGGTTTGGTTGAAAGCTTTTCAGATAGTGTGATT  
GTAGAATATATCTTAAAGCTTTATGTAAACGCTATTGAGTTTGCATCTTTTTCTGCACTCCTTTAGCAT  
TAGATTGTTTGGTTGTAGGATACCTTCAGTCCAAGGCATTATTGAAAAAAGAGGATATAAAGAGA  
ATCTTTATTGAAGAAAGAGAAGGGAAAGCTCATGTGAAATTCTTAAAAGTATAGATGCTTCTTCAGT  
GAAGAATCTATTTATAATGAGTAGCGGAGAAAAAACATTTGTTTTCATGATCAGTTAAAGATAGGCAA  
GACCTGTTGCTCACTGCAACTTCACATGCAATCCCTGCATTTGTTTTCTGAGCAGTTAAACATAGGCC  
CAATAACAAGCAACATTAATAACAAGTTAAAGGATATAATCAATCTATCAGAGAGATTTAACAATGGCT  
CGGGCTTGTCAAGATAACAGGGGGAGTACACAGCTGTGCGATTGCTGATGACAAGGATTTTATAAT



TTTTTCATGAAGATATAGGTAGGCATAACGCTTTTGATAAAGCGTTTGGGCAGGCTCTTTTAGATGGTA  
TAGACCTTCAGGATAAAGCTGTTTTACAAGCGGAAGGATATCCGTTCGAAATGTTATTAAGCAGCT  
AAAAGGAAGGTACCTGTAGTGGTGTCCATTCAGCTCCTACTGCTTTAGCCGTTGAGGTTGGAAGAA  
AATTAACATAAC

## 7.2 Deletion of *cooS* gene in *T. kivui*

### 7.2.1 UFR of *cooS* gene

GCAGGAAGATTGGAAGTCATGAGGAAACAGCCTTATGTGGTGATAGATGGAGCTCATAATCCTCAAG  
GAATTTCTGTGCTAAAAAATTCTTTAAAGCTATTTAATTACGACAGACTGATTCTTGTGGTAGGGATGC  
TTAAGGACAAGGACACTCAAATATGCTTAATATAATTGTGCCAAAGGCGGATGTAATAATAACGACG  
ATGCCAATAAGTGAAAGAGCTTATAGGGCAAGTGAAGTTGCACAAAAGATAGATAAAGAAAACGTAAT  
TCCAATTGAAAATATTGAAGAGGCGGTAAAATACGCCCTTGATATAGCTAAGGAAGAGGATATGGTG  
CTTTTTTGTGGGTCCTCTACATGATAGGTCATGTGAGATCATTACTTAAAAAGGTAATATTTAAGGGA  
GGGTTTTAATATAATGTAAGGTGTAAGGACATAATAAGAAGGTGGTTGTTATGGAAATAAATAACT  
ACGTTGCTACAGGAGATAGATAAGGCACTAAAGGTTATGAAAGAAGCAGAGAGAAATTTGGAGATGA  
TAGAAAATGACAACTACCTTAAGACGAAATTGGCGAGATTAATAACGATTTTGAAGGCAGGAGTAT  
ATAAGACTTTTGGAGAATTGCCAAAGAACAATAAAAGTACAACATGAATGAGCTGATGGAAAAAAT  
AATAGACGCATGATAAAAGCAGTTTTGTTTTATCGAATTATTATAAGAATAATAGCTTATCTCAAAATTA  
TTAATGTAGGCCTTATGTGAGAAATAATTAATTTTATTTCCACATAAGGCAATTTTCATCTTAACATTCA  
TTCTGTTGCTACGCTCTAGCACAAAAGTGTATAAAGACAAGTGTATAGTTCTTGTGTAATCATTTTAAA  
TTAAAAACAACATTAAGCGAAAAAATTATTAATTAGTATTGACTTTGATTTATAATGAAAGTAAAATT  
ATATTATAACAATAAATAAATAAAAAAGGAGTTGTGATAATA

### 7.2.2 DFR of *cooS* gene

ATTGAAAAATATGGGAGGAATAAAATATGGATGTCAAAGCGGCACAAAATATATATTTGCTGATATA  
AAAAATGTCTCGGATGCCGTTGCTGCGAACAAGCCTGTGCTGATGCTAATGGAAACCGACCATATT  
GGGAGCTTTTAGGGTCTGGAATTCCTTTAAGCCCAATATAAATATTTTATATATTTTCTACAGGATA  
AAAATTATCCTGTTATGGCTCAGGCAGTATGCCGACAATGTGAAGATGCTCCTTGTGTTAAAATATGT  
CCGGTAAAGGCTATAAGTGTAAATCCAGACGGTATAAAAGTAATTGATAAACAGCGTTGTATTGGATG  
CCACAGTTGCTCAATTGTATGTCCTTTTGGTGCAGTATATATTCCGGATAAACATGCCGTTGCGACAA  
AGTGTACACTTTGCATAGAAAGAAAAGGTGCGGAAGGGCAACCAGCCTGCGTAGAGGCGTGTCCAA

ACGGTGCTTTGCAATTAGTTGATACAAAAGAAATTGGACGGGAAAAAGTCAAAAAAATCGTTAGTGAC  
ACATTCTCAAATAAATAATAAACTCCCCATCAAAGGGACTCCCCATAAGGTTTGTCAACAACTAAA  
GCGGTCTTTTGACCGCTTAATTTATTGCTCAGGTATTTTGGTTTCTTCGTGAAAATCGCATTTAGAATC  
TTTAAAGGCAATGCAAAAGCCGCTACAATTATAGATGCATGTAATTGCATTACATTTCTTCATACATTT  
AAGAGGTATATTTGCTGGCTTTGAAGAGCGCATAAATGCTATTTCTAAATAATTCATAGTAATCGCCCT  
TTCTAGTTTGATAACTTTATTATAGACATAATTCATTTATCTGTGAAATGCGGGTTTTATTTCACTTATT  
GAAAAAGAGAAAGAGTGTGGTAAATGAATATTGCGTCGGGGCATGGCGCAGCGGTAGCGCGCGC  
GGTTCGGGACCGTGAGGTCGCAGGTTCAAATCCTGTTGCCCGACCAG

### 7.3 Deletion of *hydAB* gene in *T. kivui*

#### 7.3.1 UFR of *hydAB* gene

CCACCTTCATATGACACAGCCCCAGTTAGCCAAGCAATTGCCGAACCTTGAGGAATATTATGGAGTA  
AAACTGTTTGAACGCTTTGGGCGAAAAATCTATCTTACCAACGAAGGTGAAAACTCTATTCGTATGC  
TTCTCACATATTGGCTTTGGCAGATGAAGCACAAAAGCAGCTTTTGGACCTTTCTCAAACGGCATCT  
TGCGAGTTGGAGCAAGTATGACAATTGAACTGCAATTTTGCCCTTTATAATAAAAGATTTTTATCAAT  
CTTACCCTAAGACTTATATTCAACCAGTGGTGGACAACACCACAACAATAATTAATGATTGAACT  
GCCAAGCTTGATATGGCCATCGTAGAAGGGCTGGTCTCAAGCGCAGATATAATCAAATTCCTGTAT  
ATGATGATGAACTTGTTTTGATATGTCCGTCAGAGCATCCATATGCAAAGAAAAAGATAATTGAACCC  
CACGAGCTTGAAAATCAGCACTTTGTGATTCGCGAGGAAGGAAGCGGAACACGCGAAATTTTTGAAG  
CCGCCATGCACGAATATAACATCAAATGGAATATTGCAGGAGTGTTAACAGCACTGAAGCAATCATC  
AACGCCGTTCACTGCGGCTTGGGCTTTTCATTCATATCTCAACTTTTAGCCGATGAAGCTATAAAAAG  
GCAAAAAGTGGAAGTGGTAAAAGTTCCTAACTCAAATCAAGCGCAAATTCATATCGTATACCATA  
AGAACAAGTTCATCTCTAATGCTATGGAAAAATTCTTAGGCTATTGCCAAAGATATTTTGGTTCTATAG  
CATATGTTGGGGTGGGTAAGAACCACCTTTTCAATGTATGAAATTGCTAACAATTACGTTATATTTTGA  
TATGAAAATAAGGGCAGGCATTCAGAAAATACCTACCCCAACTCTAACAAAGAACCTTAATTTTTT

#### 7.3.2 DFR of *hydAB* gene

TTAAACCACACCTCCCACAATCATACTTAATTTTTATTGTGCAGAAGCTGCTGCTTCCACATCACTGTA  
CTCTTTTAATACCTCGCTAACCTTCTCAGGAGTCATTTTACCATAAGTTTTTTCATTTACCATGACAGT  
TGGTGCCAAACCGCATGCACCAAGACATCCAACTCTCTCAAAGTGAATTTCAAATCACTTGTGGTC  
TCTCCAGCTTTAATACCCAACTGCTTCTCGAACTCCGCAAGAATTTTGTAGCACCTTTAACATGGCA

AGCAGTCCCAAGACAAACTCTGATAACATATTTCCCCCTTGGTTTTAGATGGAAGTGTGCATAGAAAG  
TAGCAACACCATAAATCTTGCTGGCAGGAATTCCTGTTTTGCTTGCAATGTAGAAAATTACATCTTCA  
GGCAAATATCCAAATTCATGTTGAACATGCTGAAGAATAGCGATAAGCGCTCCTCTCTCATTGCGAG  
CTTGGATAATATCTCATCGACTTTCTCAAACCTTGGATCTTTACTTCCTTTGCAGCAGCAATTACACAT  
CAGATTTAAACCTCCTTTAAACATTTTTAATTTAATAATATTAGTAAACTTATAAATTATTAGCACAGC  
CCAAAATGATAAAATTCACGTTGCGTTTTAGTACTTTAATCCTGTTATTAAACCTTTTTCAATTTCTTCT  
TACCTCACCTCCAGAATTTAGCTTCCACCACCTTGCAACACCTTTCTTTCAAGCTATGGGCTACTCAC  
AACTCAAACATCTCTTCTAACTCCTTTTTGCCCTTGACTGAGCTTAGGCCTTTTAACACAAGACAA  
CACCTCTCTTCCGCAACTTTTGAATTTTGTTTCATGTTATCACCTCCTGGTTATGGGTTTTTCTGTCAC  
TTATTTTTTTTACCATGAGGGTTTTGTTTTTGCAAAGACTATTTTAATTTATTAGGAATTCTCGTATATAA  
AAATTCCTCTTTACAAATTTTCTCCTGTTGTTGTCATCGC

## 8. References

- Aufurth, S., M. Madkour, F. Mayer and V. Müller (1998) Structure of the Na<sup>+</sup>-driven flagellum from the homoacetogenic bacterium *Acetobacterium woodii*. FEBS Lett. **434**: 325-328.
- Balch, W. E., S. Schoberth, R. S. Tanner and R. S. Wolfe (1977) *Acetobacterium*, a new genus of hydrogen-oxidizing, carbon dioxide-reducing, anaerobic bacteria. Int. J. Syst. Bact. **27**: 355-361.
- Bartholomew, G. W. and M. Alexander (1979) Microbial metabolism of carbon monoxide in culture and in soil. Appl. Environ. Microbiol. **37**: 932-7.
- Basen, M., I. Geiger, L. Henke and V. Müller (2018) A genetic system for the thermophilic acetogenic bacterium *Thermoanaerobacter kivui*. Appl. Environ. Microbiol. **84**: e02210-17.
- Basen, M. and V. Müller (2017) "Hot" acetogenesis. Extremophiles **21**: 15-26.
- Bertsch, J. and V. Müller (2015) CO metabolism in the acetogen *Acetobacterium woodii*. Appl. Environ. Microbiol. **81**: 5949-5956.
- Bertsch, J., C. Öppinger, V. Hess, J. D. Langer and V. Müller (2015) Heterotrimeric NADH-oxidizing methylenetetrahydrofolate reductase from the acetogenic bacterium *Acetobacterium woodii*. J. Bacteriol. **197**: 1681-1689.
- Biegel, E., and V. Müller (2010) Bacterial Na<sup>+</sup>-translocating ferredoxin:NAD<sup>+</sup> oxidoreductase. Proc. Natl. Acad. Sci. U.S.A. **107**: 18138-18142.
- Biegel, E., S. Schmidt, J. M. González, and V. Müller (2011) Biochemistry, evolution and physiological function of the Rnf complex, a novel ion-motive electron transport complex in prokaryotes. Cell. Mol. Life Sci. **68**: 613-634.
- Bonam, D., L. Lehman, G. P. Roberts and P. W. Ludden (1989) Regulation of carbon monoxide dehydrogenase and hydrogenase in *Rhodospirillum rubrum*: effects of CO and oxygen on synthesis and activity. J. Bacteriol. **171**: 3102-3107.
- Bott, M. and R. K. Thauer (1987) Proton-motive-force-driven formation of CO from CO<sub>2</sub> and H<sub>2</sub> in methanogenic bacteria. Eur. J. Biochem. **168**: 407-412.

- Bradford, M. M. (1976) A rapid and sensitive method for the quantification of microgram quantities of protein utilizing the principle of proteine-dye-binding. *Anal. Biochem.* **72**: 248-254.
- Breznak, J. A., J. M. Switzer and H. J. Seitz (1988) *Sporomusa termitida* sp. nov., an H<sub>2</sub>/CO<sub>2</sub>-utilizing acetogen isolated from termites. *Arch. Microbiol.* **150**: 282–288.
- Bryant, M. P. (1972) Commentary on the Hungate technique for culture of anaerobic bacteria. *Am. J. Clin. Nutr.* **25**:1324-8.
- Buckel, W. and R. K. Thauer (2013) Energy conservation *via* electron bifurcating ferredoxin reduction and proton/Na<sup>+</sup> translocating ferredoxin oxidation. *Biochim. Biophys. Acta.* **1827**: 94-113.
- Ceccaldi, P., K. Schuchmann, V. Müller, and S. J. Elliott (2017) The hydrogen dependent CO<sub>2</sub> reductase: the first completely CO tolerant FeFe-hydrogenase. *Energy. Environm. Sci.* **10**: 503-508.
- Clark, J. E. and L. G. Ljungdahl (1984) Purification and properties of 5,10-methylenetetrahydrofolate reductase, an iron-sulfur flavoprotein from *Clostridium formicoaceticum*. *J. Biol. Chem.* **259**: 10845-10849.
- Cook, G. M., J. B. Russell, A. Reichert, and J. Wiegel (1996) The intracellular pH of *Clostridium paradoxum*, an anaerobic, alkaliphilic, and thermophilic bacterium. *Appl. Environ. Microbiol.* **62**: 4576-4579.
- Coppi, M. V. (2005) The hydrogenases of *Geobacter sulfurreducens*: a comparative genomic perspective. *Microbiology* **151**: 1239–1254.
- Crable, B. R., C. M. Plugge, M. J. McInerney and A. J. Stams (2011) Formate formation and formate conversion in biological fuels production. *Enzyme Res.* **2011**: 532-536.
- Daniel, S. L., T. Hsu, S. I. Dean and H. L. Drake (1990) Characterization of the H<sub>2</sub>-dependent and CO-dependent chemolithotrophic potentials of the acetogens *Clostridium thermoaceticum* and *Acetogenium kivui*. *J. Bacteriol.* **172**: 4464-4471.
- Daniels, L., G. Fuchs, R. K. Thauer and J. G. Zeikus (1977) Carbon monoxide oxidation by methanogenic bacteria. *J. Bacteriol.* **132**: 118-126.
- Diekert, G. B. and R. K. Thauer (1978) Carbon monoxide oxidation by *Clostridium thermoaceticum* and *Clostridium formicoaceticum*. *J. Bacteriol.* **136**: 597-606.

- Diender, M., A. J. Stams and D. Z. Sousa (2015) Pathways and bioenergetics of anaerobic carbon monoxide fermentation. *Front. Microbiol.* **6**: 1275.
- Dobbek, H., V. Svetlitchnyi, L. Gremer, R. Huber and O. Meyer (2001) Crystal structure of a carbon monoxide dehydrogenase reveals a [Ni-4Fe-5S] cluster. *Science* **293**:1281-1285.
- Drake, H. L., S. Daniel, K. Küsel, C. Matthies, C. Kuhner and S. Braus-Strohmeyer (1997) Acetogenic bacteria: what are the *in situ* consequences of their diverse metabolic diversities? *Biofactors* **1**: 13-24.
- Drake, H. L., A. S. Gößner and S.L. Daniel (2008) Old acetogens, new light. *Ann. N. Y. Acad. Sci.* **1125**: 100-128.
- Drake, H. L., S. I. Hu and H. G. Wood (1981) Purification of five components from *Clostridium thermoaceticum* which catalyze synthesis of acetate from pyruvate and methyltetrahydrofolate. *J. Biol. Chem.* **56**: 11137-11144.
- Drake, H. L., K. Küsel and C. Matthies (2006) Acetogenic Prokaryotes. In: *The Prokaryotes*, edited by M. Dworkin, S. Falkow, E. Rosenberg, K.-H. Schleifer and E. Stackebrandt. Springer, New York, pp. 373.
- Eisenbrand, G. (2006) Römpp-Lexikon Lebensmittelchemie. Lebensmittelrecht. Thieme, Stuttgart, S. 494 f.
- Ensign, S. A. and P. W. Ludden (1991) Characterization of the CO oxidation/H<sub>2</sub> evolution system of *Rhodospirillum rubrum*. Role of a 22-kDa iron-sulfur protein in mediating electron transfer between carbon monoxide dehydrogenase and hydrogenase. *J. Biol. Chem.* **266**: 18395-18403.
- Ferry, J. G. (1990) Formate dehydrogenase. *FEMS Microbiol. Rev.* **87**: 377-382.
- Fiala, G. and K. O. Stetter (1986) *Pyrococcus furiosus* sp. nov. represents a novel genus of marine heterotrophic archaeobacteria growing optimally at 100°C. *Arch. Microbiol.* **145**: 56-61.
- Fischer, F., R. Lieske and K. Winzler (1932) Biologische Gasreaktionen. II. Über die Bildung von Essigsäure bei der biologischen Umsetzung von Kohlenoxyd und Kohlensäure zu Methan. *Biochem. Z.* **245**: 2-12.

- Fontaine, F. E., W. H. Peterson, E. McCoy, M. J. Johnson and G. J. Ritter (1942) A new type of glucose fermentation by *Clostridium thermoaceticum*. *J. Bacteriol.* **43**: 701-715.
- Fox, J. D., Y. He, D. Shelver, G. P. Roberts and P. W. Ludden (1996a) Characterization of the region encoding the CO-induced hydrogenase of *Rhodospirillum rubrum*. *J. Bacteriol.* **178**: 6200-6208.
- Fox, J. D., R. L. Kerby, G. P. Roberts and P. W. Ludden (1996b) Characterization of the CO-induced, CO-tolerant hydrogenase from *Rhodospirillum rubrum* and the gene encoding the large subunit of the enzyme. *J. Bacteriol.* **178**: 1515-1524.
- Freude, C. and M. Blaser (2016) Carbon isotope fractionation during catabolism and anabolism in acetogenic bacteria growing on different substrates. *Appl. Environ. Microbiol.* **82**: 2728-2737.
- Geiger, I. (2016) Untersuchungen zur DNA-Aufnahme und Genexpression im thermophilen acetogenen Bakterium *Thermoanaerobacter kivui*. Masterarbeit, Goethe-Universität Frankfurt, Frankfurt am Main.
- Gorst, C. M. and S. W. Ragsdale (1991) Characterization of the NiFeCO complex of carbon monoxide dehydrogenase as a catalytically competent intermediate in the pathway of acetyl-coenzyme-A synthesis. *J. Biol. Chem.* **266**: 20687-20693.
- Graber, J. R. and J. A. Breznak (2004) Physiology and nutrition of *Treponema primitia*, an H<sub>2</sub>-CO<sub>2</sub>-acetogenic spirochete from termite hindguts. *Appl. Environ. Microbiol.* **70**: 1307-1314.
- Green, M. R and J. Sambrook (2012) *Molecular cloning: a laboratory manual*. Cold Spring Harbor Laboratory Press, Cold Spring Harbor, New York, USA.
- Hawkins, A. B., H. Lian, B. M. Zeldes, A. J. Loder, G. L. Lipscomb, G. J. Schut, M. W. Keller, M. W.W. Adams and R. M. Kelly (2015) Bioprocessing analysis of *Pyrococcus furiosus* strains engineered for CO<sub>2</sub>-based 3-hydroxypropionate production. *Biotechnol Bioeng.* **112**: 1533–1543.
- Hedderich, R. and L. Forzi (2005) Energy-converting [NiFe] hydrogenases: more than just H<sub>2</sub> activation. *J. Mol. Microbiol. Biotechnol.* **10**: 92-104.
- Heise, R., V. Müller and G. Gottschalk (1989) Sodium dependence of acetate formation by the acetogenic bacterium *Acetobacterium woodii*. *J. Bacteriol.* **171**: 5473-5478.

- Henke, L. (2017) Genetische und physiologische Untersuchungen des thermophilen anaeroben Bakteriums *Thermoanaerobacter kivui*. Masterarbeit, Goethe-Universität Frankfurt, Frankfurt am Main.
- Henstra, A. M., C. Dijkema and A. J. Stams (2007) *Archaeoglobus fulgidus* couples CO oxidation to sulfate reduction and acetogenesis with transient formate accumulation. *Environ. Microbiol.* **9**: 1836-41.
- Hess, V., A. Poehlein, M. C. Weghoff, R. Daniel and V. Müller (2014) A genome-guided analysis of energy conservation in the thermophilic, cytochrome-free acetogenic bacterium *Thermoanaerobacter kivui*. *BMC Genomics* **15**: 1139.
- Himes, R. H. and J. A. Harmony (1973) Formyltetrahydrofolate synthetase. *CRC Crit. Rev. Biochem.* **1**: 501-535.
- Huang, H., S. Wang, J. Moll and R. K. Thauer (2012) Electron bifurcation involved in the energy metabolism of the acetogenic bacterium *Moorella thermoacetica* growing on glucose or H<sub>2</sub> plus CO<sub>2</sub>. *J. Bacteriol.* **194**: 3689-3699.
- Hugenholtz, J., D. M. Ivey and L. G. Ljungdahl (1987) Carbon monoxide-driven electron transport in *Clostridium thermoautotrophicum* membranes. *J. Bacteriol.* **169**: 5845-5847.
- Hugenholtz, J. and L. G. Ljungdahl (1990) Metabolism and energy generation in homoacetogenic clostridia. *FEMS Microbiol. Rev.* **87**: 383-389.
- Hungate, R. E. (1969) A roll tube method for cultivation of strict anaerobes. In: *Methods in Microbiology*, edited by J. R. Norris J. R. and D. W. Ribbons. Academic Press, New York and London, pp. 117-132.
- Jain, S., H. M. Dietrich, V. Müller and M. Basen (2020) Formate is required for growth of the thermophilic acetogenic bacterium *Thermoanaerobacter kivui* lacking hydrogen-dependent carbon dioxide reductase (HDCR). *Front. Microbiol.* **11**: 59.
- Jouanneau, Y., H. S. Jeong, N. Hugo, C. Meyer and J. C. Willison (1998) Overexpression in *Escherichia coli* of the *rnf* genes from *Rhodobacter capsulatus* - Characterization of two membrane-bound iron-sulfur proteins. *Eur. J. Biochem.* **251**: 54-64.



- Jorge, C. D., L. L. Fonseca, W. Boos and H. Santos (2008) Role of Periplasmic Trehalase in Uptake of Trehalose by the Thermophilic Bacterium *Rhodothermus marinus*. *J Bacteriol.* **190**: 1871–1878.
- Kamlage, B., B. Gruhl and M. Blaut (1997) Isolation and characterization of two new homoacetogenic hydrogen-utilizing bacteria from the human intestinal tract that are closely related to *Clostridium coccooides*. *Appl. Environ. Microbiol.* **63**: 1732-1738.
- Katsyv, A. and V. Müller (2020) Overcoming energetic barriers in acetogenic C1 conversion. *Front. Bioeng. Biotechnol.* **8**: 621166.
- Kelly, W. J., G. Henderson, D. M. Pacheco, D. Li, K. Reilly, G. E. Naylor, P. H. Janssen, G. T. Attwood, E. Altermann and S. C. Leahy (2016) The complete genome sequence of *Eubacterium limosum* SA11, a metabolically versatile rumen acetogen. *Stand Genomic Sci.* **11**: 26.
- Kerby, R., W. Niemczura and J. G. Zeikus (1983) Single-carbon catabolism in acetogens: Analysis of carbon flow in *Acetobacterium woodii* and *Butyribacterium methylotrophicum* by fermentation and <sup>13</sup>C nuclear magnetic resonance measurement. *J. Bacteriol.* **155**: 1208-1218.
- Kerby, R. and J. G. Zeikus, J.G. (1987) Catabolic enzymes of the acetogen *Butyribacterium methylotrophicum* grown on single-carbon substrates. *J Bacteriol.* **169**: 5605-9.
- Kerby, R. L., S. S. Hong, S. A. Ensign, L.J. Coppoc, P.W. Ludden and G.P. Roberts (1992) Genetic and physiological characterization of the *Rhodospirillum rubrum* carbon monoxide dehydrogenase system. *J. Bacteriol.* **174**: 5284-94.
- Kerby, R. L., P. W. Ludden and G. P. Roberts (1995) Carbon monoxide-dependent growth of *Rhodospirillum rubrum*. *J. Bacteriol.* **177**: 2241-2244.
- Klemps, R., S. M. Schoberth and H. Sahm (1987) Production of acetic acid by *Acetogenium kivui*. *Appl. Microbiol. Biotechnol.* **27**: 229-234.
- Kremp, F., J. Roth and V. Müller (2020) The *Sporomusa* type Nfn is a novel type of electron-bifurcating transhydrogenase that links the redox pools in acetogenic bacteria. *Sci. Rep.* **10**: 14872.

- Kuhner, C. H., C. Frank, A. Griesshammer, M. Schmittroth, G. Acker, A. Gossner and H. L. Drake (1997) *Sporomusa silvacetica* sp. nov., an acetogenic bacterium isolated from aggregated forest soil. *Int. J. Syst. Bacteriol.* **47**: 352-8.
- Kulkarni, G., T. D. Mand and W. W. Metcalf (2018) Energy conservation *via* hydrogen cycling in the methanogenic archaeon *Methanosarcina barkeri*. *mBio* **9**: e01256-18.
- Kung, Y. and C. L. Drennan (2011) A role for nickel-iron cofactors in biological carbon monoxide and carbon dioxide utilization. *Curr. Opin. Chem. Biol.* **15**: 276-83.
- Küsel, K., T. Dorsch, G. Acker, E. Stackebrandt and H. L. Drake (2000) *Clostridium scatologenes* strain SL1 isolated as an acetogenic bacterium from acidic sediments. *Int. J. Syst. Evol. Microbiol.* **50**: 537-546.
- Küsel, K., A. Karnholz, T. Trinkwalter, R. Devereux, G. Acker and H. L. Drake (2001) Physiological ecology of *Clostridium glycolicum* RD-1, an aerotolerant acetogen isolated from sea grass roots. *Appl. Environ. Microbiol.* **67**: 4734-4741.
- Lane, N. and W. F. Martin (2012) The origin of membrane bioenergetics. *Cell* **151**: 1406-1416.
- Lee, H. S., S. G. Kang, S. S. Bae, J. K. Lim, Y. Cho, Y. J. Kim, J. H. Jeon, Cha, S.-S., Kwon, K.K., Kim, H.-T., Park, C.-J., Lee, H.-W., Kim, S.I., Chun, J., Colwell, R.R., Kim, S.-J. and Lee, J.-H. (2008) The complete genome sequence of *Thermococcus onnurineus* NA1 reveals a mixed heterotrophic and carboxydrotrophic metabolism. *J. Bacteriol.* **190**: 7491-7499.
- Leigh, J. A., F. Mayer and R. S. Wolfe (1981) *Acetogenium kivui*, a new thermophilic hydrogen-oxidizing, acetogenic bacterium. *Arch. Microbiol.* **129**: 275-280.
- Leigh, J. A. and R. S. Wolfe (1983) *Acetogenium kivui* gen. nov., sp. nov., a thermophilic acetogenic bacterium. *Int. J. Syst. Evol. Microbiol.* **33**: 886.
- Li, F., J. Hinderberger, H. Seedorf, J. Zhang, W. Buckel and R. K. Thauer (2008) Coupled ferredoxin and crotonyl coenzyme A (CoA) reduction with NADH catalyzed by the butyryl-CoA dehydrogenase/Etf complex from *Clostridium kluyveri*. *J. Bacteriol.* **190**: 843-850.

- Li, L. F., L. Ljungdahl and H. G. Wood (1966) Properties of nicotinamide adenine dinucleotide phosphate-dependent formate dehydrogenase from *Clostridium thermoaceticum*. *J. Bacteriol.* **92**: 405-412.
- Liew, F., A. M. Henstra, K. Winzer, M. Köpke, S. D. Simpson and N. P. Minton (2016a) Insights into CO<sub>2</sub> fixation pathway of *Clostridium autoethanogenum* by targeted mutagenesis. *mBio* **7**: e00427-00416.
- Liew, F., M. E. Martin, R. C. Tappel, B. D. Heijstra, C. Mihalcea and M. Köpke (2016b) Gas fermentation-a flexible platform for commercial scale production of low-carbon-fuels and chemicals from waste and renewable feedstocks. *Front. Microbiol.* **7**: 694.
- Ljungdahl, L. G. (1986) The autotrophic pathway of acetate synthesis in acetogenic bacteria. *Ann. Rev. Microbiol.* **40**: 415-450.
- Ljungdahl, L. G. (1994) The acetyl-CoA pathway and the chemiosmotic generation of ATP during acetogenesis. In: *Acetogenesis*, edited by H.L. Drake. Chapman and Hall, New York, pp. 63-87.
- Lovell, C. R., A. Przybyla and L. G. Ljungdahl (1988) Cloning and expression in *Escherichia coli* of the *Clostridium thermoaceticum* gene encoding thermostable formyltetrahydrofolate synthetase. *Arch. Microbiol.* **149**: 280-285.
- Lovley, D. R. and J. G. Ferry (1985) Production and consumption of H<sub>2</sub> during growth of *Methanosarcina* spp. on acetate. *Appl. Environ. Microbiol.* **49**: 247-249.
- Lupa, B., E. L. Hendrickson, J. A. Leigh, W. B. Whitman (2008) Formate-dependent H<sub>2</sub> production by the mesophilic methanogen *Methanococcus maripaludis*. *Appl. Environ. Microbiol.* **74**: 6584-6590.
- Lupas, A., H. Engelhardt, J. Peters, U. Santarius, S. Volker and W. Baumeister (1994) Domain structure of the *Acetogenium kivui* surface layer revealed by electron crystallography and sequence analysis. *J. Bacteriol.* **176**: 1224-1233.
- Maia, L. B., J. J. Moura and I. Moura (2015) Molybdenum and tungsten-dependent formate dehydrogenases. *J. Biol. Inorg. Chem.* **20**: 287-309.
- Martin, W. F. (2012) Hydrogen, metals, bifurcating electrons, and proton gradients: the early evolution of biological energy conservation. *FEBS Lett.* **586**: 485-493.

- Matson, E. G., X. Zhang and J.R. Leadbetter (2010) Selenium controls transcription of paralogous formate dehydrogenase genes in the termite gut acetogen, *Treponema primitia*. *Environ. Microbiol. Rep.* **12**: 2245-2258.
- McDowall, J. S., B. J. Murphy, M. Haumann, T. Palmer, F. A. Armstrong and F. Sargent (2014) Bacterial formate hydrogenlyase complex. *Proc. Natl. Acad. Sci. U.S.A.* **111**: E3948-E3956.
- McTernan, P. M., S. K. Chandrayan, C. H. Wu, B. J. Vaccaro, W. A. Lancaster, Q. Yang, D. Fu, G. L. Hura, J. A. Tainer and M. W. Adams (2014) Intact functional fourteen-subunit respiratory membrane-bound [NiFe]-hydrogenase complex of the hyperthermophilic archaeon *Pyrococcus furiosus*. *J. Biol. Chem.* **289**: 19364-19372.
- Moon, J. (2018) Mannitol metabolism and ethanol production in the thermophilic acetogenic bacterium *Thermoanaerobacter kivui*. Masterarbeit, Goethe-Universität Frankfurt, Frankfurt am Main.
- Moon, J., L. Henke, N. Merz and M. Basen (2019) A thermostable mannitol-1-phosphate dehydrogenase is required in mannitol metabolism of the thermophilic acetogenic bacterium *Thermoanaerobacter kivui*. *Environ. Microbiol.* **21**: 3728-3736.
- Moon, J., S. Jain, V. Müller and M. Basen (2020) Homoacetogenic conversion of mannitol by the thermophilic acetogenic bacterium *Thermoanaerobacter kivui* requires external CO<sub>2</sub>. *Front. Microbiol.* **11**: 571736.
- Moore, M. R., W. E. O'Brien and L. G. Ljungdahl (1974) Purification and characterization of nicotinamide adenine dinucleotide-dependent methylenetetrahydrofolate dehydrogenase from *Clostridium formicoaceticum*. *J. Biol. Chem.* **249**: 5250-5253.
- Müller, D. J., N. A. Dencher, T. Meier, P. Dimroth, K. Suda, H. Stahlberg, A. Engel, H. Seelert and U. Matthay (2001) ATP synthase: constrained stoichiometry of the transmembrane rotor. *FEBS Lett.* **504**: 219-222.
- Müller, V. (2003) Energy conservation in acetogenic bacteria. *Appl. Environ. Microbiol.* **69**: 6345-6353.
- Müller, V. and S. Bowien (1995) Differential effects of sodium ions on motility in the homoacetogenic bacteria *Acetobacterium woodii* and *Sporomusa sphaeroides*. *Arch. Microbiol.* **164**: 363-369.

- Müller, V., N. P. Chowdhury and M. Basen (2018) Electron bifurcation: A long-hidden energy-coupling mechanism. *Annu. Rev. Microbiol.* **72**: 331-353.
- Müller, V. and J. Frerichs (2013) Acetogenic bacteria In: *Encyclopedia of life sciences*. John Wiley and Sons Ltd, Chichester.
- Müller, V., F. Inkamp, A. Rauwolf, K. Küsel and H. L. Drake (2004) Molecular and cellular biology of acetogenic bacteria. In: *Strict and facultative anaerobes: Medical and environmental aspects*, edited by M. Nakano and P. Zuber. Horizon Scientific Press, Norfolk, pp. 251-281.
- Mullis, K., F. Faloona, S. Scharf, R. Saiki, G. Horn and H. Erlich (1986) Specific enzymatic amplification of DNA *in vitro*: the polymerase chain reaction. *Cold Spring Harb. Symp. Quant. Biol.* **51**: 263-73.
- Nguyen, D. M. N., G. J. Schut, O. A. Zadvornyy, M. Tokmina-Lukaszewska, S. Poudel, G. L. Lipscomb, L. A. Adams, J. T. Dinsmore, W. J. Nixon, E. S. Boyd, B. Bothner, J. W. Peters and M. W. Adams (2017) Two functionally distinct NADP<sup>+</sup>-dependent ferredoxin oxidoreductases maintain the primary redox balance of *Pyrococcus furiosus*. *J. Biol. Chem.* **292**: 14603-14616.
- Nicolet, Y., C. Piras, P. Legrand, C. E. Hatchikian and J. C. Fontecilla-Camps (1999) *Desulfovibrio desulfuricans* iron hydrogenase: the structure shows unusual coordination to an active site Fe binuclear center. *Structure* **7**: 13-23.
- O'Brien, W. E., J. M. Brewer and L. G. Ljungdahl (1973) Purification and characterization of thermostable 5,10-methylenetetrahydrofolate dehydrogenase from *Clostridium thermoaceticum*. *J. Biol. Chem.* **248**: 403-408.
- Odom, J. M. and H. D. Peck Jr. (1984) Hydrogenase, electron-transfer proteins, and energy coupling in the sulfate-reducing bacteria *Desulfovibrio*. *Annu. Rev. Microbiol.* **38**: 551-92.
- Odom, J. M. and H. D. Peck Jr. (1981) Hydrogen cycling as a general mechanism for energy coupling in the sulfate-reducing bacteria. *FEMS Microbiol. Lett.* **12**: 47-50.
- Ohno, M., H. Shiratori, M. J. Park, Y. Saitoh, Y. Kumon, N. Yamashita, A. Hirata, H. Nishida, K. Ueda and T. Beppu (2000) *Symbiobacterium thermophilum* gen. nov., sp. nov., a symbiotic thermophile that depends on co-culture with a *Bacillus* strain for growth. *Int. J. Syst. Evol. Microbiol.* **50**: 1829-1832.

- Öppinger, C., F. Kremp and V. Müller (2021) Is reduced ferredoxin the physiological electron donor for MetVF-type methylenetetrahydrofolate reductases in acetogenesis? A hypothesis. *Int. Microbiol.*, in press. <https://doi.org/10.1007/s10123-021-00190-0>
- Onyenwoke, R. U. and J. Wiegel (2015) *Thermoanaerobacter*. *Bergey's Manual of Systematics of Archaea and Bacteria*, S. 71-118.
- Parshina, S. N., S. Kijlstra, A. M. Henstra, J. Sipma, C. M. Plugge and A. J. Stams (2005) Carbon monoxide conversion by thermophilic sulfate-reducing bacteria in pure culture and in co-culture with *Carboxydotherrmus hydrogenoformans*. *Appl. Microbiol. Biotechnol.* **68**: 390-6.
- Peiter, N. (2017) Genetische und physiologische Untersuchungen des Wasserstoff- und Formiat-Stoffwechsels in *Thermoanaerobacter kivui*. Bachelorarbeit, Goethe-Universität Frankfurt, Frankfurt am Main.
- Pereira, I. A. (2013) An enzymatic route to H<sub>2</sub> storage. *Science* **342**: 1329-1330.
- Pezacka, E. and H. G. Wood (1984) Role of carbon monoxide dehydrogenase in the autotrophic pathway used by acetogenic bacteria. *Proc. Natl. Acad. Sci. U.S.A.* **81**: 6261-6265.
- Pierce, E., G. Xie, R.D. Barabote, E. Saunders, C. S. Han, J. C. Detter, P. Richardson, T. S. Brettin, A. Das, L. G. Ljungdahl and S. W. Ragsdale (2008) The complete genome sequence of *Moorella thermoacetica* (f. *Clostridium thermoaceticum*). *Environ. Microbiol.* **10**: 2550-2573.
- Pikuta, E. V., R. B. Hoover, A. K. Bej, D. Marsic, E. N. Detkova, W. B. Whitman and P. Krader (2003) *Tindallia californiensis* sp. nov., a new anaerobic, haloalkaliphilic, spore-forming acetogen isolated from Mono Lake in California. *Extremophiles* **7**: 327– 334.
- Pinske, C. and F. Sargent (2016) Exploring the directionality of *Escherichia coli* formate hydrogenlyase: a membrane-bound enzyme capable of fixing carbon dioxide to organic acid. *Microbiologyopen* **5**: 721-737.
- Poehlein, A., M. Cebulla, M. M. Ilg, F. R. Bengelsdorf, B. Schiel-Bengelsdorf, G. Whited,

- J. R. Andreesen, G. Gottschalk, R. Daniel and P. Dürre (2015) The complete genome sequence of *Clostridium aceticum*: a missing link between Rnf- and cytochrome containing autotrophic acetogens. *mBio* **6**: e01168-01115.
- Ragsdale, S. W. (1991) Enzymology of the acetyl-CoA pathway of autotrophic CO<sub>2</sub> fixation. *Crit. Rev. Biochem. Mol. Biol.* **26**: 261-300.
- Ragsdale, S. W. (2000) Nickel containing CO dehydrogenases and hydrogenases. *Subcell. Biochem.* **35**: 487-518.
- Ragsdale, S. W. (2008) Enzymology of the Wood-Ljungdahl pathway of acetogenesis. *Ann. N. Y. Acad. Sci.* **1125**: 129-136.
- Ragsdale, S. W. and M. Kumar (1996) Nickel-containing carbon monoxide dehydrogenase/acetyl-CoA synthase. *Chem. Rev.* **96**: 2515-2540.
- Ragsdale, S. W. and L. G. Ljungdahl (1984) Purification and properties of NAD-dependent 5,10-methylenetetrahydrofolate dehydrogenase from *Acetobacterium woodii*. *J. Biol. Chem.* **259**: 3499-3503.
- Ragsdale, S. W., L. G. Ljungdahl and D. V. DerVartanian (1982) EPR evidence for nickel-substrate interaction in carbon monoxide dehydrogenase from *Clostridium thermoaceticum*. *Biochem. Biophys. Res. Commun.* **108**: 658-663.
- Ragsdale, S. W., L. G. Ljungdahl and D. V. DerVartanian (1983) Isolation of carbon monoxide dehydrogenase from *Acetobacterium woodii* and comparison of its properties with those of the *Clostridium thermoaceticum* enzyme. *J. Bacteriol.* **155**: 1224-1237.
- Ragsdale, S. W. and E. Pierce (2008) Acetogenesis and the Wood-Ljungdahl pathway of CO<sub>2</sub> fixation. *Biochim. Biophys. Acta* **1784**: 1873-1898.
- Ragsdale, S. W. and H. G. Wood (1985) Acetate biosynthesis by acetogenic bacteria. Evidence that carbon monoxide dehydrogenase is the condensing enzyme that catalyzes the final steps in the synthesis. *J. Biol. Chem.* **260**: 3970-3977.
- Raybuck, S. A., N. R. Bastian, W. H. Orme-Johnson and C. T. Walsh (1988) Kinetic characterization of the carbon monoxide-acetyl-CoA (carbonyl group) exchange activity of the acetyl-CoA synthesizing CO dehydrogenase from *Clostridium thermoaceticum*. *Biochemistry* **27**: 7698-7702.

- Robb, F. T. and S. M. Techtmann (2018) Life on the fringe: microbial adaptation to growth on carbon monoxide. *F1000Res.* **7**: 1981.
- Rother, M. and W. W. Metcalf (2004) Anaerobic growth of *Methanosarcina acetivorans* C2A on carbon monoxide: an unusual way of life for a methanogenic archaeon. *Proc. Natl. Acad. Sci. U.S.A.* **101**: 16929-16934.
- Ruan, Z., Y. Wang, C. Zhang, J. Song, Y. Zhai, Y. Zhuang, H. Wang, X. Chen, Y. Li, and B. Zhao (2014) *Clostridium huakuii* sp. nov., an anaerobic, acetogenic bacterium isolated from methanogenic consortia. *Int. J. Syst. Evol. Microbiol.* **64**: 4027–4032.
- Savage, M. D., Z. G. Wu, S.L. Daniel, L. L. Lundie, Jr. and Drake, H. L. (1987) Carbon monoxide-dependent chemolithotrophic growth of *Clostridium thermoautotrophicum*. *Appl. Environ. Microbiol.* **53**: 1902-1906.
- Schaupp, A. and L. G. Ljungdahl (1974) Purification and properties of acetate kinase from *Clostridium thermoaceticum*. *Arch. Microbiol.* **100**: 121-129.
- Schmehl, M., A. Jahn, A. Meyer zu Vilsendorf, S. Hennecke, B. Masepohl, M. Schuppler, M. Marxer, J. Oelze and W. Klipp (1993) Identification of a new class of nitrogen fixation genes in *Rhodobacter capsulatus*: a putative membrane complex involved in electron transport to nitrogenase. *Mol. Gen. Genet.* **241**: 602-615.
- Schmidt, K., S. Liaaen-Jensen and H. G. Schlegel (1963) Die Carotinoide der Thiorhodaceae. *Arch Mikrobiol.* **46**: 117-126.
- Schoelmerich, M. C. and V. Müller (2019) Energy conservation by a hydrogenase-dependent chemiosmotic mechanism in an ancient metabolic pathway. *Proc. Natl. Acad. Sci. U.S.A.* **116**: 6329-6334.
- Schoelmerich, M. C. and V. Müller (2020) Energy-converting hydrogenases: The link between H<sub>2</sub> metabolism and energy conservation. *Cell. Mol. Life Sci.* **77**: 1461-1481.
- Schuchmann, K., N. P. Chowdhury and V. Müller (2018) Complex multimeric [FeFe] hydrogenases: Biochemistry, physiology and new opportunities for the hydrogen economy. *Front. Microbiol.* **9**: 2911.
- Schuchmann, K. and V. Müller (2012) A bacterial electron bifurcating hydrogenase. *J. Biol. Chem.* **287**: 31165–31171.



- Schuchmann, K. and V. Müller (2013) Direct and reversible hydrogenation of CO<sub>2</sub> to formate by a bacterial carbon dioxide reductase. *Science* **342**: 1382-1385.
- Schuchmann, K. and V. Müller (2014) Autotrophy at the thermodynamic limit of life: A model for energy conservation in acetogenic bacteria. *Nat. Rev. Microbiol.* **12**: 809-821.
- Schuchmann, K. and V. Müller (2016) Energetics and application of heterotrophy in acetogenic bacteria. *Appl. Environ. Microbiol.* **82**: 4056-4069.
- Schuchmann, K., J. Vonck and V. Müller (2016) A bacterial hydrogen-dependent CO<sub>2</sub> reductase forms filamentous structures. *FEBS J.* **283**: 1311-1322.
- Schut, G. J. and M. W. Adams (2009) The iron-hydrogenase of *Thermotoga maritima* utilizes ferredoxin and NADH synergistically: a new perspective on anaerobic hydrogen production. *J. Bacteriol.* **191**: 4451-4457.
- Schut, G. J., O. Zadvornyy, C. H. Wu, J. W. Peters, E. S. Boyd and M. W. Adams (2016b) The role of geochemistry and energetics in the evolution of modern respiratory complexes from a proton-reducing ancestor. *Biochim. Biophys. Acta* **1857**: 958-970.
- Schwarz, F. M., S. Ciurus, S. Jain, C. Baum, A. Wiechmann, M. Basen and V. Müller (2020) Revealing formate production from carbon monoxide in wild type and mutants of Rnf- and Ech-containing acetogens, *Acetobacterium woodii* and *Thermoanaerobacter kivui*. *Microb. Biotechnol.* **13**: 2044-2056.
- Schwarz, F. M., K. Schuchmann and V. Müller (2018) Hydrogenation of CO<sub>2</sub> at ambient pressure catalyzed by a highly active thermostable biocatalyst. *Biotechnol. Biofuels* **11**: 237.
- Seravalli, J., M. Kumar, W. P. Lu and S. W. Ragsdale (1997) Mechanism of carbon monoxide oxidation by the carbon monoxide dehydrogenase/acetyl-CoA synthase from *Clostridium thermoaceticum*: Kinetic characterization of the intermediates. *Biochem.* **36**: 11241-11251.
- Shao, X., J. Zhou, D. G. Olson and L. Lynd (2016) A markerless gene deletion and integration system for *Thermoanaerobacter ethanolicus*. *Biotechnol. Biofuels.* **9**:100.

- Shelver, D., R. L. Kerby, Y. He and G. P. Roberts (1997) *CooA*, a CO-sensing transcription factor from *Rhodospirillum rubrum*, is a CO-binding heme protein. *Proc. Natl. Acad. Sci. U. S. A.* **94**:11216-11220.
- Simankova, M. V., O. R. Kotsyurbenko, E. Stackebrandt, N. A. Kostrikina, A. M. Lysenko, G. A. Osipov and A. N. Nozhevnikova (2000) *Acetobacterium tundrae* sp. nov., a new psychrophilic acetogenic bacterium from tundra soil. *Arch. Microbiol.* **174**: 440-447.
- Singer, S. W., M. B. Hirst and P. W. Ludden (2006) CO-dependent H<sub>2</sub> evolution by *Rhodospirillum rubrum*: role of CODH:CooF complex. *Biochim. Biophys. Acta* **1757**: 1582-91.
- Slobodkin, A. I., T. P. Tourova, B. B. Kuznetsov, N. A. Kostrikina, N. A. Chernyh and E. A. Bonch-Osmolovskaya (1999) *Thermoanaerobacter siderophilus* sp. nov., a novel dissimilatory Fe(III)-reducing, anaerobic, thermophilic bacterium. *Int. J. Syst. Bacteriol.* **49**: 1471-8.
- Soboh, B., D. Linder and R. Hedderich (2002) Purification and catalytic properties of a CO-oxidizing:H<sub>2</sub>-evolving enzyme complex from *Carboxydothemus hydrogenoformans*. *Eur. J. Biochem.* **269**: 5712-5721.
- Sokolova, T. G., A. M. Henstra, J. Sipma, S. N. Parshina, A. J. Stams and A. V. Lebedinsky (2009) Diversity and ecophysiological features of thermophilic carboxydophilic anaerobes. *FEMS Microbiol. Ecol.* **68**: 131-141.
- Svetlitchnyi, V. A., T. G. Sokolova, M. Gerhardt, M. Ringpfeil, N. A. Kostrikina and G.A. Zavarzin (1991) *Carboxydothemus hydrogenoformans* gen. nov. sp. nov., a CO-utilizing thermophilic anaerobic bacterium from hydrothermal environments of Kunashir Island. *Syst. Appl. Microbiol.* **14**: 254-260.
- Tanner, R. S., L. M. Miller and D. Yang (1993) *Clostridium ljungdahlii* sp. nov., an acetogenic species in clostridial rRNA homology Group-I. *Int. J. Syst. Bacteriol.* **43**: 232-236.
- Tersteegen, A. and R. Hedderich (1999) *Methanobacterium thermoautotrophicum* encodes two multisubunit membrane-bound [NiFe] hydrogenases. Transcription of the operons and sequence analysis of the deduced proteins. *Eur. J. Biochem.* **264**: 930-943.

- Thauer, R. K., K. Jungermann and K. Decker (1977) Energy conservation in chemotrophic anaerobic bacteria. *Bacteriol. Rev.* **41**: 100-180.
- Trchounian, K. and A. Trchounian (2014) Different role of *focA* and *focB* encoding formate channels for hydrogen production by *Escherichia coli* during glucose or glycerol fermentation. *Int. J. Hydrogen Energy* **39**: 20987-20991.
- Tschech, A. and N. Pfennig (1984) Growth yield increase linked to caffeate reduction in *Acetobacterium woodii*. *Arch. Microbiol.* **137**: 163-167.
- Uffen, R. L. (1976) Anaerobic growth of a *Rhodopseudomonas* species in the dark with carbon monoxide as sole carbon and energy substrate. *Proc. Natl. Acad. Sci. U.S.A.* **73**: 3298-3302.
- Uffen, R. L. (1983) Metabolism of carbon monoxide by *Rhodopseudomonas gelatinosa*: cell growth and properties of the oxidation system. *J. Bacteriol.* **155**: 956-965.
- Vignais, P. M. and B. Billoud (2007) Occurrence, classification, and biological function of hydrogenases: an overview. *Chem. Rev.* **107**: 4206-4272.
- Voneysmond, J., D. Vasicracki and C. Wandrey (1990) Acetic acid production by *Acetogenium kivui* in continuous culture — kinetic studies and computer simulations. *Appl. Microbiol. Biotechnol.* **34**: 344-349.
- Wang, S., H. Huang, J. Kahnt, A.P. Müller, M. Köpke and R. K. Thauer (2013a) NADP-specific electron-bifurcating [FeFe]-hydrogenase in a functional complex with formate dehydrogenase in *Clostridium autoethanogenum* grown on CO. *J. Bacteriol.* **195**: 4373-4386.
- Wang, S., H. Huang, J. Kahnt and R. K. Thauer (2013b) A reversible electron-bifurcating ferredoxin- and NAD-dependent [FeFe]-hydrogenase (HydABC) in *Moorella thermoacetica*. *J. Bacteriol.* **195**: 1267-1275.
- Weghoff, M. C. and V. Müller (2016) CO metabolism in the thermophilic acetogen *Thermoanaerobacter kivui*. *Appl. Environ. Microbiol.* **82**: 2312-2319.
- Weiss, M. C., F. L. Sousa, N. Mrnjavac, S. Neukirchen, M. Roettger, S. Nelson-Sathi and W. F. Martin (2016) The physiology and habitat of the last universal common ancestor. *Nat. Microbiol.* **1**: 16116.

- Welte, C., V. Kallnik, M. Grapp, G. Bender, S. Ragsdale and U. Deppenmeier (2010) Function of Ech hydrogenase in ferredoxin-dependent, membrane-bound electron transport in *Methanosarcina mazei*. *J. Bacteriol.* **192**: 674-678.
- Westphal, L., A. Wiechmann, J. Baker, N. P. Minton and V. Müller (2018) The Rnf complex is an energy coupled transhydrogenase essential to reversibly link cellular NADH and ferredoxin pools in the acetogen *Acetobacterium woodii*. *J. Bacteriol.* **200**: e00357-18.
- Wiechmann, A., S. Ciurus, F. Oswald, V. N. Seiler and V. Müller (2020) It does not always take two to tango: "Syntrophy" *via* hydrogen cycling in one bacterial cell. *ISME J.* **14**: 1561-1570.
- Wieringa, K. T. (1939) The formation of acetic acid from carbon dioxide and hydrogen by anaerobic spore-forming bacteria. *Antonie van Leeuwenhoek* **6**: 251-262.
- Wohlfarth, G., G. Geerligs and G. Diekert (1990) Purification and properties of a NADH-dependent 5,10-methylenetetrahydrofolate reductase from *Peptostreptococcus productus*. *Eur. J. Biochem.* **192**: 411-417.
- Wolin, E. A., M. J. Wolin and R. S. Wolfe (1963) Formation of methane by bacterial extracts. *J. Biol. Chem.* **238**: 2882-2886.
- Wood, H. G. and L. G. Ljungdahl (1991) Autotrophic character of the acetogenic bacteria. In: *Variations in autotrophic life*, edited by J.M. Shively and L.L. Barton. Academic press, San Diego, pp. 201-250.
- Wu, M., Q. Ren, A. S. Durkin, S. C. Daugherty, L. M. Brinkac, R. J. Dodson, R. Madupu, S. A. Sullivan, J. F. Kolonay, D. H. Haft, W. C. Nelson, L. J. Tallon, K. M. Jones, L. E. Ulrich, J. M. Gonzalez, I. B. Zhulin, F. T. Robb and J. A. Eisen (2005) Life in hot carbon monoxide: the complete genome sequence of *Carboxydotherrmus hydrogenoformans* Z-2901. *PLoS Genet.* **1**: e65.
- Yang, H. and H. L. Drake (1990) Differential effects of sodium on hydrogen- and glucose-dependent growth of the acetogenic bacterium *Acetogenium kivui*. *Appl. Environ. Microbiol.* **56**: 81-86.
- Yamamoto, T., K. Maruta, K. Mukai, H. Yamashita, T. Nishimoto, M. Kubota, S. Fukuda, M. Kurimoto, Y. Tsujisaka (2004) Cloning and sequencing of kojibiose

---

phosphorylase gene from *Thermoanaerobacter brockii* ATCC35047. J Biosci Bioeng. **98**: 99-106.

## 9. Acknowledgements

First of all, I am thankful to the German Academic Exchange Service (DAAD) for providing the financial support for this PhD work. This study could not have been realised without the support of many people whom I would like to acknowledge.

My special thanks to Prof. Dr. Volker Müller for giving me the opportunity to conduct this research work with the continuous support and motivating supervision. Also, I would like to express my heartfelt gratitude to Dr. Mirko Basen for his support. He contributed a lot in planning and discussion of research work, manuscripts as well as helped me throughout with every small thing. I would also like to acknowledge Prof. Dr. Claudia Büchel for accepting to be second corrector of this thesis.

I am thankful to Prof. Dr. Beate Averhoff for many lively discussions. A big thank you goes to all the current and former colleagues of the research groups for introducing me with the anaerobic techniques and assistance in the lab. The open, friendly and free working atmosphere contributed to a great extent to the success of the dissertation. A special thanks to Jennifer Bereich and Helge Dietrich for proofreading my Deutsche Zusammenfassung. Also, special thanks to Nilanjan Pal Chowdhury for all scientific discussions and career advice. I also want to thank Florian Rosenbaum and Jan Daniel Enzmann for helping me to understand and practice German.

I am indescribably thankful to my parents and in-laws for their continuous support and believing in me to study abroad. Special thanks to Ankit (my husband) and Prateek (my brother) for being my lifetime strengths without which this work could not have been accomplished. A special note of thanks goes to my friends (especially Shivam and Nandita) for their emotional and kind support during my stay in Germany.

## 10. Curriculum vitae

### Surbhi Jain

Date of birth: 11<sup>th</sup> October 1991

Place of birth: Alwar, India



### Education

- Since 04/2018 beginning of the experimental work for the present dissertation under guidance of Prof. Dr. Volker Müller at Goethe-University Frankfurt, Frankfurt am Main, Germany
- 07/2013 - 05/2015 Master of Science (M.Sc.) in Industrial Biotechnology at B.R.D. School of Biosciences, Sardar Patel University, Gujarat, India
- Master Thesis with the topic “Studies on Lipase Production, Purification and its Molecular Characterization” under guidance of Prof. Prof. R.B. Subramnian and Dr. Ujjwal Trivedi at B.R.D. School of Biosciences, Sardar Patel University, Gujarat, India
- 07/2009 - 04/2010 Bachelor of Science (B.Sc.) in Botany honors at Miranda House, Delhi University, New Delhi, India
- 07/2009 - 04/2010 High school at St. Anselms School, Alwar, India  
Majors: Biology, Chemistry and Physics

## Publications

**Jain, S.**, A. Katsyv, M. Basen and V. Müller (2021) The monofunctional CO dehydrogenase CooS is essential for growth of *Thermoanaerobacter kivui* on carbon monoxide. *Extremophiles* (submitted).

Katsyv, A., **S. Jain**, M. Basen and V. Müller (2021) Electron carriers involved in autotrophic and heterotrophic acetogenesis in the thermophilic bacterium *Thermoanaerobacter kivui*. *Extremophiles* (submitted).

**Jain, S.**, H. M. Dietrich, V. Müller and M. Basen (2020) Formate is required for growth of the thermophilic acetogenic bacterium *Thermoanaerobacter kivui* lacking hydrogen-dependent carbon dioxide reductase (HDCR). *Front. Microbiol.* **11**: 59.

Moon, J., **S. Jain**, V. Müller and M. Basen (2020) Homoacetogenic conversion of mannitol by the thermophilic acetogenic bacterium *Thermoanaerobacter kivui* requires external CO<sub>2</sub>. *Front. Microbiol.* **11**: 571736.

Schwarz, F. M., S. Ciurus, **S. Jain**, C. Baum, A. Wiechmann, M. Basen and V. Müller (2020) Revealing formate production from carbon monoxide in wild type and mutants of Rnf- and Ech-containing acetogens, *Acetobacterium woodii* and *Thermoanaerobacter kivui*. *Microb. Biotechnol.* **13**: 2044-2056.